THE ROLES OF PODOPLANIN AND CLEC-2 IN THE DEVELOPMENT AND MAINTENANCE OF THE CEREBRAL VASCULATURE

By

Kate L Lowe

UNIVERSITY OF BIRMINGHAM

A thesis is submitted to the University of Birmingham for the degree of

DOCTOR OF PHILOSOPHY

Institute of Biomedical Research
College of Medical and Dental Science
The University of Birmingham

September 2014

Abstract

The C-type lectin-like receptor, CLEC-2, is constitutively expressed on platelets, with reported expression on a number of leukocyte subsets in adult mice. Constitutive or platelet-specific deletion of CLEC-2 in mice induces cerebral haemorrhaging by mid-gestation. In this thesis, I investigated the basis of this defect, hypothesising that it is mediated by the loss of CLEC-2 activation by its endogenous ligand, podoplanin, expressed on the developing neural tube. *Podoplanin*$^{fl/fl}$ mice were crossed to mice expressing PGK-Cre to induce deletion of podoplanin at the two-cell stage. Developing blood vessels were visualized by 3-dimensional microscopy and found to be aberrantly patterned in CLEC-2- and podoplanin-deficient mice, culminating in widespread cerebral haemorrhaging by mid-gestation. Haemorrhages were also observed following Nestin-Cre driven deletion of podoplanin on neural progenitors and following deletion of the platelet integrin, αIIbβ3. Together these studies support that neuro-epithelial-derived podoplanin interacts with platelet-CLEC-2 to guide the maturation and integrity of the cerebral vasculature and to prevent haemorrhage by stimulating platelet aggregation. Using tamoxifen-inducible deletion of CLEC-2 in adult mice, the expression profile of CLEC-2 was investigated and shown to be restricted to platelets and circulating B-lymphocytes and CD11b^{high} Gr1^{high} myeloid cells. Furthermore, loss of CLEC-2 in adult mice was shown to be dispensable for maintaining blood-brain barrier permeability.

Publications arising from this thesis

Lowe, K.L., B.A. Finney, R. Hägerling, C. Deppermann, J. Frampton, B. Nieswandt, C. Buckley, F. Kiefer and S.P. Watson., 2015. Podoplanin and CLEC-2 drive cerebrovascular patterning and integrity in development. *Submitted*.

Lowe, K.L., L. Navarro-Núñez, C. Bénézech, S. Nayar, F. Barone, B. Nieswandt, S.P. Watson, C.D. Buckley and G.E. Desanti., 2015. The expression of murine CLEC-2 on leukocyte subsets varies according to their anatomical location and inflammatory state. *Submitted*.

Bénézech, C., S. Nayar, B.A. Finney, D.R. Withers, **K.L. Lowe**, G.E. Desanti, C.L. Marriot, S.P. Watson, J.H. Caamaño, C.D. Buckley and F. Barone., 2014. CLEC-2 is required for development and maintenance of lymph nodes. *Blood*, 123(20), pp.3200-3207.

Lowe, K.L., L. Navarro-Núñez. S.P. Watson., 2012. Platelet CLEC-2 and podoplanin in cancer metastasis. *Thrombosis Research*, 129 Suppl 1, pp S30-7

Finney, B.A., E. Schweighoffer, L. Navarro-Núñez, C. Bénézech, F. Barone, CE. Hughes, S.A. Langan, **K. L. Lowe**, A.Y. Pollitt, D. Mourao-Sa, S. Sheardown, G. Nash, N. Smithers, C. Reis e Sousa, V.L.J. Tybulewicz and S.P. Watson., 2012. CLEC-2 and Syk in the megakaryocytic/platelet lineage are essential for development. *Blood,* 119(7), pp. 1747-1756.

Acknowledgments

I would like to thank my supervisor Steve Watson for giving me the opportunity to do my PhD in his lab, for being supportive and giving me the freedom to express my ideas, and to the Medical Research Council for funding. I would like to thank Friedemann Kiefer and René Hägerling at the Max Planck Institute in Münster for being so welcoming and supportive of my research. Thank you to all of our external collaborators for providing reagents, mice and helpful discussions, particularly Bernhard Nieswandt and Carsten Deppermann in Würzburg and Hugh Perry and Jessica Teeling at University of Southampton. Thank you to University of Birmingham Biomedical Services Unit for all their help and support with animal work, the Centre for Electron Microscopy and the Musculoskeletal Pathology Unit at the Queen Elizabeth Hospital.

I would particularly like to thank all members of the Watson group, past and present, for making the past three years so much fun. Particularly Brenda for being a great mentor but more important a fabulously fabulous friend! Alice, Danai and Natalie for all the girly chats along the way. Craig H and Steve T for all the tea breaks, biscuits, and riveting 'random' discussions. Neil for all the donuts. Ale Bellissima for singing every morning. All the students, particularly Sam for making us warm up before netball. Gayle for being a general goddess and most of all Beata and Stef for always smiling and for all your help over the years. Outside of the Watson lab, thank-you to Ana Maria Gonzalez for all your guidance and Guillaume for being a great mentor and a pleasure to work with.

Finally, to my Corisanders; Aliesha, Annika and Claire, you are in alphabetical order to remove bias, thank you for being insane and keeping me sane-ish. To Charl for all the wine and cake. Thank you to Matthew for working abroad and giving me the freedom to work hard but for all the spontaneous exotic holidays in-between. And most importantly, to all my family and friends, in particular for Sunday face-timing with Leila and Jackson, thank you.

Table of Contents

List of Figures

CHAPTER 1

CHAPTER 2

CHAPTER 3

Page numbers represent the preceding page

CHAPTER 4

Page numbers represent the preceding page

List of Tables

Page numbers represent the preceding page

CHAPTER 1

CHAPTER 2

CHAPTER 3

Abbreviations

ACD	Acid citrate dextrose
ACK	Ammonium-Chloride-Potassium
Ang	Angiopoietin
APC	Antigen presenting cell
BABB	Benzyl alcohol:benzyl benzoate
BBB	Blood-brain barrier
BSA	Bovine serum albumin
CLEC-2	C-type lectin-like receptor 2
CNS	Central nervous system
CSF	Cerebrospinal fluid
CFU	Colony forming unit
DC	Dendritic cell
DMSO	Dimethylsulfoxide
E	Embryonic day
ECM	Extracellular matrix
EDTA	Ethylenediamine tetra-acetic acid
EMT	Epithelial-mesenchymal transition
EGF	Epidermal growth factor
ERM	Ezrin-radaxin-moesin
FBS	Fetal bovine serum
FRC	Fibroblastic reticular cell
GFAP	Glial fibrillary acidic protein
GPVI	Glycoprotein VI
Grb2	Growth factor receptor bound protein-2
H&E	Haematoxylin & Eosin
HEV	High endothelial venule
Ig	Immunoglobulin
ITAM	Immunoreceptor tyrosine based activation motif
IVH	Intraventricular haemorrhage
kDa	Kilodalton
LAT	Linker for activation of T-cells
LEC	Lymphatic endothelial cell
LPA	Lysophosphatidic acid
LPS	Lipopolysaccharide
mAb	Monoclonal antibody
MHC	Major histocompatibility complex
MS	Multiple sclerosis
NBEAL-2	Neurobeachin-like-2
Nrp2	Neuropilin-2
NVU	Neurovascular unit
OD	Optical density
P	Postnatal day
PBS	Phosphate buffered saline
PBST	Phosphate buffered saline/0.1% Tween
PDGFβ	Platelet derived growth factor β
PDGFRβ	Platelet derived growth receptor factor β
PFA	Paraformaldehye
PLC	Phospholipase C

PNVP	Perineural vascular plexus
PRP	Platelet-rich plasma
S1-P	Sphingosine-1-phosphate
SH2	Src homology 2
S1PR	Sphingosine-1-phosphate receptor
SLP76	SH2 containing leukocyte protein of 76 kDa
SPK	Sphingosine kinase
TCA	Trichloroacetic acid
TGF-β	Transforming growth factor-β
TEM	Transmission electron microscopy
TLR	Toll-like receptor
T_H17	T-helper 17
VEGF	Vascular endothelial growth factor
VEGFR	Vascular endothelial growth factor receptor
WT	Wild-type
VWF	Von Willebrand Factor

CHAPTER 1

GENERAL INTRODUCTION

1.1 Platelet function and physiology

1.1.1 Overview of platelet function

Platelets are anucleate blood cells that continually circulate the vascular system in a resting state ready to respond and plug areas of vascular damage to fulfill their major role in haemostasis. Platelets are packed with signalling proteins and surface receptors that are primed to mediate a robust activation response when in contact with exposed endothelial matrix (Gibbins, 2004). Their contact with the vessel wall is dependent on their small size (2-3 μm) that allows their margination towards vascular endothelial cells within the laminar flow of the blood vessels (Green, 2011). Inappropriate activation of platelets is associated with atherothrombotic disease such as myocardial infarction or stroke and is responsible for over 25% of deaths globally, making it the leading cause of mortality (Ho-Tin-Noe *et al*., 2011).

1.1.2 Platelet production

Platelets are derived from megakaryocytes, which in the embryo arise in the fetal liver and the yolk sac. In the adult, platelets reside in the osteoblastic niche of the bone marrow where they are formed from common myeloid progenitors (*Figure 1.1*) (Green, 2011). Platelets are released directly into the blood stream from megakaryocyte pro-platelet processes that extend between sinusoidal endothelial cells of the bone marrow (Italiano & Shivdasani, 2003). The rapid, dynamic nature of this process is highlighted by the short lifetime (5-7 days in mice and 8-10 days in humans) and large volume of circulating platelets (90-160 x 10^{10} in mice and 15-40 x 10^{10} in humans) (Kaushansky, 2005).

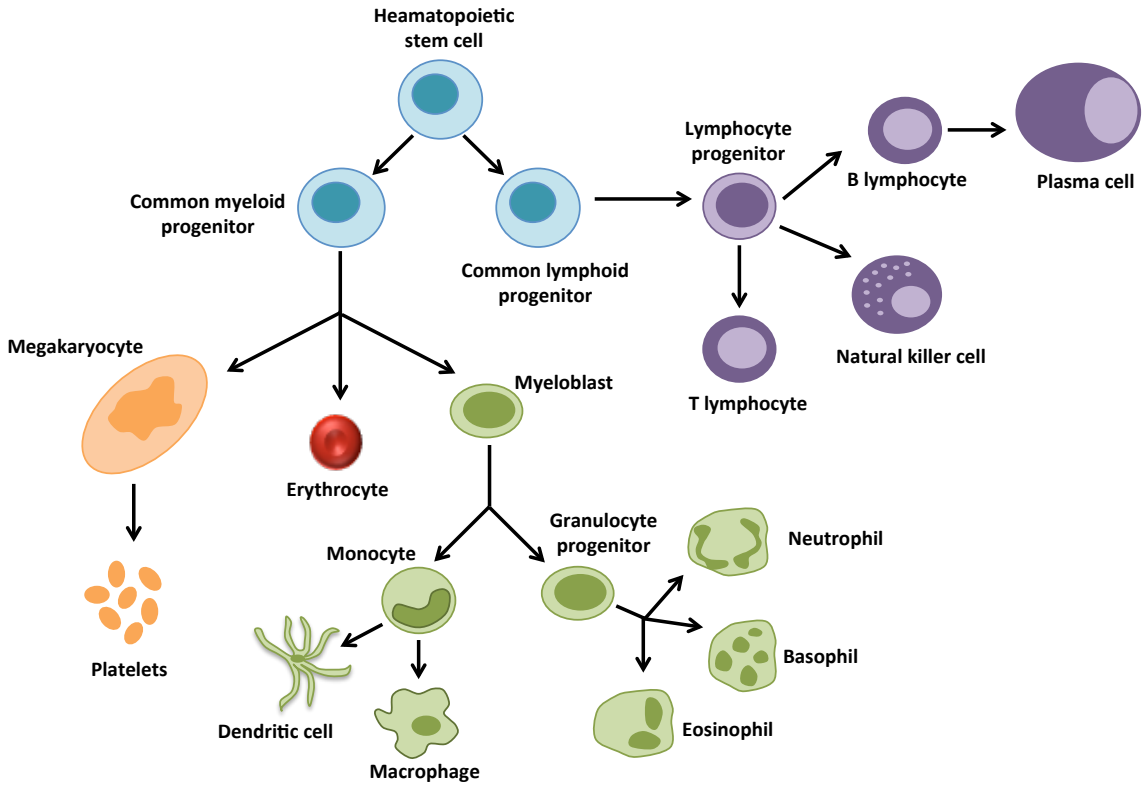

Figure 1.1. Hematopoietic stem cell lineages. Hematopoietic stem cells (HSCs) are multi-potent cells that self-renew to continually generate new HSCs to replenish cells of the blood system. HSCs can differentiate to commit to the myeloid or lymphoid lineage, giving rise to common myeloid progenitors or common lymphoid progenitors, respectively. Progenitor cells differ from stem cells in that they lack self-renewal capacity but can be multipotent or unipotent. Common lymphoid progenitors predominantly generate B- and T- lymphocytes as well as natural killer cells (and some dendritic cell subsets). Common myeloid progenitor lineage pathways include the generation of erythrocytes, the megakaryocyte pathway to generate platelets, or the myeloblast pathway to generate monocyte derived macrophages, dendritic cell subsets and granulocytes, including basophils, neutrophils and eosinophils. *Figure reconstructed from* (Katsura, 2002).

1.1.3 Platelet signalling

Platelet adhesion and activation involves a multi-step cascade of receptor interactions. The initial tethering of platelets to exposed collagen in the vessel wall is mediated through the platelet glycoprotein GPIb-V-IX binding to von Willebrand factor (VWF). This interaction brings the platelet receptor GPVI in close proximity to collagen, mediating platelet activation and the release of the secondary mediators, thromboxane and adenosine diphosphate, which in combination with locally generated thrombin creates a feedback loop to initiate further platelet activation and platelet capture. Stable adhesion and platelet aggregation relies on the major platelet integrins, αIIbβ3 and α2β3, reviewed in (Green, 2011; Nieswandt *et al*., 2011).

1.1.4 Roles of platelets outside of haemostasis and thrombosis

Platelets have been shown to critically contribute to a range of both inflammatory and developmental processes. Inflammation is tightly coupled to thrombosis and relies on an imbalance in the pro- and anti-coagulant properties of the endothelium (Wagner & Burger, 2003). Platelets have been shown to contribute to both the onset and progression of atherosclerosis amongst other thrombo-inflammatory disorders, such as ischaemic stroke and inflammatory bowel disease (Nieswandt *et al*., 2011; McNicol & Israels, 2008; Gawaz *et al*., 2005). Platelets have also been shown to facilitate the growth of tumour cells, their extravasation into the blood stream and their evasion from the immune system to promote cancer metastasis, reviewed in (Lowe *et al*., 2012; Gay & Felding-Habermann, 2011). Furthermore, platelet interactions with bacteria have been implicated in infective endocarditis, coronary artery disease and atherosclerosis, reviewed in (Fitzgerald *et al*., 2006). Interestingly, thrombi have also been implicated in immune defense, whereby

pathogens are captured and contained within a platelet rich thrombus, limiting their dissemination and effectively compartmentalising them for immune cell targeting (Engelmann & Massberg, 2013). Platelet receptors that signal through a specific, conserved motif, known as the immunoreceptor tyrosine-based activation motif (ITAM), are particularly implicated in these pathways (Boulaftali *et al*., 2013). Of particular interest is the platelet C-type lectin-like receptor 2 (CLEC-2) and its endogenous ligand podoplanin. During development, CLEC-2 has been shown to interact with podoplanin to mediate the separation of the blood and lymphatic vasculatures, which will be discussed in *Section 1.4* (Suzuki-Inoue *et al*., 2010).

1.2 C-type lectin-like receptor 2 (CLEC-2)

1.2.1 Identification of CLEC-2

CLEC-2 (gene name *Clec-1b*) was first identified in a bioinformatics study and found on chromosome 12 of the human genome in a cluster of six other C-type lectin receptors (Colonna *et al*., 2000). Years later CLEC-2 was identified on platelets as a novel receptor for the snake venom toxin rhodocytin and further isolated as a 30kDa protein by mass spectrometry (Suzuki-Inoue *et al*., 2006). Subsequently, CLEC-2 mRNA was found to be abundantly expressed in the megakaryocyte/platelet lineage of the mouse genome through use of serial analysis of gene expression (SAGE) (Senis *et al*., 2006). CLEC-2 has since been reported to be expressed on subsets of murine myeloid cells, such as neutrophils, dendritic cells (DCs) and natural killer cells, however, the reliability of this data is now questionable and will be discussed in *Chapter 4* (Mourao-Sa *et al*., 2011; Kerrigan *et al*., 2009).

1.2.2 CLEC-2 signalling

CLEC-2 is a type II transmembrane glycoprotein, however its C-type lectin-like extracellular domain lacks the conserved structural features required for binding to carbohydrate moieties, which suggested its endogenous ligand may be a protein (A. A. Watson *et al*., 2006). CLEC-2 signals through its cytoplasmic tail in a sequential multi-step pathway similar, yet distinct, to that of the major platelet collagen receptor, GPVI (S. P. Watson *et al*., 2010). A single YxxL motif found downstream of a conserved triacidic amino acid sequence in the CLEC-2 cytoplasmic tail is known as a hem-ITAM. Two ITAM sequences are found in the GPVI-FcRγ complex amongst other immunoglobulin receptors that play a critical role in platelet, B- and T-lymphocyte signalling. CLEC-2 is expressed as a dimer on the platelet surface where it interacts with its only known endogenous ligand, podoplanin (*Section 1.3*). Ligand engagement triggers the phosphorylation of the signalling molecule SYK by SRC family kinases (SFKs). Activated SYK phosphorylates the YxxL motifs in the CLEC-2 cytoplasmic tail, allowing its association to the dimeric form of CLEC-2 through its tandem SH2 domains. A complex signalling cascade ensues, resulting in the formation of the LAT signalasome encompassing an array of adaptor proteins and other effector molecules that mediate activation of PLCγ2, culminating in platelet activation (*Figure 1.2*), reviewed in (S. P. Watson *et al*., 2010; Underhill & Goodridge, 2007).

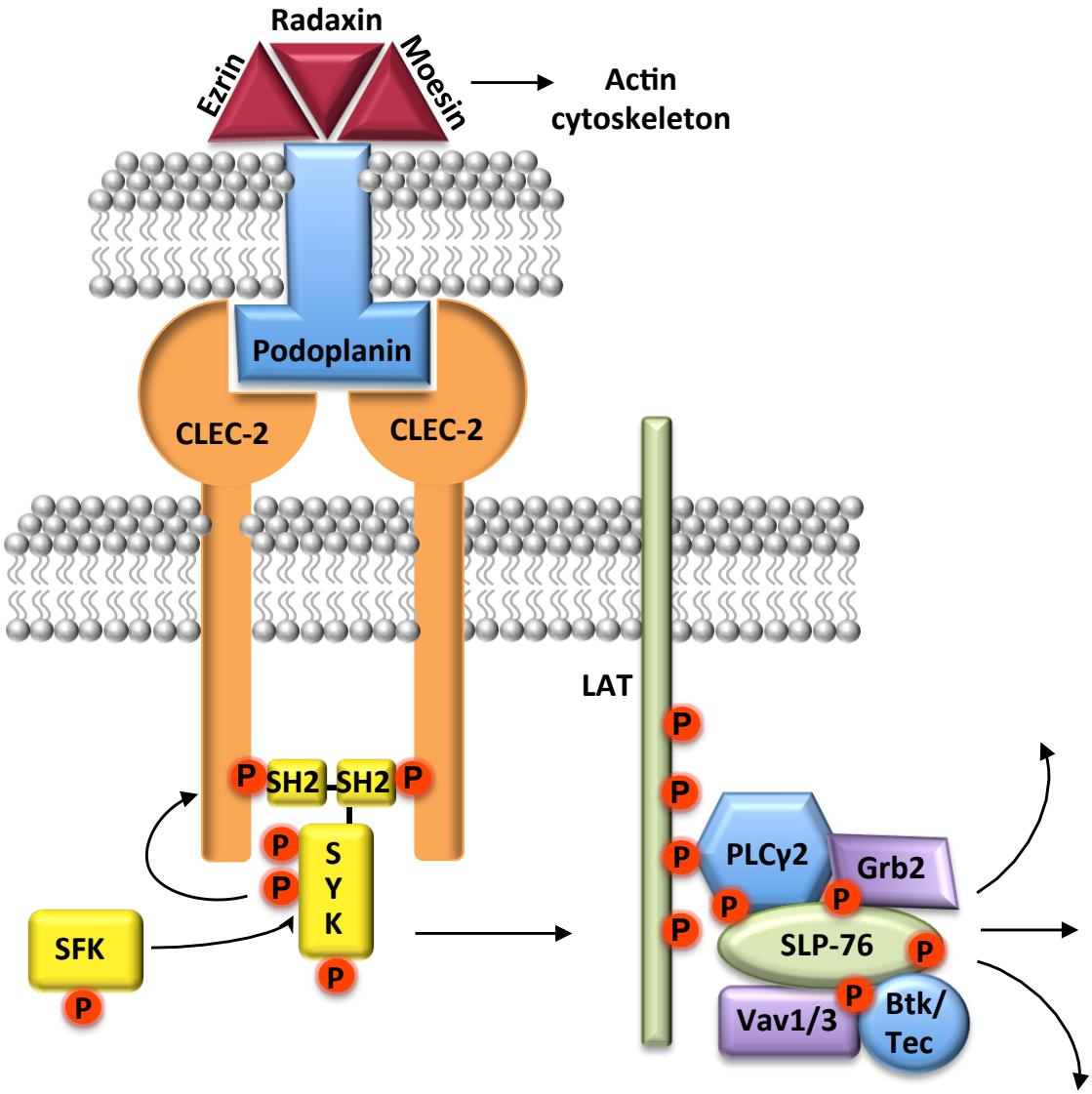

Figure 1.2. CLEC-2-podoplanin signalling axis. CLEC-2 interacts with podoplanin stimulating phosphorylation of the tyrosine kinase SYK, by SRC family kinases (SFKs). Activated SYK phosphorylates (P) the YxxL motifs in the CLEC-2 cytoplasmic tails, permitting their association with dimeric CLEC-2 through its tandem SH2 domains. A complex signaling pathway ensues involving the adaptor proteins LAT, SLP-76, Grb2, Tec family kinases, including Btk, and the Vav family of guanine exchange factors, which together support the activation of a number of effector molecules, including the enzyme PLCγ2, culminating in platelet activation. Meanwhile podoplanin signals through its short cytoplasmic tail through the interaction with the ezrin, radaxin & moeisin (ERM) family proteins, influencing actin cytoskeletal re-arrangements. *Figure reconstructed from* (S. P. Watson *et al*., 2010).

1.3 Podoplanin

1.3.1 Identification of podoplanin as a ligand for CLEC-2

Evidence for an endogenous ligand for CLEC-2 came from studies investigating the causative receptor mediating the viral capture of human immunodeficiency virus-1 (HIV-1) by platelets, found to be CLEC-2 (Chaipan *et al*., 2006). The capture of HIV-1 by CLEC-2 on platelets was independent of a viral envelope protein and was instead found to be a protein from the virus producing cell line, human embryonic kidney 293T (HEK-293T), incorporated during viral budding (Christou *et al*., 2008). Podoplanin was later identified on the surface of tumour cells as a potent inducer of platelet aggregation (Kato *et al*., 2003). Furthermore, induction of platelet aggregation was shown to rely on a key amino acid sequence within the highly glycosylated extracellular domain $(EDxxVTPG)_3$, designated the platelet aggregation (PLAG) stimulating domain (Kaneko *et al*., 2004). Independently, Suzuki-Inoue *et al* (2007) were able to show the ligand for podoplanin to be CLEC-2 by demonstrating that tumour cells induce platelet aggregation with similar kinetics to the exogenous ligand for CLEC-2, rhodocytin, and through a similar signalling pathway involving SRC and PLCγ2 (Suzuki-Inoue *et al*., 2007). Using podoplanin-expressing Chinese hamster ovary (CHO) cells they were able to confirm the interaction between CLEC-2 and podoplanin, and further show that lymphatic endothelial cells (LECs) that endogenously express podoplanin, were able to initiate platelet aggregation in a CLEC-2-dependent manner (Suzuki-Inoue *et al*., 2007). Following the identification of podoplanin as an endogenous ligand for CLEC-2, the HEK-293T protein ligand for CLEC-2 was also confirmed to be podoplanin, with an interaction affinity of 25 μM, as confirmed by surface plasmon resonance (Christou *et al*., 2008).

1.3.2 Tissue expression pattern of podoplanin

Podoplanin is a 36-43 kDa type-1 transmembrane glycoprotein first identified in kidney podocytes (Breiteneder-Geleff *et al*., 1997). Its expression is however widespread, with varying names connected to its pattern of discovery. It was identified on thymic epithelial cells and lymphoid fibroblastic reticular cells as gp38 (Farr *et al*., 1992), on alveolar type-1 epithelial cells, the cerebral choroid plexus, ciliary epithelium of the eye, oesophagus and intestine as T1α (M. C. Williams *et al*., 1996), on osteoblasts as 0TS-8 (Nose *et al*., 1990), on LECs as the E11 antigen (Wetterwald *et al*., 1996), on induced skin keratinocytes as PA2.26 (Scholl *et al*., 1999) and on tumour cells as the platelet aggregating protein, aggrus (Kato *et al*., 2003). Podoplanin has since been shown to be expressed on mucosal epithelial cells of the salivary glands (Hata *et al*., 2010), the myocardium, pericardium and epicardium of the heart (Mahtab *et al*., 2008; Gittenberger-De Groot *et al*., 2007) and on T-helper 17 (T_H17) cells and inflammatory macrophages (A. Peters *et al*., 2011; Hou *et al*., 2010; Kerrigan *et al*., 2012). However, the function of podoplanin in each of these tissues remains speculative.

During development, the expression pattern of podoplanin is more transient than in adulthood. In tissues such as the heart, brain, oesophagus, intestine and kidney, expression is high early in development (around embryonic day (E) 9.0), and becomes more spatially restricted in adulthood. For example, podoplanin is expressed throughout the central nervous system (CNS) at E9.0 and becomes restricted to the choroid plexus by mid-gestation. The opposite pattern is seen in the lung, where expression in early development is negligible, with a dramatic increase on alveolar type I cells by postnatal day (P)0 (M. C. Williams *et al*., 1996; Mahtab *et al*., 2008).

1.3.3 Podoplanin signalling

The extracellular domain of podoplanin is a highly glycosylated, rigid structure that makes up over 90% of its molecular weight. This is followed by a single transmembrane domain, leaving only a short 9 amino acid cytoplasmic tail for intracellular signalling (Cueni *et al*., 2010; Martin-Villar *et al*., 2006). Despite this, podoplanin is able to dynamically regulate cell motility through its interaction with ezrin-radaxin-moesin (ERM) family proteins, forming a bridge between the integral membrane surface and the actin cytoskeleton (Fehon *et al*., 2010; Martin-Villar *et al*., 2006) (*Figure 1.2*). Rho-dependent kinase phosophorylates ERM proteins, initiating a conformational change that exposes binding sites to permit their association with integral membrane proteins and F-actin (Bretscher *et al*., 2002). Overexpression of podoplanin is associated with increased phosphorylation of ERM proteins (Martin-Villar *et al*., 2006; Wicki *et al*., 2006). Furthermore, when upregulated in keratinocytes, podoplanin was shown to co-localise with ERM family proteins at filopodia and lamellipodia to mediate an increase in cell motility (Scholl *et al*., 1999). In cancer cell lines, up-regulation of podoplanin is associated with an increase in RhoA activity and the acquisition of a migratory phenotype. As expression of epithelial markers such as E-cadherin decrease, these cells undergo an epithelial to mesenchymal transition (EMT), during which they are transformed from non-invasive cells into having an invasive pro-migratory phenotype (Martin-Villar *et al*., 2006). Similarly, siRNA knockdown of podoplanin on LECs correlates with a decrease in RhoA expression (Navarro *et al*., 2008). Conversely, Wicki *et al* (2006) found that up-regulation of podoplanin led to a decrease in RhoA activity while still promoting tumour invasion. Furthermore, the acquisition of a migratory phenotype was in the absence of EMT (Wicki *et al*., 2006). In the absence of EMT, mucin-like proteins have been shown to increase the migratory properties of cells by masking adhesion receptors with their

extensive ectodomains, thereby inhibiting their function (Komatsu *et al*., 1997). These conflicting mechanisms likely reflect the multiple roles of podoplanin, depending on the cell type in which it is expressed.

1.3.4 Binding partners of podoplanin

Podoplanin has been shown to associate with transmembrane domains 1 and 2 of the tetraspanin CD9, through homophillic interactions. The full impact of this interaction remains to be explored, but has been shown to directly suppress the platelet aggregating ability of podoplanin (Nakazawa *et al*., 2008). The major hyaluronan receptor CD44 (otherwise known as Lyve-1) has also been found as a novel binding partner for podoplanin. During EMT in cancer cell lines, podoplanin and CD44 are mutually upregulated and co-associate at cell protrusions to mediate cell migration (Martín-Villar *et al*., 2010).

1.3.5 Other endogenous ligands for podoplanin

Given the vast expression pattern of podoplanin and the highly restricted expression of CLEC-2, it is feasible to assume a number of ligands exist for podoplanin, which, in time, will unravel its physiological role and function. Two such ligands have been identified, galectin-8 and CCL21, whose interaction with the podoplanin ectodomain is glycosylation dependent. Galectin-8 is highly expressed on LECs, where it promotes LEC migration and adhesion. Physiologically, galectin-8 is suggested to associate with podoplanin on lymphatic endothelium and promote its association with the extracellular matrix (ECM) (Cueni & Detmar, 2009). CCL21 is a lymphatic specific chemokine and although the significance of its association with podoplanin is unknown, its expression on LECs and fibroblastic reticular cells gives interesting potential in light of recent studies demonstrating a role for podoplanin in the trafficking of DCs to lymph nodes (Kerjaschki

et al., 2004; Acton *et al*., 2012).

1.4 Podoplanin and CLEC-2 in the development of the lymphatic vasculature

(Refer to *Table 1.1* for summary)

Nearly two decades ago, mice deficient in the tyrosine kinase SYK were shown to present with subcutaneous haemorrhaging in the skin and oedema throughout the back at E14.5 (Turner *et al*., 1995; Cheng *et al*., 1995). The same phenotype was observed in mice deficient in the adaptor protein SLP-76 (Clements, 1998; Clements *et al*., 1999; Pivniouk *et al*., 1998) and the effector enzyme PLCγ2 (Wang *et al*., 2000). This phenotype was later shown to result from defective lymphatic function, attributable to erroneous connections between the blood and lymphatic circulations (Abtahian *et al*., 2003; Ichise *et al*., 2008). In the same time frame, mice deficient in podoplanin were generated and found to die at birth due to respiratory failure (Ramirez *et al*., 2003). Pups also developed severe lymphedema at birth resulting from impaired lymphatic drainage (Schacht *et al*., 2003) and were later shown to harbour blood filled lymphatic vessels in the skin and gut (Fu *et al*., 2008). CLEC-2-deficient mice were further shown to die within the first postnatal week, attributable to impaired lung inflation (Finney *et al*., 2012). Embryonic studies found both CLEC-2- and podoplanin-deficient mice to harbour the characteristic phenotype of blood-filled lymphatic vessels in the skin from E13.5 and oedema in the back and limbs, phenocopying SYK-, SLP-76- and PLCγ2-deficient mice (Suzuki-Inoue *et al*., 2010; Bertozzi, Schmaier, *et al*., 2010b). All surviving podoplanin, CLEC-2-, SYK-, SLP-76- and PLCγ2-deficient pups developed chylous ascites in the abdomen, further highlighting impaired lymphatic function, with many dying in the early postnatal period. The glycosylation of the podoplanin extracellular domain is dependent on the activity of a

key glycosyltransferase enzyme T-synthase, which catalyses the biosynthesis of O-glycans. Mice constitutively deficient in T-synthase are embryonic lethal by E14.5, while endothelial specific deletion (*Tie2-Cre*) results in the characteristic blood-filled lymphatic phenotype (Xia *et al*., 2004; Fu *et al*., 2008). The requirement for podoplanin expression specifically on the endothelium is shown in Tie2-Cre transgenic mice, which exhibit blood-filled lymphatic vessels, while no phenotype is observed in radiation chimeric mice reconstituted with podoplanin-deficient fetal liver (Bertozzi, Schmaier, *et al*., 2010b; Herzog *et al*., 2013). These data support a role for the podoplanin on the endothelium with a specific requirement for its glycosylated extracellular domain.

1.4.1 Identifying the CLEC-2-expressing cell type

The group of Mark Kahn initially pinpointed the activity of SYK and SLP-76 signalling in a circulating cell to be involved in the defective separation of the blood and lymphatic vasculatures, later suggesting this to be a bone marrow-derived circulating lymphatic endothelial progenitor cell (Abtahian *et al*., 2003; Sebzda *et al*., 2006). Lineage tracing studies later identified cells of the myeloid lineage, within the haematopoietic compartment, to be the causative cell type (Bohmer *et al*., 2010). This was supported through the generation of a range of cell-specific Cre deleters, showing that mice deficient in SLP-76 or SYK in the haematopoietic lineage (*Vavi-Cre*), and not in endothelial cells (*Tie2-Cre*), present with the characteristic blood-filled lymphatic phenotype, albeit this phenotype was of varying severity with a low level of perinatal mortality (Finney *et al*., 2012; Bertozzi, Schmaier, *et al*., 2010b). Furthermore, a role for SYK in macrophages, T- and B-lymphocytes was eliminated, while the loss of CLEC-2, SYK and SLP-76 in the megakaryocyte/platelet lineage (*PF4-Cre*) was shown to be indispensable for blood-lymphatic separation (Finney *et al*., 2012; Bertozzi, Schmaier, *et al*., 2010b). The severity

of the phenotype resulting from *PF4-Cre*–mediated deletion of CLEC-2, SYK or SLP-76 was variable, mimicking that seen using the *Vavi-Cre* transgene, and is suggested to be attributable to the onset of Cre activity. Although Bertozzi *et al* (2010) find the activity of the *PF4-Cre* transgene to be specific to the megakaryocyte/platelet lineage, other studies suggest this not to be the case, opening up the possibility for the contribution of another haematopoietic lineage (Calaminus *et al*., 2012; Bertozzi, Schmaier, *et al*., 2010b). However, a role for platelets is supported by the description of a blood-lymphatic mixing phenotype in mice lacking functional megakaryocytes, owing to a deficiency in the transcription factor Meis-1, following selective ablation of the megakaryocyte/platelet lineage using diphtheria toxin, or through treating with the anti-platelet agent aspirin (Carramolino *et al*., 2010; Uhrin *et al*., 2010). Furthermore, the contribution of platelet-specific effects over contributions by megakaryocytes is shown in the development of blood-lymphatic mixing in the intestines of radiation chimeric mice reconstituted with SYK-, SLP-76-, PLCγ2- or CLEC-2-deficient bone marrow, where the numbers of circulating megakaryocytes are negligible (Bertozzi, Schmaier, *et al*., 2010b; Finney *et al*., 2012; Ichise *et al*., 2008).

Table 1.1. Mouse models portraying blood-lymphatic separation defects

Reference	Background	Lethality	Reported phenotype
CLEC-2			
Tang ***et al*** (2010)	C57BL/6*	The majority of pups die in the first postnatal weeks	Subcutaneous haemorrhages throughout the embryo at E13.0. Haemorrhages in the developing brain at E12.0
Bertozzi ***et al*** (2010)	C57BL/6; 129sv	100% lethality within the first postnatal weeks	Blood-filled lymphatic vessels at E14.5. Oedema through the back and limbs. Reduced airspaces in the lungs. Chylous ascites in the abdomen of pups
Suzuki Inoue ***et al*** (2010)	C57BL/6*	Mendelian up to E15.5, majority of pups die at birth, 99.4% lethality at 8 weeks	Blood filled lymphatic vessels at E13.5. Oedema in the back
Finney ***et al*** (2012)	C57BL/6*	Mendelian up to P0, the majority of pups die at birth, 98.6% lethality at 4 weeks	Blood-filled lymphatic vessels at E14.5. Oedema through the back and limbs. Reduced airspaces in the lungs. Chylous ascites in the abdomen of pups. Haemorrhaging in the brain at E12.5
Podoplanin			
Ramirez ***et al*** (2003) Schacht ***et al*** (2003) Fu ***et al*** (2008)	129sv*	Mendelian up to P0. 100% lethality within 4 hours	Death due to respiratory failure. Impaired formation of alveolar spaces. Oedema in the limbs of neonates. Blood-filled lymphatic vessels
Bertozzi ***et al*** (2010)	C57BL/6; 129sv		Blood-filled lymphatic sacs and cutaneous vessels at E11.5 and E14.5, respectively. Oedema through the back at E14.5. Chylous ascites in the small intestine of neonates
Mahtab ***et al*** (2008)	129sv; Swiss	40% lethality by E16.5 and 50% lethality within 1 week	Myocardial pathology related to reduced epithelial to mesenchymal transitions
Uhrin ***et al*** (2010)	C57BL/6	55% lethality within 1 week. 20% had a normal life span	Blood-filled cutaneous lymphatic vessels at E13.5. Chylous ascites in the small intestine of neonates

T-synthase	***C1galt1***		
Xia ***et al*** (2004)	C57BL/6*	100% lethality by E14.5	Haemorrhaging in the central nervous system at E12.0 (See text on lineage specific deletions).
SYK			
Turner ***et al*** (1995)	$(B6D2)F_1$*	Mendelian up to E18.5. Only 1 pup survived >3 weeks	Subcutaneous haemorrhages throughout embryo at E16.5 in 45% of knockouts. Chylous ascites in the small intestine.
Cheng ***et al*** (1995)		Majority of pups die by P1, all pups die within 3 weeks	Subcutaneous haemorrhages throughout the embryo at E14.5 Oedema in the limbs at E14.5 and in neonates.
SLP-76			
Clements at al (1998) Clements ***et al*** (1999)	C57BL/6*	Mendelian up to P0. Majority of pups die by P7	Subcutaneous haemorrhages throughout the embryo. Bleeding in abdominal cavity of neonates.
Pivniouk ***et al*** (1998)		Majority of pups die by P7	Subcutaneous haemorrhages, swollen footpads and bleeding in abdominal cavity of pups
PLCγ2			
Wang ***et al*** (2000)	C57BL/6*	Mendelian up to E19.0. One third of pups die at birth	Subcutaneous haemorrhages at E12.0. Bleeding in the small intestine and the abdominal cavity.
Ishise ***et al*** (2009)	C57BL/6; 129Sv		Blood-filled lymphatic sacs at E13.5. Adults have blood-lymphatic shunts in the intestine, heart, diaphragm and skin and chylous ascites in the abdomen
* No detail into the number of backcrosses is given			

1.4.2 Function and development of the lymphatic system

The primary function of the lymphatic system is to regulate tissue homeostasis, lipid absorption and facilitate immune cell trafficking (*Figure 1.5*). Fluid from lymphatic vessels drains into the venous system through either one of only two points of contact with the subclavian vein, the thoracic duct and the right lymphatic vein, both of which encompass bicuspid lympho-venous valves to prevent backflow into the venous system, reviewed in (Tammela & Alitalo, 2010; Schulte-Merker *et al*., 2011). It was suggested in 1902 that the lymphatic system develops from the venous system, which has since been confirmed by lineage tracing studies (Srinivasan *et al*., 2007). The current mechanism underlying the initial specification of the lymphatic system is complex and involves over 20 genes, reviewed in (Tammela & Alitalo, 2010; Schulte-Merker *et al*., 2011). Briefly, lymphatic progenitor cells can be detected at the cardinal vein at E10.0 by the activity of the transcription factor Sox18, which induces expression of prox-1, both of which are indispensible for lymphatic specification and function (François *et al*., 2008; Wigle *et al*., 2002). Prox-1-expressing lymphatic progenitor cells migrate from the dorsal side of the cardinal vein as a polarised stream of cells that rapidly acquire a pro-migratory phenotype. This is dependent on the expression of vascular endothelial growth factor receptor 3 (VEGFR-3), its co-receptor neuropilin-2 (Nrp-2) and the presence of the growth factor VEGF-C (Xu *et al*., 2010; Dumont *et al*., 1998; Karkkainen *et al*., 2003). From E11.0, these 'immature' LECs, now expressing podoplanin, rapidly coalesce to form a luminised vessel from which the superficial lymphatic vessels develop, further differentiating into dermal lymphatics in the skin from E12.0. Simultaneously, the primary thoracic duct forms adjacent to the cardinal vein from a subset of aggregating LECs (Hägerling *et al*., 2013; Yang *et al*., 2012).

1.4.3 Unraveling the mechanism behind the blood-lymphatic mixing phenotype

The mechanism by which podoplanin on LECs interacts with and induces signalling in a CLEC-2-expressing cell to mediate blood and lymphatic vessel separation remains controversial. Direct interactions between platelets and newly specified LECs at the cardinal vein at E11.5 were initially proposed to 'clot off' and aid the budding of primary lymphatic structures (Uhrin *et al*., 2010; Bertozzi, Hess, *et al*., 2010a). This was disputed because of the presence of blood-filled lymphatic shunts in adult radiation chimeric mice reconstituted with CLEC-2- or SYK-deficient bone marrow, in which the lymphatic system is already developed (Bertozzi, Schmaier, *et al*., 2010b; Finney *et al*., 2012). The requirement for platelet aggregation is disputed because of the presence of a non-separation phenotype in mice lacking the gene kindlin-3, essential for platelet aggregation, while no requirement was found for the major platelet integrin αIIβ3 (Hodivala-Dilke *et al*., 1999; Uhrin *et al*., 2010). Recently, it was proposed that podoplanin-induced CLEC-2 signalling in platelets stimulates thrombus formation at the joining of the thoracic duct and subclavian vein. This interaction was shown to be required throughout development and adulthood to prevent backflow of lymphatic fluid into the venous system. However, no explanation as to how a thrombus can prevent backflow while permitting flow through from the lymphatic system was provided (Hess *et al*., 2014). Alternatively, any of the vast array of bioactive molecules and growth factors released from platelet secretory granules upon their activation could influence LEC behaviour (Suzuki-Inoue, 2011). Finney *et al* (2012) observed an inhibition in LEC migration when crosslinking podoplanin, which may result from a direct effect, the effect of a secretory molecule, or from podoplanin signalling within the LEC, whereby the CLEC-2 interaction is suggested to induce receptor clustering to sustain or enhance signalling events (Finney *et al*., 2012).

1.5 Podoplanin and CLEC-2 in the development of cerebral haemorrhages

In addition to the blood-filled lymphatic phenotype, mice deficient in CLEC-2 or SYK are reported to develop haemorrhages within the CNS. In CLEC-2-deficient embryos, multiple haemorrhages were first reported in the midbrain parenchyma from E12.0 (Tang *et al*., 2010). Similar findings were reported by Finney *et al* (2012) at E12.5, although haemorrhages appeared more severe (Finney *et al*., 2012). In the initial paper describing a SYK-deficient mouse, brain haemorrhages were visible in embryos at E14.0, yet they were not reported in the text (Cheng *et al*., 1995). Later, characterisation of these embryos by our group showed that these haemorrhages were consistently present from E12.0, but appeared less severe than in CLEC-2-deficient embryos. Furthermore, haemorrhages were also observed in megakaryocyte/platelet specific CLEC-2- and SYK-deficient mice, although they were less severe (Finney *et al*., 2012). Haemorrhages in the CNS have never been reported in podoplanin-deficient mice, yet the loss of T-synthase caused severe haemorrhaging through the brain parenchyma, ventricles and spinal column between E12.0-E14.0, with mice perishing by E14.0 (Xia *et al*., 2004). These haemorrhages were not observed in endothelial specific T-synthase deficient mice, suggesting the involvement of podoplanin, or another substrate, on a different cell type (Fu *et al*., 2008).

1.5.1 Podoplanin expression in the CNS through development

The expression of podoplanin on the choroid plexus at E16.5 is well documented (M. C. Williams *et al*., 1996; Kaji *et al*., 2012), albeit its function on this structure, which forms the blood-cerebrospinal fluid (CSF) barrier, is not known. Williams *et al* (1996) detected

podoplanin mRNA in the neural tube at E13.5 and visualised podoplanin expression diffusely through the neural tube by immunohistochemistry, with increased expression on cells close to the ventricular lumen between E13.0-E15.0 (M. C. Williams *et al*., 1996). Podoplanin was later shown to be expressed throughout the neural tube at E10.5 by immunofluoresence, yet the specific cell type and function remains unknown (Schacht *et al*., 2003).

1.6 Development of the mouse brain

The development of the nervous system is a highly complex process, involving the simultaneous, highly regulated expression of thousands of genes. The spatio-temporal pattern of gene expression allows a multitude of different structures to develop alongside one another, culminating in the formation of a highly specialised, functional nervous system (Liscovitch & Chechik, 2013).

1.6.1 Development of the neural tube and ventricular system

In the early stages of embryogenesis, a double-layered structure is formed termed the 'primitive streak stage embryo', consisting of an inner layer of ectoderm cells enclosing the pro-amniotic canal, surrounded by a mesoderm layer and outer endoderm layer. A critical 'turning' step is required to re-organise the layers such that the ectodermally-derived neural plate becomes situated at the outer aspect of the embryo, while the endodermally derived gastro-intestinal tract becomes centrally located. The amniotic canal inverts to form the characteristic sac surrounding a now fetal-like embryo (*Figure 1.3A*), reviewed in (Kaufman, 1992).

The neural plate is an unpatterned, undifferentiated primordium that through the process of neuralation will go on to form the brain and spinal cord. At around E8.0, bilateral folds develop in the neural plate at its junction with the surrounding non-neural ectodermal layer that fuses to form the neural tube (*Figure 1.3B*) (Copp *et al*., 2003; Greene & Copp, 2009). Between E8.5-9.0 neural folds overlaying the primitive fore-, mid- and hindbrain appose and subsequently fuse at either end to form vesicles, the walls of which form the prosencephalon, mesencephalon and rhombencephalon, respectively. Between E9.0-10.0, the primitive forebrain vesicle expands, culminating in the subdivision of the prosencephalon into the diencephalon and the telencaephalon (*Figure 1.3C*). Within the telencephalon, two telenphalic vesicles develop, encompassing the lateral ventricles connected to the third ventricle within the developing diencephalon by a canal named the intraventricular foramen. Within the mesencephalon, the cerebral aqueduct forms connecting the lateral and third ventricles to the developing fourth ventricle within the rhombencephalon. As development progresses, the telencephalon subdivides into the cerebral cortex, the caudate putamen and the palidium. Several thalmic structures develop within the diencephalon, including the thalamus and hypothalamus. The substantia nigra develops within the primitive midbrain (mesencephalon), and the pons, cerebellum and medulla oblongata are differentiated within the developing hindbrain (*Figure 1.3D*) (Kaufman, 1992; C. Watson *et al*., 2012).

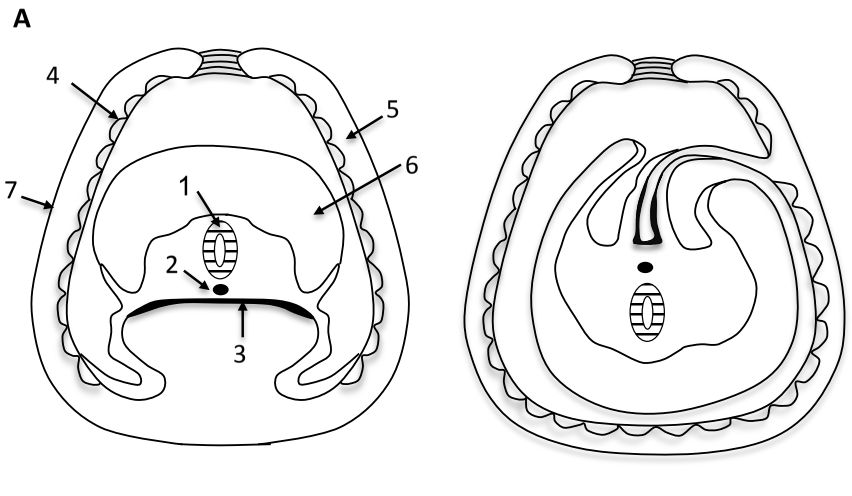
A
4
5
6
7
1
2
3

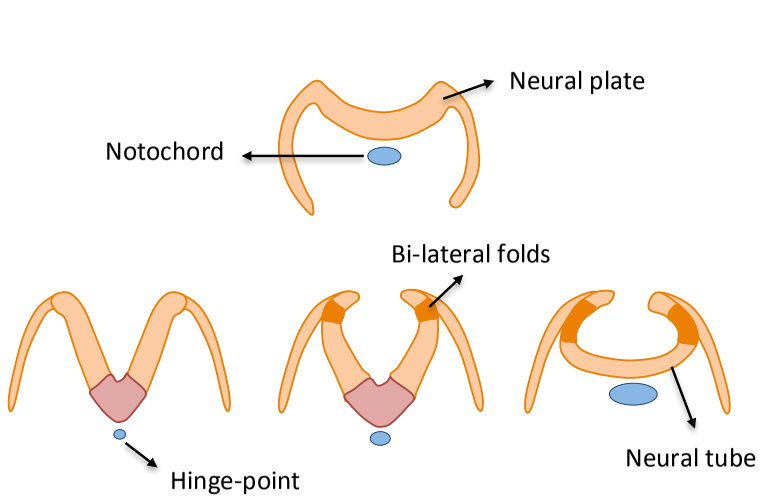
B
Neural plate
Notochord
Bi-lateral folds
Hinge-point
Neural tube

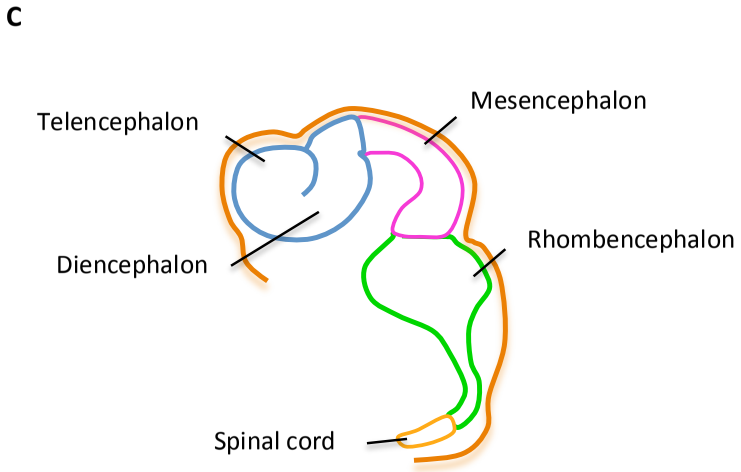
C
Telencephalon
Mesencephalon
Diencephalon
Rhombencephalon
Spinal cord

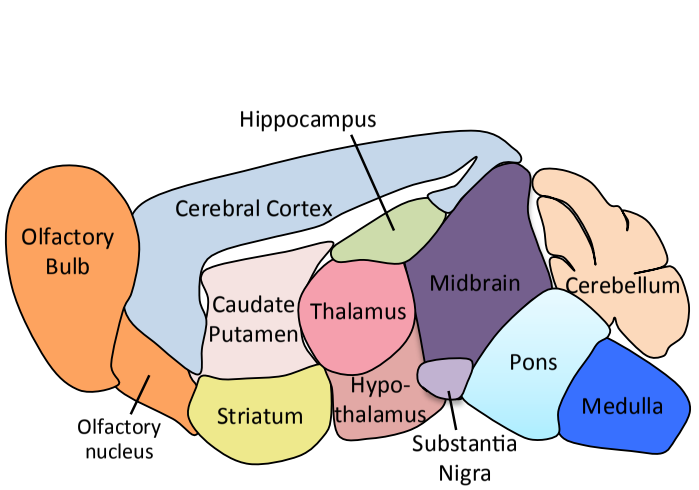
D
Hippocampus
Cerebral Cortex
Olfactory Bulb
Caudate Putamen
Thalamus
Midbrain
Cerebellum
Pons
Medulla
Striatum
Hypo-thalamus
Olfactory nucleus
Substantia Nigra

Figure 1.3. Development of the CNS. (**A**) A simplified diagram to illustrate the beginning and end point of embryonic 'turning' visualised as vertical sections looking towards the caudal aspect of the embryo. 1, neural tube (ectoderm); 2, notochord; 3, prospective midgut endoderm; 4, yolk sac; 5, yolk sac cavity; 6, amniotic cavity; 7, endoderm layer. *Reconstructed from* (Kaufman, 1992). (**B**) Neural tube formation from the neural plate. *Reconstructed from* (Copp *et al*., 2003). As development progresses the primitive fore-, mid- and hindbrain regions are formed (**C**) which are further differentiated into their unique structured compartments (**D**). *Reconstructed from* (C. Watson *et al*., 2012).

1.6.2 Neuro-epithelial cell fate

Prior to the onset of neurogenesis, the neural tube consists of a single layer of neuro-epithelial cells. This neuro-epithelium has characteristic epithelial properties in that it is highly polarised and pseudostratified. The term stem cell can only be loosely associated with neuro-epithelial cells because their ability to self-renew is often restricted to a limited time and they have an undefined uni- or multi-potency.

Subsequent to the onset of neurogenesis, a multi-layered neuro-epithelium is formed with a dense progenitor cell layer forming adjacent to the apical ventricular wall, termed the ventricular zone. This region is abundant in neuro-epithelial-derived radial glial cells (*Figure 1.4*). Characteristically, radial glial cells maintain some neuro-epithelial cell properties, such as their apical to basal polarity, the association of the zonula occludin protein 1 (ZO-1) with apical adherens junctions and the expression of the intermediate filament protein, nestin. Conversely, radial glial cells adopt some astroglial properties, expressing the glial fibrillary acidic protein, GFAP. Radial glial cells differ from neuro-epithelial cells in that their progeny are fate-restricted to form neurons or glial cells, such as astrocytes, oligodendrocytes or ependymal cells (*Figure 1.4*). Astrocytes have a multitude of functions in the brain, providing structural support at the blood-brain barrier and assisting in synaptic transmission through their close association with the surrounding neurons. Oligodendrocytes form the basis of the myelin sheath, an electrical insulation layer surrounding the axons of the CNS. Ependymal cells line the ventricle walls and the choroid plexus, where their apical surface is abundant in cilia to promote the circulation of CSF (*Figure 1.4*). Between E10.0 and E12.0, most neuro-epithelial cells within the brain will become radial glial cells. In contrast, neuro-epithelial cells of the retina and spinal cord are less fate-restricted, since they retain some neuro-epithelial cell characteristics.

A second important progenitor of neuro-epithelial cells is the basal progenitor cell. Following cell division, basal progenitors migrate away from the ventricular zone to form a second germinal layer named the sub-ventricular zone, providing an important source of neurons. Reviewed in (Götz & Huttner, 2005; Farkas & Huttner, 2008).

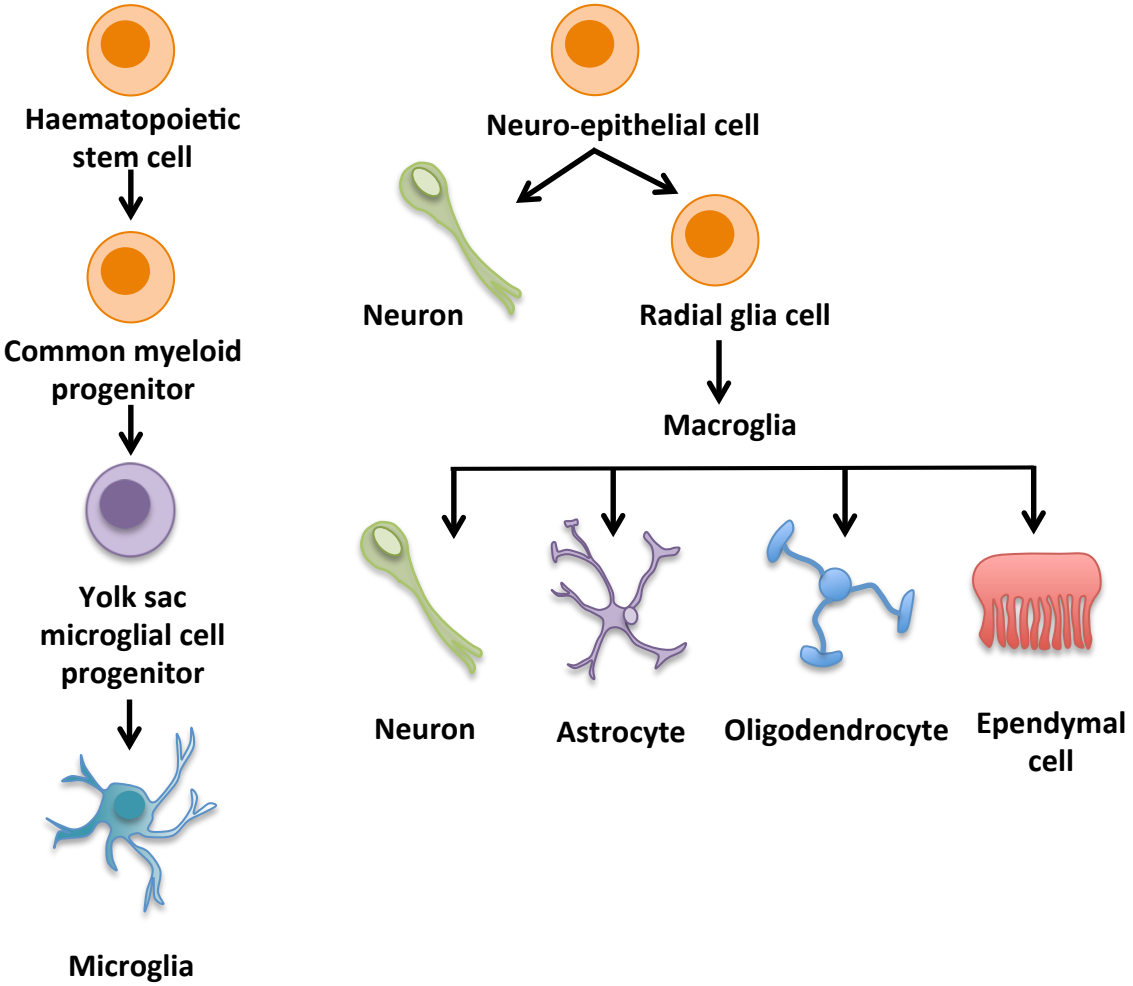

Figure 1.4. Cell lineages within the CNS parenchyma. Microglia are the only haematopoietic cells found in the parenchyma of the CNS in the steady state. On entering neurogenesis, neuro-epithelial cells can differentiate into neurons or the more fate-restricted progenitors, radial glial cells, which give rise to neurons, astrocytes, oligodendrocytes or ependymal cells. *Reconstructed from* (Ransohoff & Cardona, 2010).

1.6.3 Development of the cerebral vascular system

The cardiovascular system is the first functional organ system to develop, with the first mesodermally derived 'haemangioblasts' emerging around E7.0. Haemangioblasts are said to be common precursor cells that migrate to the mesoderm where they differentiate to form haematopoietic stems cells or angioblasts (non-lumenised vascular endothelial cell precursors). During differentiation, blood islands are formed, consisting of an inner core of haematopoietic cells surrounded by clusters of endothelial cells. By E8.0, a primitive vascular network is formed by the coalescence of neighbouring blood islands to form the heart, dorsal aorta and the yolk sac plexus, which subsequently remodel to form a complex vascular tree (Marcelo *et al*., 2013; Anon, 1998; Kaufman, 1992). Meanwhile, some angioblasts can migrate to distant sites to commence the vasculogenesis of organs, such as the formation of the perineural vascular plexus (PNVP) that surrounds the neural tube and the spinal cord between E8.5-E9.5, where it provides essential nutrients and oxygen to developing neural tissue (Walls *et al*., 2008).

The brain is distinct from most other organs in that the entire vascularisation of the neural tube subsequent to the formation of the PNVP is derived through angiogenesis. Angiogenesis is distinct from vasculogenesis in that new vessels are formed by sprouting, bridging and intussuscepted growth from existing vessels, which can all occur concurrently (Jain, 2003). In the brain, angiogenesis occurs predominantly through sprouting angiogenesis due to the absence of pre-existing angioblasts in the neural tissue itself (Risau, 1997). The first blood vessels invade the neural tube around E10.0, stimulated by a multitude of signalling pathways. VEGF is highly expressed in the ventricular zone where it is shown to provide an important signal to stimulate the migration of invading capillaries from the PNVP along the pre-formed lattice network of

neuro-epithelial cells (Breier & Risau, 1996; Walls *et al*., 2008). The Wnt-β-catenin pathway also plays an important role in CNS specific angiogenesis. Wnt ligands are released from the neuro-epithelium and bind to endothelial cells to influence the transcription of genes involved in angiogenesis through the stabilisation of the intracellular signal transducer, β-catenin. Inhibition of Wnt or β-catenin results in impaired invasion of endothelial cells into the neural tube from the PNVP, culminating in widespread cerebral haemorrhaging by E12.5 (Daneman *et al*., 2009; Stenman *et al*., 2008). The role of Wnt-β-catenin signalling has also been shown to be important post-natally in maintaining the integrity of tight junctions between cerebral endothelial cells (Liebner *et al*., 2008).

1.6.4 Development of the blood-brain barrier (BBB)

The formation of the blood-brain barrier (BBB) is a complex multi-step pathway, whereby nascent angiogenic vessels are transformed into a structurally supported and functional vascular network. As nascent angiogenic vessels form they are characteristically 'leaky', since their formation relies on the degradation of the existing ECM by matrix metalloproteases in order to free endothelial cells so that they can migrate and proliferate to form new lumenised vessel tubes (Winkler *et al*., 2011). Their transformation into a functional vascular network requires the recruitment of a wide range of ECM proteins forming a basement membrane coat over the albuminal vessel wall. Among the ECM proteins are integrins that mediate the adhesion, migration and the organisation of cells to the vessel wall (Proctor *et al*., 2005). Among these cells are mural cells which include vascular smooth muscle cells and pericytes, both of which are perivascular cells of mesenchymal origin and to date cannot be definitively distinguished from one another but

are instead identified on the basis of their location and protein expression. In general, vascular smooth muscle cells predominantly line the larger arteries and veins, while pericytes function to support smaller arterioles, capillaries and venules. Pericytes overlay endothelial cell junctions and their processes intimately associate with the underlying basement membrane, providing structural support. The density of pericytes is highest in the cerebral vasculature highlighting their critical role in supporting vascular integrity, reviewed in (Armulik *et al*., 2010). The ensheathed vessel is then coated in astrocytes, neurons and microglia to form what is referred to as the neurovascular unit (NVU). The NVU is a tightly regulated interface between the CNS and the circulation that forms the basis of a functional BBB. The NVU critically enables efficient nutrient and oxygen exchange through the CNS to establish proper brain function (Hawkins & Davis, 2005). A number of key molecules and signalling pathways which regulate the recruitment, association and proliferation of mural cells to the developing cerebral vasculature will be discussed, since their disruption often leads to extensive haemorrhaging and embryonic lethality.

1.6.4.1 Integrins

To date, only integrins containing subunits β8 or α5 have been shown to be specifically involved in cerebral vascular development, where their loss results in severe haemorrhage and neonatal death. No gross abnormalities in brain development or in the initial angiogenic endothelial cell proliferation, migration and sprouting were observed. Instead, cerebral haemorrhage results from the severe distension and aberrant patterning of vessels resulting in their 'leakiness' (McCarty *et al*., 2002; Bader *et al*., 1998; Zhu *et al*., 2002). Furthermore, deletion of integrin β8 specifically from the neuro-epithelium (driven by the *Nestin-Cre8* promoter) results in altered capillary morphology and cerebral haemorrhage,

proposed to result from aberrant connections between capillaries and the surrounding neuro-epithelial cells and glial cells (Proctor *et al*., 2005). Integrin α5β8 is also expressed on astrocytic processes where it activates transforming growth factor β (TGFβ) which acts on endothelial cells to influence the transcription of anti-angiogenic factors (Cambier *et al*., 2005).

1.6.4.2 Tyrosine kinase pathways

The receptor tyrosine kinase family are fundamental to the formation of a secure cerebral vascular network. Of specific relevance are the VEGF-VEGFR-1 and -2 axis and the angiopoietin (Ang)-Tie receptor axes. Mice deficient in Tie2, which is expressed throughout the developing vasculature, die at E9.5 resulting from impaired survival and maturation of angiogenic endothelial cells (Dumont *et al*., 1994; Sato *et al*., 1995). The lethality is prior to the development of the cerebral vasculature, however, the loss of Tie1, for which the expression is later, results in widespread cerebral haemorrhage by E13.0, thought to result from the defective integrity of the angiogenic derived microvasculature (Puri *et al*., 1995; Partanen *et al*., 1996). Such defects are subsequent to those seen in mice deficient in VEGFR-1 and VEGFR-2, where defects arise during early vasculogenesis resulting in lethality between E8.5-9.5 (Ferrara *et al*., 1996).

1.6.4.3 Platelet derived growth factor β (PDGFβ)

The platelet derived growth factor β (PDGFβ)-PDGFβ receptor (PDGFRβ) axis is involved in the recruitment, proliferation and longitudinal spreading of mural cells across vessels. Pericytes express PDGFRβ allowing them to migrate towards endothelial cells that actively secrete PDGFβ. PDGFRβ$^{-/-}$ mice fail to recruit pericytes to nascent blood vessels, leading to endothelial hyperplasia and aberrant morphology and architecture of

the microvasculature, culminating in embryonic lethality. Importantly, the density, length and branching of vessels was unchanged, showing that the PDGFβ-PDGFRβ axis functions after the formation of a primitive vascular network (Hellström *et al*., 2001).

1.6.4.4 Sphingosine-1-Phosphate (S1-P)

Sphingosine-1phosphate (S1-P) is a blood borne bioactive lipid stored at a high concentration in platelets and secreted upon platelet activation. Sphingosine is generated from ceramide and further phosphorylated by sphingosine kinases (SPK) 1 and 2. S1-P binds to a family of G protein-coupled receptors, the endothelial differentiation gene (Edg) family, referred to as S1-P receptors (S1PRs). S1PRs 1-3 are widely expressed, including on embryonic endothelial cells and have roles in directing growth, survival, migration and morphogenesis. S1PRs 4 and 5 have a more restrictive expression pattern, on lymphoid tissue or lung and in the CNS, respectively, reviewed in (Gaengel *et al*., 2009). Deletion of $S1PR_1$ results in extensive haemorrhaging and embryonic lethality between E12.5 and E14.5, thought to be due to the defective recruitment of mural cells to developing vessels (Liu *et al*., 2000). This defect was later shown to specifically involve $S1PR_1$ expression on endothelial cells (Allende *et al*., 2003). Furthermore, whereas the loss of $S1PR_2$ and $S1PR_3$ alone exhibit no phenotypic abnormalities, the loss of $S1PRs_{1-3}$ exacerbate the phenotype, highlighting their co-operative functions in stabilising the developing vasculature (Kono *et al*., 2014). Interestingly, the loss of SPKs 1 and 2 was shown to eliminate circulating S1-P levels and caused severe defects in neurogenesis and in cerebral angiogenesis, as shown by delayed neural tube closure and haemorrhaging in the brain and spinal cord at E11.5. The cerebral phenotype is more severe than that seen in $S1PR_1$ -deficient mice, suggesting the involvement of additional S1PRs (Mizugishi *et al*., 2005). However, the distribution and function of S1PRs in the brain is largely

uncharacterised, with the majority of work based on *in vitro* studies that demonstrate multiple functions for S1PRs, including in the growth and survival of oligodendorocytes and in the activity of hippocampal neurons, reviewed in (Bryan *et al*., 2008). Consequently, a mechanistic role for S1-P in neurogenesis has not yet been investigated.

1.6.5 Connections between the nervous and blood vascular system

It has long been recognised that the vascular and nervous systems are intricately connected, both through observations of their perfect overlay and the functional requirement for the vascular system to provide oxygen and nutrients, while the nervous system controls vascular tone and blood flow, reviewed in (Tam & Watts, 2010; Chauvet *et al*., 2013). From a developmental aspect, the patterning of nerves is driven by a unique axon 'growth cone' that forms at the leading edge of migrating neurons. The axon 'growth cone' has a distinct morphology that has been shown to be remarkably similar to structures identified on the terminal end of migrating blood vessels, 'tip cells'. Both are rich in lamellipodia and filopodia and respond to an array of environmental factors to guide their growth (de Castro *et al*., 2007; Gerhardt *et al*., 2003). While the role of VEGFs/VEGFRs are critical in guiding developing capillaries (Ruhrberg *et al*., 2002), endothelial tip cells also respond to a range of neural guidance signals, including the Slit/Robo, semaphorin/plexin/neuropilin, Netrin/Unc5/DCC and Ephrin/Eph signalling axes, reviewed in (Chauvet *et al*., 2013; Tam & Watts, 2010). Briefly, neuropilin-1 (Nrp-1) is an axon guidance molecule expressed on neurons and endothelial cells where it can act as a co-receptor for VEGFR2. In Nrp-1 deficient mice, while blood vessels can extend into the neural tube from the PNVP to the sub-ventricular zone (albeit this is delayed from E9.0 to E10.0), they experience defects in tip cell guidance and sprouting resulting in

aberrant vessel patterning and lethality by E13.0 (Kawasaki *et al*., 1999; Gerhardt *et al*., 2004; Fantin *et al*., 2013).

1.6.6 Maintenance of the blood-brain barrier

Once formed, the BBB constitutes a unique interface between the circulation and the CNS. Its key function is to control leukocyte trafficking and the passage of molecules and ions across the endothelium. Although the BBB exists at all levels of the CNS vascular tree, environmental factors influence vessel function, for example, capillaries adjacent to neurons become specialised in nutrient transport, while post-capillary venules protruding into perivascular spaces adapt to regulate leukocyte trafficking. Despite this, the fundamental principles of a functional BBB are conserved, where endothelial cells are sealed together by tight junctions (e.g. claudins, occludins and ZO-1), adherens junctions (e.g. VE-cadherin) and junctional adhesion molecules. This endothelial barrier is overlaid with the multiple cellular components that constitute the NVU. Many studies have shown that disrupting the intimate associations within the NVU leads to BBB permeability and is associated with a range of neurological disorders, including ischemic stroke, multiple sclerosis (MS), Alzheimer's disease, HIV-induced dementia, epilepsy and intra-ventricular haemorrhage in premature infants. In many cases, it is unknown as to whether the onset of neurological damage instigates vascular permeability, or vice versa. In general, endothelial damage is associated with cytokine release, a loss of tight junctional molecules and an increase in leukocyte migration into the CNS. For this reason, BBB permeability is rarely associated with the resolution of disease and more often its progression, reviewed in (Obermeier *et al*., 2013; Engelhardt & Sorokin, 2009; Hawkins & Davis, 2005; Ballabh *et al*., 2004). Therapeutic targets are focused on restoring BBB permeability with an aim to resolve neurological symptoms. Platelets have become a key

candidate in this area and will be discussed in more detail in *Chapter 5*.

1.7 CLEC-2 and podoplanin in inflammation

Beyond their roles in development, podoplanin and CLEC-2 have been implicated in a range of inflammatory processes. To better understand the nature of their roles, first, some key principles will be summarised.

1.7.1 Innate vs adaptive immunity

The innate immune system forms the first line of defense against foreign pathogens. This is non-specific targeting that is mediated mostly by phagocytic macrophages that engulf bacteria and microorganisms that have penetrated epithelial barriers. Tissue resident inflammatory cells such as DCs release inflammatory mediators such as cytokines, which stimulate the recruitment of neutrophils and monocytes (see *Figure 1.1* for haematopoietic cell tree). The build up of immune cells and inflammatory mediators that function to clear foreign pathogens is the hallmark of 'inflammation'. Key players in this initial line of defense become critical to prime the adaptive arm of the immune response, which is an antigen-specific system that functions to allow the host to discriminate between self and non-self. This system relies on antigen presenting cells (APCs) that can be in the form of B-lymphocytes in the blood system, DCs in the lymphatic system or tissue resident stromal cells and DCs. The key characteristics of APCs are their ability to present foreign antigens on major histocompatibility complex (MHC) proteins and to express co-stimulatory molecules to activate T-lymphocytes. DCs are derived from the bone marrow and are released as immature cells that survey the local environment until they interact

with an antigen, at which point they are activated to become an APC. Once activated, APCs migrate to secondary lymphoid organs to initiate the adaptive immune response, reviewed in (Janeway, 2001; Alberts, 2008).

1.7.2 Secondary lymphoid organs

Secondary lymphoid organs include the spleen, lymph nodes, tonsils and Peyers patches. Each secondary lymphoid organ is uniquely designed to provide an optimal environment for B- and T-lymphocytes to survey circulating antigens. These secondary lymphoid organs are critically connected by the blood and lymphatic vasculatures (Turley *et al*., 2010). Lymphatic vessels start as blind ended capillaries, drawing in fluid and DCs from the interstitial fluid in surrounding tissues. These initial lymphatic vessels drain into collecting vessels that converge at multiple points at lymph nodes (*Figure 1.5*) (Randolph *et al*., 2005). Lymph enters the lymph node in 'afferent' lymphatic vessels that carry DCs and flow them through the sinuses, bringing them into contact with naïve lymphocytes, which are imported from the blood system. The interaction between DCs and naïve lymphocytes is facilitated by the fibroblastic reticular cell (FRC) network in the T-lymphocyte rich paracortex, which serves as a highway for migrating cells. The FRC network is lined with macrophages, which mop up bacteria and debris, while also functioning as APCs alongside the FRCs themselves and circulating DCs. Lymphocytes enter the FRC network through high endothelial venules (HEVs), the permeability of which are heavily influenced by inflammatory mediators. T-lymphocytes then survey APC niches before either leaving through the efferent lymphatics to continue their search for antigen in other secondary lymphoid organs, or, they become activated, stimulating their proliferation. Dispersed around the paracortex are follicles, rich in B-lymphocytes and tissue resident follicular DCs that present antigen to B-lymphocytes. Upon antigen

recognition, B-lymphocytes proliferate to form germinal centres and can additionally be induced to transform into antibody secreting plasma cells in response to secondary stimulation by helper T-lymphocytes, reviewed in (Willard-Mack, 2006; Turley *et al*., 2010).

Like the lymph nodes, the spleen is uniquely compartmentalised to maximise interactions between APCs and circulating lymphocytes, however, there are a few key differences in its structure. B- and T-lymphocytes do not enter through HEVs but instead, they enter through the afferent artery. Specific chemokines direct the migration of B- and T-lymphocytes through a meshwork of APCs within the marginal zone, towards the B-cell follicles or the T-cell zone, respectively. DCs can migrate towards the T-cell zone and activate T-lymphocytes, which, in turn, hover at the periphery of B-cell follicles to activate B-lymphocytes. Activated B-lymphocytes can proliferate within follicles or migrate out to be further induced to form plasma cells by DCs or T-lymphocytes. Interestingly, S1-P receptors have been implicated in both the organisation of the marginal zone and the migratory capacity of B- and T-lymphocytes, reviewed in (Mebius & Kraal, 2005).

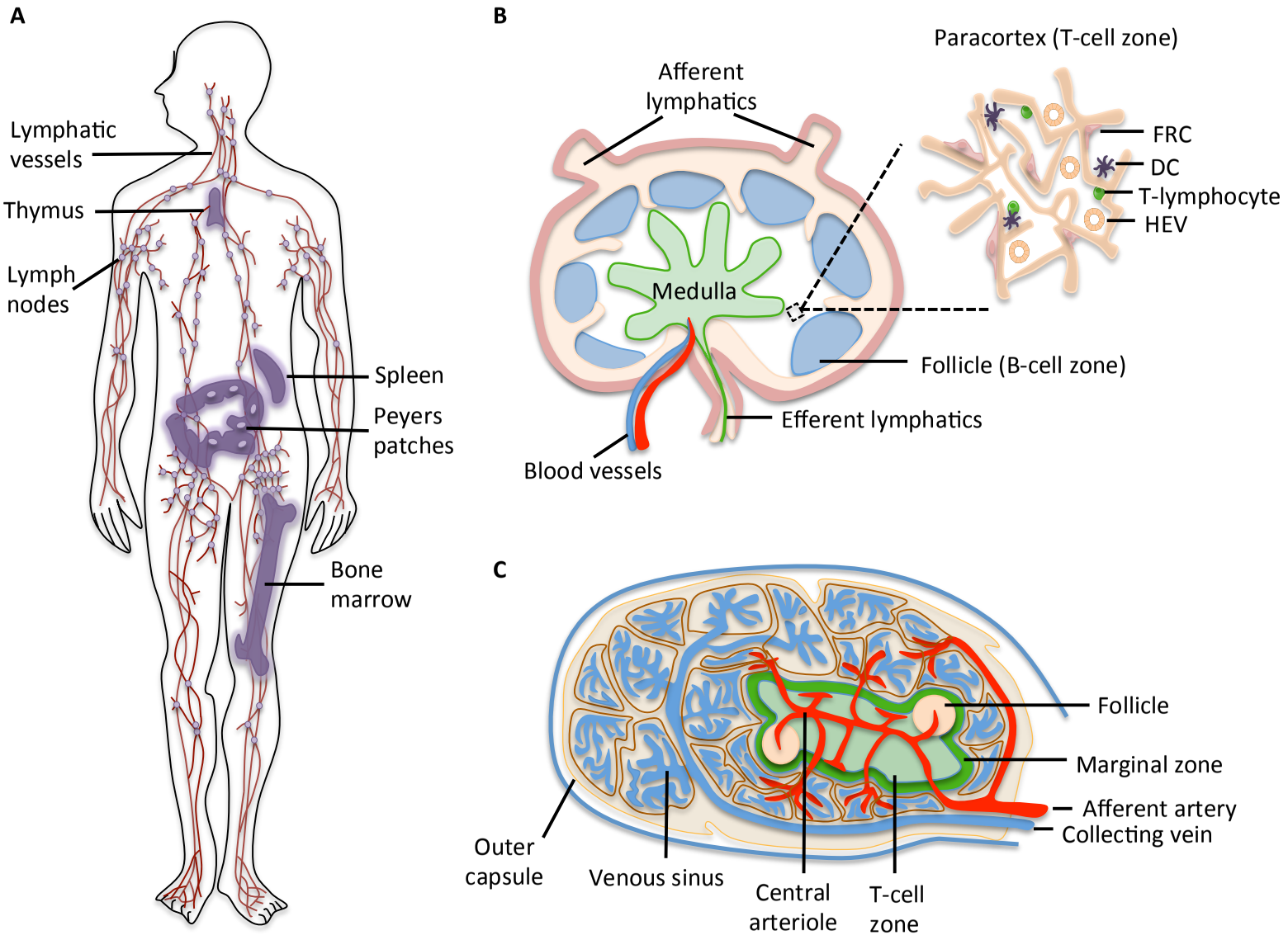
A
Lymphatic vessels
Thymus
Lymph nodes
Spleen
Peyers patches
Bone marrow
B
Paracortex (T-cell zone)
Afferent lymphatics
FRC
DC
T-lymphocyte
HEV
Medulla
Follicle (B-cell zone)
Efferent lymphatics
Blood vessels
C
Follicle
Marginal zone
Afferent artery
Collecting vein
Outer capsule
Venous sinus
Central arteriole
T-cell zone

Figure 1.5. Lymphatic vascular networks connect secondary lymphoid organs to mediate effective immune regulation. (**A**) The lymphatic system consists of a vast network of lymph nodes connected by lymphatic vessels. A key function of the lymphatic vasculature is to circulate immune cells between secondary lymphoid organs, such as the lymph nodes, spleen and peyers patches. Immune cells are initially generated in primary lymphoid tissues such as the bone marrow. T-lymphocyte precursors subsequently migrate to the thymus to mature. *Figure reconstructed from* (Janeway, 2001). (**B**) Immune cells in the lymph enter lymph nodes through afferent lymphatic vessels and percolate through the parenchymal tissue, which is lined with phagocytic macrophages, before being directed towards the T-cell rich paracortex or B-cell follicles. Lymphocytes enter the T-cell zone through high endothelial venules (HEVs) that are positioned within the fibroblastic reticular cell (FRC) network, in close proximity to dendritic cells (DCs). Immune cells leave the lymph through the efferent lymphatic vessels to continue their search, or prime other immune cells in other secondary lymphoid organs. Blood vessels carry antigens, antibodies and patrolling lymphocytes and antigen presenting cells (APCs) in and out of secondary lymphoid organs to survey the immune system. *Figure reconstructed from* (Turley *et al*., 2010). (**C**) The spleens major function is to filter blood, which flows through the cords of the 'red pulp' before filtering into the venous sinuses through a unique fibrous membrane. Aged erythrocytes are then phagocytosed by red pulp macrophages. Immune modulation occurs in the 'white pulp', where B- and T-lymphocytes enter the marginal zone from the afferent blood system and are screened by a network of APCs, before being directed towards the follicles or T-cell zone, respectively. *Figure reconstructed from* (Mebius & Kraal, 2005).

1.7.3 Podoplanin in inflammation

Podoplanin was identified on FRCs within the splenic white pulp and the medullary and paracortical areas of the lymph node over two decades ago (Farr *et al*., 1992), yet the significance of its expression within secondary lymphoid organs was, until recently, largely unexplored. Podoplanin is now used as a common marker for FRCs, where it is critical for the correct separation of B- and T-lymphocyte compartments in the spleen (Bekiaris *et al*., 2007). Podoplanin was further shown to be highly expressed on human follicular DCs, yet its function on these cells is unknown (Yu *et al*., 2007). More recently podoplanin expression on lymphatic endothelium and on FRCs was shown to be specifically required to mediate the entry and trafficking of CLEC-2 expressing DCs to the lymph nodes in mice (Acton *et al*., 2012). In an independent study, podoplanin expressing FRCs were shown to interact with CLEC-2 on platelets, inducing the release of a number of mediators, including S1-P, that were shown to be critical in maintaining the integrity HEV's. In this model, platelets were delivered to FRCs on the back of migrating lymphocytes (Herzog *et al*., 2013). In contrast to these positive regulatory roles, podoplanin expression has been shown to be specifically induced in the inflamed synovium of patients with rheumatoid arthritis, while absent from healthy controls (Del Rey *et al*., 2014). Additionally, podoplanin has been shown to be expressed on T_H17 cells which, when transferred into mice, can simulate the pathogenesis of MS, known in mice as experimental autoimmune encephalomyelitis (EAE). Blocking podoplanin significantly reduced the number of lymphoid aggregates forming adjacent to inflamed blood vessels in the EAE model, suggesting an important regulatory role for podoplanin in T-lymphocyte physiology during inflammation (A. Peters *et al*., 2011). Podoplanin has also been shown to be expressed on $F4/80^+$ phagocytic macrophages in the splenic red pulp and in the inflamed peritoneum, where they are proposed to aid the resolution of inflammation (Hou

et al., 2010). These F4/80^{+} macrophages were further shown to induce CLEC-2-mediated platelet aggregation, proposed to enhance the recruitment of inflammatory cells (Kerrigan *et al*., 2012). Together these findings indicate that podoplanin has many immunological roles varying from day to day-immune homeostasis, to either the onset, or resolution of inflammation, depending on the tissue and cell types involved. Whether the podoplanin-CLEC-2 axis is immunologically beneficial or detrimental to the host remains controversial, which is reflected in the growing wealth of literature debating their roles in tumour progression and metastasis, reviewed in (Lowe *et al*., 2012; Gay & Felding-Habermann, 2011). Given the recent acceleration in this field, the mechanisms behind these processes are likely to be unraveled in the near future. Although CLEC-2 expression is much more restricted, within the haematopoietic compartment, the specific CLEC-2-expressing cell subsets involved in these immune processes is equally as controversial and will be discussed in detail in *Chapter 5*.

1.7.4 Immune surveillance in the CNS

While secondary lymphoid organs are specifically designed to enhance immune cell interactions, the CNS functions to limit these interactions and is often considered 'immune privileged'. However, this is only partial and regulated transfer of immune cells between the circulation and parenchymal tissue is fundamental for CNS immune homeostasis. The most abundant immune cells in the CNS are macrophages, with microglial constituting 5-12% of all the cells within the CNS (D'Agostino *et al*., 2012). Microglia are yolk sac derived macrophages, typically high in Cd11b and F4/80, which infiltrate the neuro-epithelium as early as E8.0 (*Figure 1.6*) (Perry & Teeling, 2013). The mechanism that regulates the renewal of microglia is highly controversial, but it is thought

that the vast majority of microglia self-renew, with only minimal replenishment from infiltrating bone marrow-derived monocytes, in the steady state. Microglia are highly plastic molecules with long projections that function to sense and respond to their environment, stimulating shape change and cytokine secretion, which enable them to prime neighbouring microglia. A key function of microglia is their capacity to mop up cellular debris, the importance of which is echoed in Alzheimer's patients, where the defective clearance of amyloid β peptide results from impaired microglial activity (Prinz *et al*., 2011). In addition to microglia, distinct macrophage subsets also occupy perivascular spaces, the meninges, as well as the choroid plexus and other circumventricular organs. These macrophages are generally derived from blood monocytes and have a much more rapid turnover than microglia, where as few as 1% of cells turn over in 90 days (K. Williams *et al*., 2001). In the steady state, non-microglial macrophages are excluded from the CNS parenchyma, yet they hover at the parenchymal borders providing key signals to parenchymal cells (*Figure 1.6*). The exclusion of immune cells from the CNS parenchyma is determined by a unique set of barriers that function within the CNS. Foremost is the BBB, which in the steady state is largely impenetrable to immune cells, but is critical for immune surveillance by allowing circulating T- and B-lymphocytes, as well as free antigens, to communicate systemic messages across the endothelium to the underlying microglial cells and vice versa (*Figure 1.6*) (Schwartz *et al*., 2013). Within the CNS, several distinct structures, termed circumventricular organs, lack a BBB. The choroid plexus is the main circumventricular organ, located throughout the four interconnecting ventricles of the brain, where it forms the blood-CSF interface. The choroid plexus is formed from an epithelial membrane which encloses a highly vascularised core of connective tissue, consisting fibroblasts, macrophages, DCs and a rich supply of fenestrated capillaries (*Figure 1.6*). Fenestrated capillaries lack endothelial

tight junctions, thereby facilitating the interaction between circulating cytokines and inflammatory mediators with resident macrophages and DCs (Wolburg & Paulus, 2010). However, the passage of molecules into the CNS parenchyma at the circumventricular organs is selectively regulated, depending on the requirements of the CNS. A unique population of $CD4^+$ T-lymphocytes, specific for CNS antigens, reside in the choroid plexus and regulate trafficking by controlling local cytokine levels (Schwartz *et al*., 2013). This equilibrium can become disturbed during ageing, or in certain neurological disorders, resulting in the inappropriate influx of lymphocytes, e.g. in MS or its animal model, EAE. The specific subsets of lymphocytes and other inflammatory cells that occupy different niches of the CNS is still a developing field. The underlying dogma is the balance between regulated infiltration of immune cells to clear infection, as apposed to inappropriate uncontrolled entry (Ransohoff & Brown, 2012). In the context of neurodegenerative diseases, the lab of Hugh Perry have recently communicated the principle of 'microglial priming', whereby microglia become primed by an on-going pathology, appearing activated, but exhibiting a 'anti-inflammatory' phenotype with decreasing functional responses. A second systemic stimulus can re-activate microglia, but overtime may exacerbate this response and severely advance disease severity (Perry *et al*., 2007).

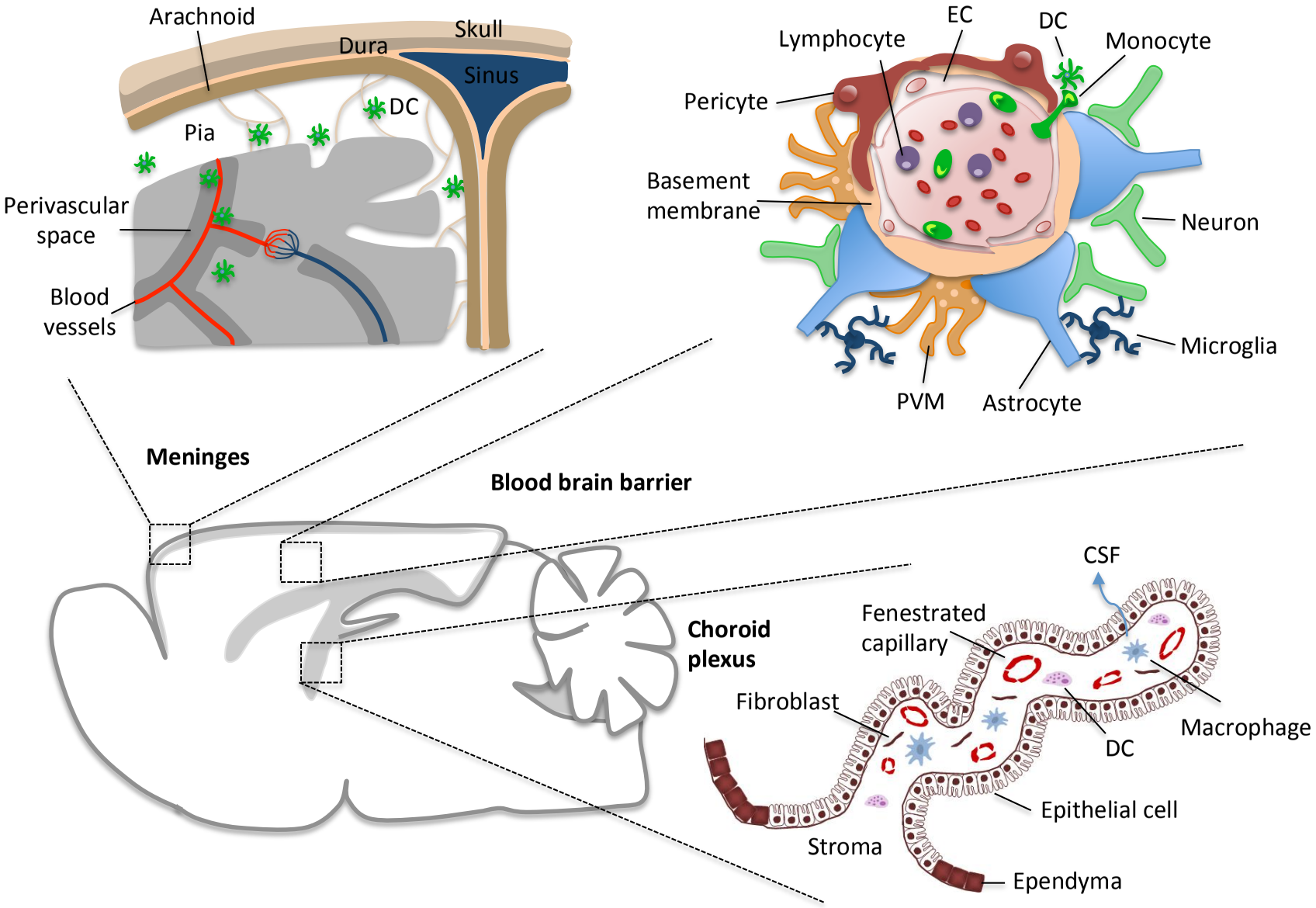
Arachnoid
Dura
Skull
Sinus
DC
Pia
Perivascular space
Blood vessels
Lymphocyte
EC
DC
Monocyte
Pericyte
Basement membrane
Neuron
Microglia
PVM
Astrocyte
Meninges
Blood brain barrier
Choroid plexus
CSF
Fenestrated capillary
Fibroblast
DC
Macrophage
Epithelial cell
Stroma
Ependyma

Figure 1.6. Immune barriers in the adult brain. Unique cellular environments exist within the brain to regulate immune homeostasis. Under pathological conditions these barriers can become increasingly permeable. The meninges is abundant in monocyte-derived macrophages and dendritic cells (DCs) that continually enter perivascular compartments to communicate with circulating leukocytes and antigens in parenchymal vessels. Parenchymal vessels are characteristically impermeable due to the tight interplay between adjacent endothelial cells (EC) and the surrounding glia and neurons that constitute the blood-brain barrier. Perivascular macrophages (PVMs) and microglia resident in the apical compartments communicate environmental signals to circulating immune cells across the endothelium and vice versa to influence blood-brain barrier permeability. The choroid plexus is the hub of CNS immune surveillance with a highly vascularised stroma formed of permeable fenestrated capillaries allowing continued crosstalk between circulating and resident immune cells. Despite the inherent permeability within the stroma, the trafficking of molecules across the epithelium and into the CSF is highly regulated. *Reconstructed from* (D'Agostino *et al*., 2012; Hawkins & Davis, 2005; Emerich *et al*., 2005).

1.8 Aims

The role of podoplanin and its receptor CLEC-2 in the separation of the blood and lymphatic vasculatures during development has now been well characterised. However, their role in the development of the cerebral vasculature, which forms independently of a lymphatic system, remains largely unexplored. Furthermore, the expression of podoplanin in the adult brain has only recently been investigated, and its function in this tissue remains unknown. Therefore, the aim of the work undertaken in this thesis was;

1. To investigate a role for podoplanin and CLEC-2 in the development of the brain vasculature.
2. To explore a role for podoplanin and CLEC-2 in the adult brain in the steady state and in response to inflammatory challenge.
3. To characterise a range of CLEC-2- and podoplanin-deficient mouse models to investigate points 1 and 2.

CHAPTER 2

MATERIALS AND METHODS

2.1 Materials

2.1.1 Antibodies and reagents

The antibodies used during the course of this thesis are listed in *Table 2.1*. If unstated, materials used are from Sigma (Poole, UK).

Table 2.1 Antibodies

Antibody	Host species	Dilution	Source
PRIMARY			
Podoplanin	Hamster	IF – 1/600* IHC – 1/400* WM-IF – 1/200	EBioscience (Hatfield, UK)
PECAM-1	Rat	WM-IF – 1/200 IF – 1/200*	Dr S Butz (Max Planck Institute for Molecular Biomedicine, Germany)
Endomucin	Rat	IF – 1/200**	Santa Cruz Biotechnology (Heidelberg, Germany)
Pre-albumin	Sheep	IF – 1/200**	Abcam (Cambridge, UK)
F480	Rat	IF – 1/100**	AbD Serotech (Kidlington, UK)
CD11b	Rat	IF – 1/100**	AbD Serotech (Kidlington, UK)
CD41	Rat	IF – 1/100**	BD Pharmingen™ (Oxford, UK)
NG2	Rabbit	IF – 1/200**	Millipore (Co Durham, UK)
$F(ab)_2$-IgG-H&L	Goat	IF – 1/50**	Thermo Scientific (Loughborough, UK)
Nestin	Rat	IF – 1/50**	Developmental studies hybridoma bank (Iowa, US)
TER-119	Rat	IF – 1/200**	Cambridge Bioscience (Cambridge, UK)
ZO-1	Rabbit	IF – 1/200**	Invitrogen (Paisley, UK)
CD41-FITC	Rat	FC – 1/100	BD Bioscience (Oxford, UK)
CD41-PE	Rat	FC - 1/800	EBioscience (Hatfield, UK)
CLEC-2 (17D9) (AlexaFluor®488 conjugated – see text)	Rat	FC – 1/100	Reis e Sousa (Cancer Research UK, London, UK)

INU1-FITC	Rat	FC - 1/10	Bernhard Nieswandt (University Hospital Würzberg, Germany)
INU1 (AlexaFluor®488 conjugated – see text)	Rat	FC – 1/100	Bernhard Nieswandt (University Hospital Würzberg, Germany)
Gr1-APC	Rat	FC – 1/3000	EBioscience (Hatfield, UK)
CD11b-PerCP-Cy5.5	Rat	FC – 1/1000	EBioscience (Hatfield, UK)
CD3e-Cy7	Rat	FC – 1/200	EBioscience (Hatfield, UK)
CD19-APC-Cy7	Rat	FC – 1/100	BD Pharmingen™ (Oxford, UK)
CD45.2-eF780	Rat	FC – 1/200	EBioscience (Hatfield, UK)
CD19-APC	Rat	FC – 1/100	BD Pharmingen™ (Oxford, UK)
Streptavidin-PE	Rat	FC – 1/100	EBioscience (Hatfield, UK)
GPIbα		Platelet depletion – 1.5 µg/g	Emfret (Eibelstadt, Germany)
SECONDARY			
IgG-H&L-Cy3® (hamster)	Goat	IF – 1/500	Abcam (Cambridge, UK)
AlexaFluor®488 (rat)	Goat	IF – 1/500	Invitrogen (Paisley, UK)
AlexaFluor®488 (hamster)	Goat	IF – 1/500	Invitrogen (Paisley, UK)
AlexaFluor®647 (rat)	Goat	IF – 1/500	Invitrogen (Paisley, UK)
IgG-FITC (rabbit)	Donkey	IF – 1/150	Dako Cytomation
IgG-H&L-Biotin (hamster)	Goat	IHC – 1/100	Vector laboratories (Peterborough, UK)

*1 hour incubation time. ** Overnight incubation. WM, whole-mount;
IF, immunofluorescence; IHC, immunohistochemistry; FC, flow cytometry

2.2 Mice

All animal experimentation was performed under a license from the UK Home Office. Constitutive deletion of CLEC-2 (*Clec-2*$^{-/-}$) and conditional deletion of CLEC-2 (*Clec-2*$^{fl/fl}$) on a C57BL/6 background have been previously described (Hughes *et al*., 2010; Finney *et al*., 2012). *Clec-2*$^{fl/fl}$*PF4-Cre* mice have been described previously (Finney *et al*., 2012) and *Clec-2*$^{fl/fl}$*ER*^{T2}*-Cre* mice were generated by breeding *Clec-2*$^{fl/fl}$ mice to mice expressing *ER*^{T2}*Cre* recombinase driven by the *ROSA*^{26} locus obtained from Jackson Laboratories (B6.129-Gt(ROSA)26Sortm1(cre/ESR1)Tyj/J), backcrossed 8 times onto a C57BL/6 background. Mice with a conditional deletion of podoplanin (*Pdpn*$^{fl/fl}$) were generated at Taconic Artemis and provided on a C57BL/6 background. *Pdpn*$^{fl/fl}$ mice were crossed to mice expressing *PGK-Cre* recombinase (*Pdpn*$^{fl/fl}$*PGK-Cre*), obtained from Cancer Research UK, Manchester, mediating constitutive deletion of podoplanin from the two-cell stage (Lallemand *et al*., 1998). *Pdpn*$^{fl/fl}$ mice were also crossed to mice expressing Cre recombinase driven by the nestin promoter (*Nes-Cre*), obtained from Cancer Research UK, London, to delete podoplanin in the neural tube (Petersen *et al*., 2002). *αIIb*$^{-/-}$ mice on a C57BL/6 background were provided by Professor John Frampton, University of Birmingham, UK (Emambokus & Frampton, 2003). Embryos from NBEAL-2-deficient mice (*Nbeal-2*$^{-/-}$) on a C57BL/6 background were provided by Professor Bernhard Nieswandt, University of Wurzburg, Germany (Deppermann *et al*., 2013). Genotyping was performed by PCR using primers listed in *Table 2.2,* using genomic DNA isolated from ear/tail tissue.

Table 2.2 PCR Primers

Primer	Sequence
Clec-2 wildtype forward primer	GATGAGTCTGCTAGGGATGC
Clec-2 knockout forward primer	CAGAGGAAGAAAACTCAGAAGG
Clec-2 common reverse primer	AGCCTGGAGTAACAAGATGG
Clec-2^{fl} forward primer	TTTCTGCCTCTCTGCCTTGC
Clec-2^{fl} reverse primer	CGTCATGAACAGAAAACTGACG
PF4-Cre forward primer	CCCATACAGCACACCTTTTG
PF4-Cre reverse primer	TGCACAGTCAGCAGGTT
ER^{T2}*-Cre* primer 1	CCT GAT CCT GGC AAT TTC
ER^{T2}*-Cre* primer 2	AAA GTC GCT CTG AGT TGT TAT
ER^{T2}*-Cre* primer 3	GGA GCG GGA GAA ATG GAT ATG
Pdpn^{fl} wildtype/floxed forward primer	TATGTATGTCTACCCCAACTCCTG
Pdpn^{fl} wildtype/floxed reverse primer	TAAGTACACTGTCGCTGTCTTCG
Pdpn^{fl} knockout forward primer	AGATGTGATGATATGTGGTACTTGC
Pdpn^{fl} knockout reverse primer	GTACACGGTTCTTAACGGTGG
PGK-Cre common primer	TCGTTGCATCGACCGGTAAT
PGK-Cre forward primer	GCGCAGGTCTCCTCTTCCTC
PGK-Cre wildtype reverse primer	GACCAATGAAACGTGGGCG
αIIb forward primer	CAGACTCCTGGCTCATCTAC
αIIb reverse primer	TCTGCCTAACTCTGCTTTCC
αIIb Cre forward primer	TCGATGCAACGAGTGATGAG
αIIb Cre reverse primer	TTCGGCTATACGTAACAGGG
Nes-Cre forward primer	GCCTGCATTACCGCTCGATGCAACGA
Nes-Cre reverse primer	GTGGCAGATGGCGCGGCAACACCATT

2.2.1 Genomic DNA extraction

Ear clippings from adult mice or embryonic tissue samples were digested in lysis buffer (100 mM Tris-hydrochloride; pH 8.5, 5 mM ethylenediamine tetra-acetic acid (EDTA), 0.2% sodium dodecyl sulphate (SDS) and 200 mM sodium chloride (NaCl) with proteinase K (1.25 mg/ml per sample)) overnight at 56°C. Samples were centrifuged at 16000 g for 5 min at 4°C and the supernatant extracted and added to isopropanol. Samples were centrifuged at 16000 g for 5 min at 4°C. Supernatants were removed and pellets were air dried before resuspending in ddH_20 ready for PCR amplification using the

primers listed in *Table 2.2*.

2.2.2 Tamoxifen-induced depletion of CLEC-2

Clec-2$^{fl/fl}$ or *Clec-2*$^{fl/fl}$*ER*^{T2}*-Cre* mice were treated with tamoxifen by intraperitoneal injection (i.p.) or in the diet. For i.p. injections, 100 µl of tamoxifen (20 mg/ml in corn oil) was injected each day for 5 days (unless stated otherwise). Alternatively, mice were fed TAM400 diet (400 mg tamoxifen in citrate form per kg of diet (Harlan Laboratories, Indianapolis, IN)) for two weeks, or continuously. Mice on tamoxifen diet were weighed each day for 7-14 days and any mice that lost >20% of their starting total body weight were culled in line with the UK Home Office regulations.

2.2.3 Generation of radiation chimeras

Fetal livers were dissected from embryos obtained from *Clec-2*$^{+/-}$ crossed time matings, or from *Pdpn*$^{fl/+}$*PGK-Cre* crossed time matings at E16.5. Genotyping of embryos was performed as described in *Section 2.2.1*. Fetal livers were processed individually in a sterile tissue culture hood. A single cell suspension was made by passaging fetal livers through a series of 19-, 6- and 2-gauge needles into phosphate buffered saline (PBS). Cells were washed twice in PBS, pellets resuspended in 800 µl of 90% fetal bovine serum (FBS)/10% dimethyl sulfoxide (DMSO) solution and immediately cooled to –80°C before storing in liquid nitrogen. On the day of reconstitution, fetal liver cells were thawed, washed twice in PBS and resuspended in 200 µl of PBS per mouse (4 injections are expected per fetal liver). Live cell counts were determined using 0.4% trypan blue solution. Counts of approximately $1x10^6$ cells in each 200 µl injection volume were expected.

Male C57BL/6 mice were provided from Harlan Laboratories at 6 weeks of age. Mice

were given one week to rest upon arrival, followed by one week on Baytril. Mice were irradiated twice with 500 rads, 3 hours apart, followed by an intravenous (i.v.) injection of fetal liver cells 1 hour later.

2.2.4 Systemic inflammatory challenge

Wild-type or *Clec-2*$^{-/-}$ chimeras, or tamoxifen-treated *Clec-2*$^{fl/fl}$ or *Clec-2*$^{fl/fl}$*ER*^{T2}*-Cre* mice were fed normal diet for 6 weeks before administration of lipopolysaccharide (LPS) (*Escherichia coli* serotype O11:B4) in sterile PBS, or PBS only, by i.p. injection (doses stated in results). Mice were terminally anaesthetised by i.p. injection of 150 mg/kg of Euthatal. Blood was drawn by cardiac puncture into 10% acid-citrate dextrose (ACD: 120 mM sodium citrate, 110 mM glucose, 80 mM citric acid) and further diluted into 200 µl of 20 mM EDTA. Mice were perfused through the atrium with 4% paraformaldehyde (PFA)/PBS followed by PBS only until the liver was clear of erythrocytes. Organs were harvested for analysis. For measuring evans blue absorbance, mice were administered evans blue dye (4 ml/kg at 2%) by i.p injection and sacrificed as described above. Brains were isolated, weighed and half of the brain was fixed in 4% PFA/PBS for histology. The other half of the brain was homogenised in a 1:3 volume of PBS by sonication. Any undigested material was pelleted at 16000 g for 30 min. An aliquot of supernatant was added to an equal volume of trichloroacetic acid (TCA) into a 96 well plate and left overnight at 4°C. Plates were centrifuged at 3000 g for 30 min and the absorbance of supernatants at 610 nm were read using a VersusMax Microplate reader (Molecular Devices, Berkshire, UK). Whole blood counts were taken from peripheral blood samples before being processed to obtain evans blue absorbance measurements. Whole blood was centrifuged at 6000 g for 5 min, plasma volumes were recorded and an aliquot of plasma was added to an equal volume of TCA and treated as detailed above. Absorbance

measurements from the brain supernatant or blood plasma were normalised to brain weights or plasma volumes, respectively, and the absorbance value from the brain supernatant was represented as a ratio to plasma absorbance. For the thioglycolate challenge model, tamoxifen-treated *Clec-2*$^{fl/fl}$ or *Clec-2*$^{fl/fl}$*ER*^{T2}*-Cre* mice were left for 6 weeks on normal diet before administration of 3% sodium thioglycolate in 1 ml sterile PBS, or PBS only, in combination with evans blue dye (4 ml/kg at 2%) by i.p. injection. Mice were sacrificed 4 hours later and evans blue absorbance in the brain and blood plasma were measured as previously described. For the *Salmonella* infection model, tamoxifen-treated *Clec-2*$^{fl/fl}$ or *Clec-2*$^{fl/fl}$*ER*^{T2}*-Cre* mice were left for 6 weeks on normal diet before administration of $5x10^5$ colony forming units (CFU) of attenuated *Salmonella* Typhimurium in sterile PBS, or PBS only, by i.p. injection. The bacteria were prepared by Jessica Hitchcock. Briefly, *Salmonella* Typhimurium were incubated overnight in Luria-Bertani broth (Invitrogen, Paisley, UK) at 37°C with aeration (180 rpm). Bacteria were harvested at the mid-log phase (optical density (OD)λ600nm of 0.8-1.2). Bacterial cultures were centrifuged at 6000 g for 5 min at 4°C and washed twice in PBS with centrifugation before resuspending in 1 ml PBS. OD was measured and bacteria within the desired range were diluted to give $5x10^5$ CFU in 200 µl sterile PBS. The infection dose was confirmed using the Miles and Misra CFU counting technique by plating serial dilutions of bacteria onto agar plates and incubating overnight at 37°C. 7 days post *Salmonella* infection, mice were administered 25 µg LPS in 200 µl sterile PBS, or PBS only, in combination with evans blue dye (4 ml/kg at 2%), by i.p. injection. Mice were sacrificed after 24 hours and evans blue absorbance in the brain and blood plasma was measured as previously described.

2.3 Microscopy

2.3.1 Immunohistochemistry

Time mated females (day of plug = E0.5), were culled by Schedule 1 methods. Embryos were photographed and whole embryos, or dissected embryo heads, were fixed overnight in Bouin's fixative. Embryos were transferred to 70% ethanol before being processed for paraffin embedding and sectioning (Pathology Department, QE Hospital).

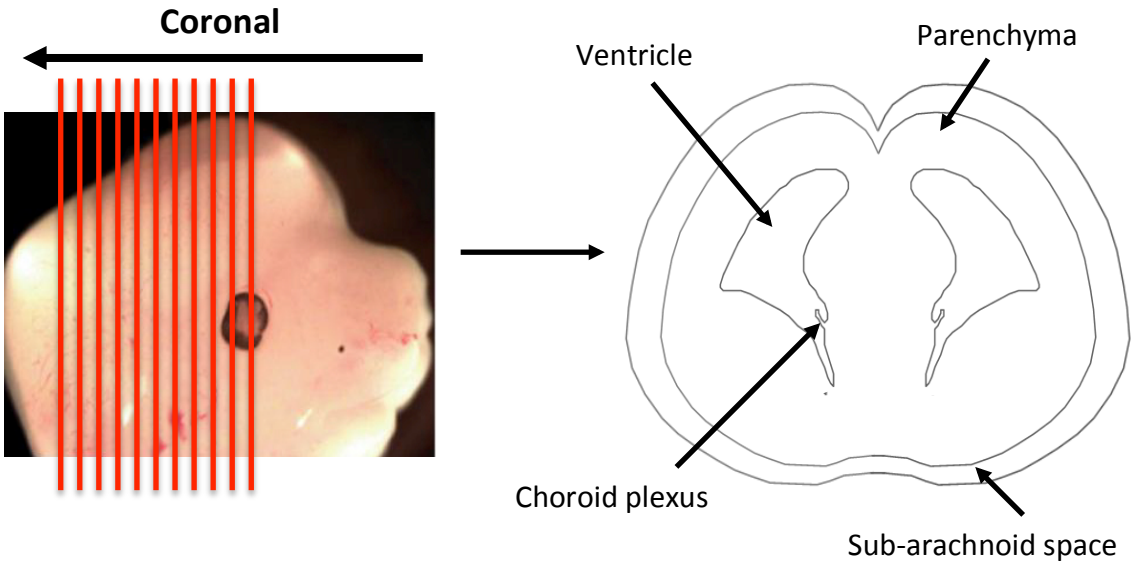

Figure 2.1. Method for sectioning through embryonic brains. Coronal sections were taken by sectioning from the rostral (anterior) side of the embryo to the caudal (posterior) side. In general, sections were collected from just past the eyes, at a point in which the lateral ventricles and a large area of brain parenchyma, choroid plexus and sub-arachnoid tissue can be visualised.

Sections were immersed in xylene before successively rehydrating in 100%, 90%, 70%, 50%, 30% ethanol and dH_20. Slides for haematoxylin and eosin (H&E) staining only were placed in Harris's haematoxylin solution for 3 min, rinsed in running tap water, dipped in 0.3% acid alcohol, incubated for 5 min in Scotts tap water (25 mM sodium bicarbonate, 0.1 M magnesium sulphate) and dipped in 1% eosin, before placing back into dH_20 and

successively dehydrating in 50%, 70%, 90%, 100% ethanol and then xylene overnight. Slides were mounted using VectaMount mounting media (Vector Laboratories, Peterborough, UK) ready for imaging.

For podoplanin staining, following rehydration (*Section 2.3.1*), slides were boiled in citrate buffer (10 mM citric acid monohydrate; pH 6.0) for 15 min. For $F(ab)_2$-HRP staining, slides were boiled in citrate buffer (1 mM EDTA, 0.1 % tween-20, pH 8.0) for 50 min. All slides were cooled to room temperature and rinsed in PBS before permeabilising in 0.3% tween-20/PBS for 10 min. Sections were circled with an ImmEdge™ hydrophobic pen (Vector Laboratories, Peterborough, UK) and incubated in 3% H_20_2 for 10 min at room temperature. Slides were washed in PBS and blocked for one hour at room temperature in 3% BSA/PBS, 0.1% tween-20 (PBST), or 10% goat serum/PBST for podoplanin or $F(ab)_2$-HRP staining, respectively. Primary antibody (diluted in 10% blocking solution/PBST) was incubated overnight at 4°C, followed by washing in PBST for 3 x 10 min (minimum). For podoplanin staining, slides were further incubated with secondary antibody (goat anti-hamster biotin) for 45 min at room temperature, followed by washes in PBST for 3 x 10 min (minimum). Slides were incubated with Avidin/Biotinylated enzyme complex from the VECTASTAIN® kit (Vector Laboratories, Peterborough, UK) for 30 min at room temperature, followed by washing for 3 x 10 min in PBST. Slides for both podoplanin and $F(ab)_2$-HRP staining were processed with 3.3'-Diaminobenzidine (DAB) liquid substrate for 30 seconds (Vector Laboratories, Peterborough, UK). Slides were immediately placed into dH_20 and stained with haematoxylin, dehydrated and mounted as described above.

Analysis was performed using a Zeiss Axiovert Zoom brightfield microscope using either

5 X or 10 X air objectives, or 40 X or 63 X oil objectives. Images were processed using Adobe Photoshop 8.0.

2.3.2 Immunofluorescence

Embryos were photographed and whole embryos, or dissected embryo heads, were fixed overnight in 4% PFA/PBS. Embryos were incubated overnight in 20% sucrose, followed by 30% sucrose overnight, before embedding in optimum cutting temperature (O.C.T) media (Tissue-Tek®, Thermo Fisher Scientific, Loughborough, UK) and snap freezing in liquid nitrogen. Samples were stored at -80°C. Cryosections between 10-20 μm were cut using a Cryostat (Bright instruments, Huntington, UK) onto Shandon™ColorFrost™ Plus microscope slides (Thermo Fisher Scientific, Loughborough, UK). Slides were immediately placed on dry ice and then stored at -80°C. In preparation for immuno-staining, slides were removed and left to dry at room temperature for 30 min, before fixing in ice cold acetone for 20 min at -20°C. Slides were left to dry for 30 min at room temperature before washing in PBS for 10 min. Sections were circled with an ImmEdge™ hydrophobic pen and incubated with ammonium chloride (20 mM) for 15 min at room temperature. Slides were washed in PBS and further permeabilised in 0.3% Tween-20/PBS before blocking in 1% BSA, 5% goat serum/PBST for 1 hour at room temperature. Slides were incubated in primary antibody (diluted in 10% blocking solution/PBST) for 1 hour at room temperature (**Table 2.1*), or overnight at 4°C (***Table 2.1*), followed by washing for 3 x 10 min (minimum) in PBST. Slides were incubated in secondary antibody (diluted in PBST) for 45 min at room temperature, followed by 3 x 10 min washes in PBST. Where applicable, further primary and secondary antibody incubations were performed, depending on species reactivity combinations. Where applicable, slides were incubated in TO-PRO-3 Iodide (Invitrogen, Paisley, UK) (diluted

1:1000 in PBS) for 10 min at room temperature. Slides were washed in PBS before mounting using VectaMount mounting media. Slides were analysed by confocal microscopy using a Leica SP2 confocal microscope. Images were processed with Adobe Photoshop 8.0.

2.3.3 Wholemount Immunofluorescence - ultramicroscopy

Embryos were prepared for ultramicroscopy as described by Hägerling *et al* (Hägerling *et al*., 2013). Embryos at E10.5, E11.5 or E12.5 were fixed for 4, 6 or 8 hours, respectively, in 4% PFA/PBS at 4°C. Embryos were permeabilised (0.5 % triton-X-100/PBS) for 2 days at 4°C and blocked in 1% BSA, 1% goat serum, 0.5% tween-20/PBS for 1 week at 4°C. Embryos were incubated in primary antibodies (diluted in blocking solution) for 1 week at 4°C, followed by washing in PBST for 2 days. Embryos were incubated with secondary antibodies (diluted in 10% blocking solution/PBS), followed by washes in PBST for 2 days. All solutions were previously filtered using a 0.22 μm filter. Embryos were embedded in 1% ultrapure, low melting point agarose. The agarose was warmed to 45°C and a small amount was placed into a mould on ice for 2 minutes before fully immersing the embryo into the agarose. Once set, samples were transferred to glass vials and successively dehydrated in 50%, 70%, 95%, 100% methanol and again in 100% methanol (anhydrous) for 1 hour per step. Samples were optically cleared by incubating overnight in benzyl alcohol:benzyl benzoate solution (BABB) (1:2):methanol (50:50) and then overnight in BABB only, ready for ultramicroscopy.

Optically cleared wholemount immunofluorescent samples were imaged on an LaVision Ultramicroscope (La Vision BioTec, Bielefeld). Stacks were captured at different

magnifications with a step size of 1 μm. 3D reconstruction, morphometric analysis and analysis of ultramicroscopy stacks were performed using IMARIS software (Version 7.6.0, Bitplane).

2.3.4 Wholemount immunofluorescence – hindbrain model

Embryos at E12.5 were isolated and hindbrains were dissected out and labelled by immunofluorescence, following the protocol by Fantin *et al* (2013) (Fantin *et al*., 2013). Briefly, the whole embryo head was isolated using forceps and the rostral half of the head was removed. The hindbrain was dissected out and placed into PBS in a 96 well plate. Hindbrains were fixed in 4% PFA for 2 hours on ice, washed in PBS and blocked in 10% goat serum in PBST for 30 min at room temperature. Hindbrains were incubated in primary antibody (diluted in blocking solution) overnight at 4°C and washed 5 x 30 min in PBST. Hindbrains were incubated in secondary antibody (diluted in blocking solution) overnight at 4°C and washed for 5 x 30 min in PBST. Hindbrains were flat mounted onto glass slides using VectaMount, overlaid with a glass coverslip and stored at 4°C. Slides were imaged by confocal microscopy using a Leica SP2 confocal microscope. Image analysis was performed using IMARIS software (Version 7.6.0, Bitplane).

2.3.5 Transmission electron microscopy (TEM)

All sample preparation for transmission electron microscopy (TEM) was performed in a fume hood. Heads of whole embryos at E11.5 were removed and the noses cut off. Embryo heads were washed in PBS before fixing overnight in 2.5% glutaraldehyde in 0.1 M sodium cacodylate buffer (pH 7.4) (Na Cacodylate) for 1 hour at 4°C. Samples were washed with Na Cacodylate buffer for 3 x 10 min prior to incubation in osmium tetroxide (1% working solution/Na Cacodylate buffer) (Agar Scientific, Stansted, UK) for 1 hour at

4°C (all subsequent steps were performed with rotation at room temperature). Samples were washed for 3 x 10 min in Na Cacodylate buffer, followed by washing in dH_20, before successively dehydrating in 70%, 80%, 90%, 96% and 2 x 100% ethanol for 30 minutes per step. Samples were immersed in 1:1 propylene oxide (Agar Scientific, Stansted, UK): epon resin overnight, before transferring into 100% epon resin overnight. Samples were transferred to a rubber mould, oriented, immersed in resin and placed in an oven at 60°C for 4 days before being removed and stored at room temperature. Samples were sectioned and stained at the Centre for Electron Microscopy (School of Metallurgy and Materials, University of Birmingham, UK). Ultrathin sections of 90-100 nm were cut using a microtome (Leica Reichert Ultracut S, Milton Keynes, UK) and stained with lead citrate (7.5 mM lead nitrate, 0.1 M sodium citrate and 1 M sodium hydroxide) and 30% uranyl acetate in methanol. Samples were imaged on a Jeol 2100 200kV LaB6 TEM. Images were processed using Adobe Photoshop 8.0.

2.4 Flow cytometry

2.4.1 CLEC-2 expression on platelets in whole blood

Blood samples were taken either directly from the tail vein into 200 µl of 20 mM EDTA, or by terminal bleeding, whereby mice were terminally anaesthetised with isofluorane anaesthesia, a laparotomy was performed exposing the descending aorta and blood was drawn into 10% ACD. Blood was further diluted into 200 µl of 20 mM EDTA.

17D9 CLEC-2 antibody was conjugated using an AlexaFluor®488 Monoclonal Antibody Labelling Kit (Invitrogen, Paisley, UK). 17D9 CLEC-2-488 antibody was diluted in PBS and added to whole blood for 20 min in the dark. Samples were analysed using a BD

FACSVerse™ (BD Bioscience, Oxford, UK) or BD FACSCalibur™ (BD Biosciences, Oxford, UK). Analysis was performed in FlowJo v10.

2.4.2 CLEC-2 expression on platelets and leukocytes in whole blood

Blood samples were taken as described in *Section 2.4.1*. Samples were centrifuged at 3000 g for 4 min, supernatants were discarded and pellets were resuspended in Ammonium-Chloride-Potassium (ACK) lysing buffer (0.15 M ammonium chloride (NH_4Cl), 1 mM potassium bicarbonate ($KHCO_3$, 0.1 mM disodium EDTA (Na_2EDTA)) for 5 min at room temperature. Samples were centrifuged at 3000 g for 4 min and pellets were resuspended in flow cytometry (FC) buffer (2 % FBS, 2 mM EDTA in PBS) before further centrifugation at 3000 g for 4 min. Supernatants were discarded and sample pellets were resuspended in antibodies (*Table 2.1*) diluted in FC-buffer for 20 min on ice, in the dark. The unconjugated CLEC-2 antibody, INU1, was conjugated using an AlexaFluor®488 Monoclonal Antibody Labelling Kit (Invitrogen, Paisley, UK). Samples were washed in FC-buffer and centrifuged at 3000 g for 4 min. Supernatants were discarded and pellets resuspended in FC-buffer before passing through a 50 μm filter (Partec Cell Trics® UK Limited, Kent, UK). Samples were centrifuged at 3000 g for 4 min and resuspended in FC-buffer only, or in 1 μg/ml Di-acetate (DAPI), diluted in FC-buffer. Samples were analysed using a CyAN^{TM} ADP analyzer (Beckman Coulter, High Wycombe, UK). Analysis was performed in FlowJo v10.

2.4.3 DNA extraction from whole blood

Blood samples were taken from the tail vein into 200 μL of 20 mM EDTA. Samples were incubated in ACK lysing buffer for 5 min at room temperature, followed by centrifugation

at 1400 rpm for 5 min. Supernatants were discarded and pellets were processed to isolate genomic DNA using the DNeasy® Blood and Tissue Kit (Qiagen, Manchester, UK). PCR amplification was performed using primers listed in *Table 2.2*.

2.5 Platelet lifetime measurements

2.5.1 Platelet half life

Mice were injected intravenously with 150 µl of 4 mg/ml N-Hydroxysuccinimidobiotin (NHS-Biotin) in PBS buffer. At 0, 1, 2, 3, 4, 5 and 7 days post injection, whole blood was sampled from the tail vein into buffer containing 5 mM EDTA and 10% FBS in PBS (FC2-buffer). Whole blood counts were measured using an ABX Pentra 60 blood counter (BIVDA, London, UK). Samples were washed in FC2-buffer and centrifuged at 6000 g for 10 min. Supernatants were discarded and pellets were resuspended in CD41-FITC, Streptavidin-PE, or the equivalent IgG controls, diluted in FC2-buffer and kept on ice for 30 minutes in the dark. Samples were washed in FC2-buffer, centrifuged at 6000 g for 10 min and supernatants were discarded and pellets resuspended in FC2-buffer for analysis using a BD FACSCalibur™ (BD Biosciences, Oxford, UK). Analysis was performed in FlowJo v10.

2.5.2 Platelet recovery

Mice were injected intravenously with anti-GPIbα, diluted in sterile PBS. At 0, 1, 3, 5, 6, 7 and 11 days post injection, whole blood was sampled from the tail vein into 20 mM EDTA. Platelet counts were measured using the whole blood counter. Expression of CLEC-2 on platelets in *Clec-2*$^{fl/fl}$ and *Clec-2*$^{fl/fl}$*PF4-Cre* mice was confirmed by flow cytometry (*Section 2.4.1*)

2.6 Cell culture

The rat choroid plexus epithelial cell (CPEC) line, Z310, was kindly provided by Dr Wei Zheng (Purdue University, IN, USA). Cells were grown in DMEN media supplemented with 10% FBS, 100 U/ml penicillin, 100 μg/ml streptomycin and 10 ng/ml recombinant rat epidermal growth factor (EGF) (Peprotech, London, UK) at 37°C, 10% CO_2. Cells were passaged using standard methods, including trypsin detachment and live cell counting using 0.4% trypan blue solution.

2.6.1 Trans-epithelial electrical resistance measurements

BD cell inserts with pore sizes of 0.45 μm (Scientific Laboratory Supplies, Yorkshire, UK) were placed in a 24 well plate and 700 μl of media (-EGF) was added to the bottom of the well. CPECs were seeded onto the insert at a density of $1x10^4$ in 200 μl of media. Where applicable, washed wild-type mouse platelets (*Section 2.6.3*) were added to the media above the insert at a final concentration of $1x10^8$/ml. Electrical resistance across CPEC monolayers was measured each day for 5 days using a Millicell-ERS Volt-Ohm meter (Millipore, Co Durham, UK), according to the manufacturers instructions. The media was changed on day 3 and where applicable, supplemented with washed wild-type mouse platelets, added at a final concentration of $1x10^8$/ml. Measurements were normalised by subtracting measurements taken from wells containing a BD cell insert without cells seeded. Measurements were then multiplied by the area of the filter, giving a resistance reading in Ω/cm^2. Images of cell monolayers were captured each day using a Zeiss Axiovert Zoom brightfield microscope with a 5 X air objective and processed using Image J64.

2.6.2 Scratch wound assay

Surfaces of wells within a 24 well plate were coated with 0.5% gelatin/PBS for 10 min at 37°C. CPECs were seeded at a density of $1x10^5$ in 800 µl of media and grown to confluence over 48 hours. Media was removed and the underside of the plate was marked to identify points for imaging. Scratches were made through the CPEC monolayer using a 20 µl pipette tip and 800 µl of media was re-introduced. Images of the scratches were taken at the designated points at 0, 12, 24, 32 and 48 hours. 24 hours was identified as the optimal time-point, with no further cell growth at 32 and 48 hours. To determine the affect of platelets on CPEC behaviour, media was supplemented with platelets at a final concentration of $1x10^7$/ml or $1x10^8$/ml, from either wild-type or megakaryocyte/platelet specific CLEC-2-deficient platelets (*Section 2.6.3*). Images were taken at 0 and 24 hours of incubation. All images were taken using a Zeiss Axiovert Zoom brightfield microscope with a 5 X air objective. Image analysis was performed in Image J64.

2.6.3 Preparation of washed mouse platelets

Mice were terminally bled under isofluorane anaesthesia. A laparotomy was performed exposing the descending aorta and blood was drawn into 10% ACD. Blood was further diluted into 200 µl of Tyrode's-HEPES buffer (134 mM NaCl, 0.34 mM Na_2HPO_4, 2.9 mM KCL, 12 mM $NaHCO_3$, 20 mM HEPES, 5 mM glucose, 1 mM $MgCl_2$, pH 7.3) and centrifuged in a microcentrifuge for 5 min at 2000 rpm. Platelet rich plasma (PRP) and the top third of erythrocytes were isolated and further centrifuged for 6 min at 200 g. Prostacyclin (10 µg/ml) was added to PRP and centrifuged for 6 min at 1000 g. Platelet pellets were resuspended in Tyrode's-HEPES buffer to a concentration of 1 $x10^9$/ml. Platelets were left rested for at least 30 min before use.

2.7 Statistical analysis

Statistical analysis was performed as appropriate for the specific data distribution and is detailed in the individual methods sections or in the figure legends. Where data was not found to be significant, this is not stated, or referred to as not significant.

CHAPTER 3

PODOPLANIN AND CLEC-2 INTERACTIONS DRIVE VASCULAR PATTERNING AND INTEGRITY IN THE DEVELOPING BRAIN

3.1 Introduction

The discovery of podoplanin as an endogenous ligand for the platelet receptor CLEC-2 triggered nearly a decade of research into its physiological role and significance (Suzuki-Inoue *et al*., 2007). A key early finding was the characterisation of the CLEC-2 signalling pathway, incorporating the signalling molecule SYK, adaptor protein SLP-76 and the enzyme PLCγ2 (Suzuki-Inoue *et al*., 2006). Previous studies had shown that mice deficient in SYK, SLP-76 or PLCγ2 developed subcutaneous haemorrhages in the skin and oedema in the back by mid-gestation (Turner *et al*., 1995; Cheng *et al*., 1995; Wang *et al*., 2000; Clements *et al*., 1999). Shortly after, podoplanin-deficient mice were generated and shown to harbor the same phenotype, which was shown to be attributable to the impaired separation of the blood and lymphatic vasculature (Fu *et al*., 2008).

Initial studies by our group set out to investigate a role for CLEC-2 in the development of this phenotype, for which mice with a constitutive loss of CLEC-2 (*Clec-2*$^{-/-}$), or mice with a specific loss of CLEC-2 in the megakaryocyte/platelet lineage (*Clec-2*$^{fl/fl}$*PF4-Cre*), were generated (*Figure 3.1*). *Clec-2*$^{-/-}$ mice were born at Mendelian frequency up to birth, however, 90% died within the first 24 hours due to respiratory failure. During development, as expected, *Clec-2*$^{-/-}$ mice presented with a number of developmental defects, most notably the formation of the characteristic blood-lymphatic mixing phenotype by E14.5. A specific role for CLEC-2 on platelets was considered, since *Clec-2*$^{fl/fl}$*PF4-Cre* and *Syk*$^{fl/fl}$*PF4-Cre* mice also exhibit this phenotype and there is no available evidence to support there being significant expression of CLEC-2 on another haematopoietic cell, at this stage of development (Finney *et al*., 2012). However, it should be noted that *PF4-Cre* is expressed on sub-populations of other lineages, leaving open the

possible involvement of another cell type (Calaminus *et al*., 2012). The mechanism of blood-lymphatic mixing has been extensively studied and is thought to be mediated by a combination of lymphatic-venous connections and retrograde flow through the thoracic duct (Discussed in *Section 1.4.3*) (Hess *et al*., 2014; Bohmer *et al*., 2010; Suzuki-Inoue *et al*., 2010).

Interestingly, when looking earlier in development, *Clec-2*$^{-/-}$ mice were found to develop haemorrhages throughout the fore-, mid- and hindbrain by E12.5, which were localised to the developing brain parenchyma and ventricles (*Figure 3.2*). A similar pattern of consistent haemorrhaging was observed in SYK-deficient mice, albeit, histological analysis revealed haemorrhages to be less severe and restricted to the parenchyma (*Figure 3.2*). Furthermore, the loss of CLEC-2 or SYK in the megakaryocyte/platelet lineage using the *PF4-Cre* transgene resulted in mild cerebral haemorrhaging (*Figure 3.2*) (Finney *et al*., 2012).

These neurovascular defects were believed to be unrelated to defects in lymphatic development, since the lymphatic system is absent from the brain and haemorrhaging in the cerebral vasculature was coincident with, or possibly occured before, blood-lymphatic mixing. Interestingly, a cerebral phenotype has not been reported in podoplanin-deficient mice, although the loss of T-synthase, a key glycosyltransferase enzyme responsible for glycosylation of the podoplanin extracellular domain, results in the formation of a disorganised microvascular network, with defective recruitment of ECM and pericytes, leading to haemorrhaging throughout the brain parenchyma and ventricles by E12.0, and lethality by E14.0 (Xia *et al*., 2004). Haemorrhages were not observed in endothelial specific T-synthase deficient mice, which exhibited blood-lymphatic mixing, consistent

with the neurovascular defect being independent of the defect in lymphatic development (Fu *et al*., 2008).

The aim of this chapter was to further characterise and investigate the mechanism of developmental defects within the central nervous system of CLEC-2-deficient mice. To achieve this, a podoplanin-floxed mouse was generated and crossed to a *PGK-Cre* or *Nestin-Cre* mouse to delete podoplanin ubiquitously at the two-cell stage, or specifically in neural progenitors, respectively. State-of-the-art 3-dimensional microscopy was used to show the localisation and extent of cerebral haemorrhages and to visualise the patterning of the developing vasculature. Immunofluoresence staining and electron microscopy were employed to further investigate the integrity of the developing NVU. To investigate a possible role for haemostasis in the neurovascular defect, mice deficient in the major platelet integrin subunit αIIb, or mice deficient in the neurobeachin-like-2 (NBEAL-2) protein, which lack platelet α-granules, were studied.

3.2 Results

3.2.1 Generation of CLEC-2-deficient mice

Clec-2$^{fl/fl}$ mice were generated as described in *Figure 3.1*, where the presence of Cre recombinase resulted in the excision of the floxed CLEC-2 allele, producing a non-functional CLEC-2 gene. A ubiquitously active, general cre deleter (rosa(SA-CrepA) was used at Taconic Artemis to generate mice constitutively deficient in CLEC-2 (*Clec-2*$^{-/-}$), while the *Clec-2*$^{fl/fl}$ mouse was crossed to the *PF4-Cre* transgene (*Clec-2*$^{fl/fl}$*PF4-Cre*) to mediate specific deletion of CLEC-2 in the megakaryocyte/platelet lineage (Tiedt *et al*., 2007). Expression of the wild-type, floxed or knock-out CLEC-2 alleles, and the presence of the *PF4-Cre* locus were confirmed by PCR as shown in *Figure 3.1*.

In this initial study, three *Clec-2*$^{-/-}$ mice survived up to P30 before being culled due to ill health (Finney *et al*., 2012). Since this time, no *Clec-2*$^{-/-}$ mice out of the expected 85.5 survived past 24 hours (*Table 3.1*). To investigate the influence of the background of the mice on their viability, *Clec-2*$^{-/-}$ mice on a C57BL/6 background were backcrossed onto a 129s/v background, but no viable *Clec-2*$^{-/-}$ offspring were obtained (*Table 3.1*).

Clec-2$^{fl/fl}$*PF4-Cre* mice, by contrast, were born at Mendelian frequency, were viable and appeared normal (*Table 3.2*). Upon dissection, *Clec-2*$^{fl/fl}$*PF4-Cre* adult mice exhibited a blood-lymphatic mixing phenotype in the abdomen, which will be discussed in *Chapter 5*.

3.2.2 Histological analysis of the developing brain in CLEC-2-deficient embryos

Progressing from published observations showing haemorrhaging in the CNS of *Clec-2*$^{-/-}$ mice at E12.5 (*Figure 3.2*), earlier developmental time points were investigated. Haemorrhages were seen to develop between E10.5 and E11.5 in *Clec-2*$^{-/-}$ embryos, becoming more substantial by E12.5 (*Figure 3.3A*). Closer inspection of H&E sections at E12.5 showed haemorrhages to displace large areas of the neuro-epithelium and protrude into ECM tissue (*Figure 3.3B*).

At this early stage in development, the only endogenous ligand for CLEC-2, podoplanin, is expressed throughout the developing neural tube on neuro-epithelial cells, as characterised by its co-expression with the intermediate filament protein, nestin (*Figure 3.4A and B*). By E14.5, podoplanin expression becomes restricted to the choroid plexus and the ependymal lining of the ventricle wall (*Figure 3.4A*). Despite the high expression of podoplanin in the neural tube, coinciding with the development of haemorrhages in both CLEC-2 and T-synthase deficient embryos, to date no study has described this phenotype in podoplanin-deficient mice.

3.2.3 Generation and characterisation of podoplanin-deficient mice

To investigate a role for podoplanin in the development of cerebral haemorrhages, a floxed podoplanin mouse was generated (*Figure 3.5*) and crossed to mice expressing Cre recombinase driven by the maternal PGK-1 promoter, to mediating constitutive recombination of the floxed allele from the two-cell stage (Lallemand *et al*., 1998), resulting in a non-functional podoplanin gene (*Pdpn*$^{fl/fl}$*PGK-Cre*). *Pdpn*$^{fl/fl}$*PGK-Cre* mice were found at Mendelian frequency up to E18.5 but found to be lethal at birth, with only one *Pdpn*$^{fl/fl}$*PGK-Cre* mouse surviving past P0 that was later culled due to ill health before weaning (*Table 3.3*). Breeding analysis from pairs set up to generate 50% heterozygous and wild-type offspring, compared to pairs set up to generate 50% heterozygous and 50% podoplanin-deficient offspring, revealed an increase in the number of pups dying by P1 and a significant decrease in the number of viable pups post-weaning in the latter breeding pair (*Figure 3.6*). Due to the marginal difference in total litter sizes recorded, it is likely that due to the severity of the phenotype in *Pdpn*$^{fl/fl}$*PGK-Cre* mice at birth, most pups will have been eaten prior to the litter being recorded.

In line with previous studies, podoplanin-deficient mice presented with a characteristic pattern of blood filled vessels on the surface of the skin at E14.5 and E16.5, indicative of a blood-lymphatic mixing phenotype (*Figure 3.21*). Reminiscent of CLEC-2-deficient embryos, *Pdpn*$^{fl/fl}$*PGK-Cre* embryos developed cerebral haemorrhages between E10.5 and E11.5 that become more prominent by E12.5 (*Figure 3.7*). H&E sections revealed haemorrhages through vast areas of the neuro-epithelium at E12.5, protruding into the surrounding ECM tissue. Blood vessels in *Pdpn*$^{fl/fl}$*PGK-Cre* embryos often appeared distended from the surrounding neuro-epithelium, in contrast to the intimate association of blood vessels with the surrounding tissue in *Pdpn*$^{fl/fl}$ littermates (*Figure 3.7*). Taken

together, the cerebral phenotype observed in podoplanin-deficient embryos mimics that of embryos deficient in its only known endogenous ligand, CLEC-2.

3.2.4 Cerebral haemorrhages in podoplanin-, CLEC-2- and SYK-deficient mice persist up to E14.5

In both *Clec-2*$^{-/-}$ and *Pdpn*$^{fl/fl}$*PGK-Cre* embryos, haemorrhages did not readily resolve and could be seen by histology at E14.5 and E16.5 to occupy large areas of the developing neuro-epithelium, accumulating in the ventricles (*Figure 3.8*). Immunofluorescence staining of wild-type and *Clec-2*$^{-/-}$ embryos at E14.5 demonstrated that the haemorrhages in the parenchyma and in the ventricles were rich in CD41+ platelets (*Figure 3.9*). Haemorrhages were also found to persist in *Syk*$^{-/-}$ embryos, where large areas of the neuro-epithelium were displaced by erythrocyte-rich haemorrhages (*Figure 3.10*). In *Clec-2*$^{fl/fl}$*PF4-Cre* embryos, substantial haemorrhages could be seen in the parenchyma of 2/6 embryos at E12.5, persisting in 1/6 embryos to E14.5 (*Figure 3.11*). As discussed in Finney *et al* (2012), the phenotype in *Clec-2*$^{fl/fl}$*PF4-Cre* mice was more variable and less severe, possibly owed to residual CLEC-2 expression during early development. Furthermore, although haemorrhages were consistently observed in the CNS upon dissection, it is likely that small haemorrhages were missed by histology, given that it was not feasible to section the entire embryo. These results demonstrate that haemorrhages in podoplanin-, CLEC-2- and SYK-deficient mice do not readily resolve and persist in the developing nervous system past mid-gestation.

3.2.5 Ultramicroscopy as a tool to visualise the developing vasculature in CLEC-2- and podoplanin-deficient mice

To investigate the cause of cerebral haemorrhaging in *Clec-2*$^{-/-}$ and *Pdpn*$^{fl/fl}$*PGK-Cre* embryos, a more in depth analysis of the developing vasculature was required. Due to the limitations of 2-dimensional microscopy, the planar illumination based microscope modality, ultramicroscopy, was used to visualise the developing cerebral vasculature in 3-dimensions. Ultramicroscopy creates stacks of optical sections that are analysed and reconstructed into a single 3D image, thereby allowing the localisation and scale of haemorrhages to be better studied. The vasculature in *Clec-2*$^{-/-}$, *Pdpn*$^{fl/fl}$*PGK-Cre* and wild-type littermates (+/+ includes *Pdpn*$^{fl/fl}$ littermates) was analysed at E10.5 and E12.5 by immunofluorescently labeling embryonic heads with PECAM-1. Prior to the appearance of haemorrhages, the vasculature at E10.5 appeared tortuous and abnormally patterned in *Clec-2*$^{-/-}$ and *Pdpn*$^{fl/fl}$*PGK-Cre* embryos, compared to the organised, characteristic branching patterns of wild-type embryos (*Figure 3.12A*). By E12.5, haemorrhages were clearly visible throughout the developing fore-, mid- and hindbrain in CLEC-2- and podoplanin-deficient mice, as indicated by dense areas of PECAM-1 staining (*Figure 3.12B*, red arrows). The size and localisation of haemorrhages can only fully be appreciated by a complete spatial reconstruction of the entire embryonic brain that is provided by the ultramicroscopy approach. Higher magnification images of the vasculature at E12.5 revealed the presence of large haemorrhages amongst aberrantly patterned vascular networks in *Clec-2*$^{-/-}$ and *Pdpn*$^{fl/fl}$*PGK-Cre* embryos (*Figure 3.12B*, right panel, red dashed lines outline haemorrhages). Developing blood vessels were discontinuous and appeared prone to haemorrhage compared to the intricately branched sheets of vessels that were observed in wild-type (+/+) littermates (*Figure 3.12B*, right panel).

Imaris software was used to quantify the area and branching patterns of the developing vasculature of *Clec-2*$^{-/-}$ and *Pdpn*$^{fl/fl}$*PGK-Cre* embryos compared to littermate controls. Due to the complexity and size of the images obtained, regions were cropped to dimensions of x-503 μm, y-503 μm, z-100 μm for analysis. An algorithm was optimised to create a surface over the PECAM-1 vascular network, allowing surface area measurements to be extracted (*Figure 3.13B* and *Figure 3.14A and C*). Once optimised, the parameters were applied equally to all samples. To extract measurements of filament length and branch points, the filament tracer tool was used, which again required optimisation (*Figure 3.13C*). Both the surface area and filament tracer tools allowed for haemorrhagic areas to be excluded (*Figure 3.14C*). Nevertheless, in highly complex areas of the images, surface and filament traces could not be perfectly extracted. At E10.5, the total surface area and total length of all vessels were comparable between *Clec-2*$^{-/-}$ embryos and wild-type littermates, while in *Pdpn*$^{fl/fl}$*PGK-Cre* embryos, there was a trend for the vessel area and vessel length to be reduced compared to wild-type littermates, although this difference was not significant (*Figure 3.14B*). By E12.5, the surface area of vessels and the total vessel length in *Pdpn*$^{fl/fl}$*PGK-Cre* embryos was similar to wild-type littermates, and while an increase was observed in *Clec-2*$^{-/-}$ embryos, this was not significant (*Figure 3.14D*). The total number of vessel branch points and the number of branched vessels was comparable between *Clec-2*$^{-/-}$, *Pdpn*$^{fl/fl}$*PGK-Cre* embryos and wild-type littermates at both E10.5 and E12.5 (*Figure 3.14B and D*). Taken together, it was concluded that there was no major change in vessel branching in podoplanin- or CLEC-2-deficient embryos. However, it cannot be excluded that a more subtle change was masked by limitations in the analysis, as described above.

3.2.4 Quantifying vascular networks using the hindbrain model

Due to the difficulty experienced in quantifying blood vessel network parameters from complex 3-dimensional images, a new method was trialed, developed by Fantin *et al* (2013) that allowed the architecture of the vasculature in the hindbrain to be studied. The hindbrain model was specifically designed to study cerebral angiogenesis, given that the hindbrain tissue is isolated from its surrounding vascular plexus (Fantin *et al*., 2013). Preliminary analysis of hindbrains from *Clec-2*$^{-/-}$, *Pdpn*$^{fl/fl}$*PGK-Cre* embryos and wild-type littermates, revealed a trend towards a small (<20%) increase in the surface area of vessels, number of branch points and branched vessels in *Clec-2*$^{-/-}$ and *Pdpn*$^{fl/fl}$*PGK-Cre* embryos, corresponding with a decrease in the average vessel length (*Figure 3.15*), albeit these were not significant. Further imaging and analysis could provide a more detailed insight into the patterns of vessel sprouting, for example, specifically focusing on PECAM-1 dense tip cell projections and monitoring vessel growth at different embryonic stages.

3.2.5 Quantifying pericyte coverage in CLEC-2- and podoplanin-deficient mice

Both ultramicroscopy and hindbrain model imaging showed that despite vessels appearing tortuous in CLEC-2 and podoplanin-deficient embryos, they were able to successfully sprout from the PNVP and extend through the neuro-epithelium. This indicated that the initial stages of angiogenesis driven primarily by the VEGF and Wnt-β-catenin pathways were largely unperturbed (Walls *et al*., 2008; Breier *et al*., 1992; Obermeier *et al*., 2013). As a result, further work was focused on the maturation of cerebral vessels, a process by which nascent angiogenic vessels, are transformed into a structurally supported vascular network, through the recruitment of mural cells, ECM proteins and neurons. Amongst these mural cells are pericytes, which overlay endothelial cell junctions to support smaller arterioles, venules and capillaries (Armulik *et al*., 2010). Immunostaining of tissue sections revealed a significant reduction in the number of NG2+ pericytes recruited to PECAM-1+ blood vessels in the neuro-epithelium of *Clec-2*$^{-/-}$and *Pdpn*$^{fl/fl}$*PGK-Cre* embryos, compared to wild-type littermates at E11.5 (*Figure 3.16*). Similar to the observations taken from the analysis of H&E sections, blood vessels often appeared distended from the surrounding neuro-epithelium (*Figure 3.16*).

In light of the clear visualisation of vascular networks that was seen by whole-mount immuno-staining of isolated hindbrains (Figure *3.15*), this model was used to quantify pericyte recruitment to developing cerebral vessels, in order to verify observations seen from tissue sections. Pericyte coverage on hindbrain vessels was quantified by comparing the intensity of immunostaining for the pericyte marker NG2, relative to that of PECAM-1 positive blood vessels (*Figure 3.17*). No significant difference in pericyte coverage was observed between *Clec-2*$^{-/-}$and *Pdpn*$^{fl/fl}$*PGK-Cre* embryos, compared to wild-type littermates at E12.5.

3.2.6 Ultrastructural analysis of cerebral microvessels by electron microscopy

To investigate the ultrastructure of developing cerebral microvessels in more detail, CLEC-2- and podoplanin-deficient embryos were taken at E11.5 and processed for electron microscopy. In wild-type littermate controls, the blood vessel endothelium could be seen to enclose a lumen containing a nucleated fetal red blood cell (*Figure 3.18*). At this stage of development, the thick, supportive basal lamina characteristic of mature microvessels could not be observed, but tight junctions were seen connecting adjacent endothelial cells. Pericytes and neuro-epithelial cells were visibly associated with the endothelium, providing structural support for developing microvessels. By contrast, although endothelial cell junctions appeared well established in *Clec-2*$^{-/-}$and *Pdpn*$^{fl/fl}$*PGK-Cre* embryos, shown by visible endothelial cell flaps, vascular lumens appeared expanded and the endothelium was rich in vacuoles, appearing fragile, tortuous and prone to haemorrhage (*Figure 3.18*). Large gaps were visible between the blood vessel endothelium and the surrounding pericytes and neuro-epithelial cells, precluding their critical structurally supportive role.

3.2.7 Generation of neural-specific podoplanin-deficient mice

Earlier in this Chapter, podoplanin was shown to be expressed throughout the neural tube at E11.5, where it was co-expressed with the intermediate filament protein nestin (*Figure 3.4*). To confirm that podoplanin expression on neuro-epithelial cells is required for the development and integrity of cerebral vessels, $Pdpn^{fl/fl}$ mice were crossed to mice expressing cre recombinase under the control of the nestin promoter (*Nes-Cre*). There are at least three Nes-Cre lines that have been generated and this transgenic line was chosen because of its early onset, targeting neural progenitors from E8.5, before the onset of brain vascularisation (Petersen *et al*., 2002). $Pdpn^{fl/fl}$*Nes-Cre* mice were present at Mendelian frequency up to E14.5, but were found to be lethal at birth, with only one pup successfully weaned (*Table 3.4*). By comparing mating pairs that were expecting all heterozygous or wild-type offspring, to pairs expecting 50% $Pdpn^{fl/fl}$*Nes-Cre* mice, it was apparent that $Pdpn^{fl/fl}$*Nes-Cre* mice were lethal within the first post-natal days, with smaller litter sizes recorded, more deaths by P1 and fewer pups successfully weaned (*Figure 3.19*). Analysis of more offspring may increase the certainty of these initial observations which are currently not statistically significant.

The successful deletion of podoplanin on neuro-epithelial cells by the nestin promoter was confirmed by immunofluorescence staining on tissue sections from E11.5 $Pdpn^{fl/fl}$*Nes-Cre* embryos, compared to the maintained expression of podoplanin that was seen in $Pdpn^{fl/fl}$ littermate controls (*Figure 3.4C*).

3.2.8 Histological analysis of *Pdpn$^{fl/fl}$Nes-Cre* embryos

Pdpn$^{fl/fl}$Nes-Cre embryos appeared identical to *Pdpn$^{fl/fl}$PGK-Cre* and *Clec-2$^{-/-}$* embryos, with haemorrhages developing in the fore-, mid and hindbrain between E11.5 and E12.5 (*Figure 3.20A*). H&E sections revealed a comparable phenotype to constitutive CLEC-2- and podoplanin-deficient mice, with haemorrhages displacing vast regions of the neuro-epithelium and collecting in the ventricles by E12.5 (*Figure 3.20B*). Haemorrhages were still present at E14.5, occupying large areas of the developing neural tissue (*Figure 3.20C*).

Intriguingly, *Pdpn$^{fl/fl}$Nes-Cre* embryos developed a characteristic pattern of blood-filled vessels on the surface of the skin at E14.5 and E16.5, reminiscent of the blood-lymphatic mixing phenotype observed in *Pdpn$^{fl/fl}$PGK-Cre* embryos (*Figure 3.21*). This suggests that nestin may be expressed outside of neural cells during development.

3.2.9 Defining the mechanism by which CLEC-2 activated platelets influence cerebral vascular development

Taken together, results so far suggest that podoplanin on neuro-epithelial cell progenitors, interacts with CLEC-2-expressing haematopoietic cells, to drive the maturation of cerebral vessels and prevent haemorrhage. During development, the only known haematopoietic cells with significant CLEC-2 expression are platelets, and it has been shown that the loss of CLEC-2 in this lineage results in cerebral haemorrhaging (*Figure 3.12*) (Finney *et al*., 2012). Furthermore, the loss of the downstream tyrosine kinase SYK, both constitutively and in the megakaryocyte/platelet lineage, mirrors the observations in CLEC-2-deficient mice, thus indicating a specific role for CLEC-2-induced platelet activation in cerebral vascular development (*Figure 3.10*) (Finney *et al*., 2012). A role for podoplanin-CLEC-2 interactions in a developing vascular environment as apposed to within a fully mature vascular network is supported by the absence of cerebral haemorrhage in mice where CLEC-2 was depleted post-development (discussed in *Chapter 5*). In a developmental setting, nascent angiogenic vessels continually remodel their extracellular matrix coating to allow for the generation of new vascular networks. This presents a pathway for platelets to interact with surrounding podoplanin-expressing neuro-epithelial cells. In support of this, platelets were often seen outside of blood vessels within the neuro-epithelium on frozen sections of wild-type embryos, early in development (*Figure 3.22*). Despite efforts to ensure all embryos were collected within the same time frame, rapid changes early on in development are likely to account for the variability in results (*Figure 3.22B*). Very rarely were platelets seen outside of mature blood vessels within the vascular beds that surround the neural tube. Furthermore, by E14.5, platelets were rarely seen outside of blood vessels within the neuro-epithelium itself. A small number of platelets were identified outside of blood vessels in each group,

likely due to the inherent errors introduced when dealing with 2-dimensional imaging (*Figure 3.22*).

To begin to understand a mechanism by which CLEC-2-induced platelet activation safeguards the developing cerebral vasculature from lethal haemorrhage, embryos deficient in αIIb were studied, which together with β3 forms the major platelet integrin. Haemorrhages were seen to develop in the nervous system of *αIIb*$^{-/-}$ embryos by E11.5, persisting at E12.5 and appearing to resolve by E14.5 (*Figure 3.23A*). The neuro-epithelium of *αIIb*$^{-/-}$ embryos at E10.5 appeared disorganised on H&E histological sections, with nucleated cells penetrating the ventricle walls (*Figure 3.23B*). By E11.5, eosin-stained erythrocytes accumulated in the ventricles, persisting to E12.5. Haemorrhages at E11.5 and E12.5 were consistently observed, but were less substantial than in CLEC-2-, podoplanin- and SYK-deficient embryos, with no large haemorrhagic areas seen in the neuro-epithelial tissue. By E14.5, cerebral haemorrhages in *αIIb*$^{-/-}$ embryos had largely resolved, and histologically, the developing neural system appeared identical to littermate controls (*Figure 3.23B*).

In addition to their adhesive properties, platelets are powerful secretory cells that release a range of bioactive molecules upon activation. In this study, a role for platelet α-granules was considered, because they are enriched in both angiogenic and haemostatic molecules, such as VEGF and VWF (Deppermann *et al*., 2013). Neurobeachin-like-2 (NBEAL-2) was identified as an important regulator in the biogenesis of platelet α-granules and as the causative gene for Grey platelet syndrome, a rare congenital disorder characterised by a mild thrombocytopenia and moderate bleeding tendency, due to the absence of α-granules (Albers *et al*., 2011; Kahr *et al*., 2011; Gunay-Aygun *et al*., 2011). Deppermann el al

(2013) used a mouse model of Grey platelet syndrome (*Nbeal-2*$^{-/-}$) that recapitulates many of the phenotypic tendencies of patients, including an absence of characteristic α-granules, although a small number of aberrantly formed α-granule-like structures could be observed (Deppermann *et al*., 2013). The loss of NBEAL-2 caused a mild cerebral haemorrhagic phenotype in 2/12 embryos at E12.5, while 4/4 littermate controls appeared normal (*Figure 3.24A*). On H&E coronal sections, no clear haemorrhagic regions could be observed, with only occasional blood vessels appearing dissociated from an otherwise organised neuro-epithelium (*Figure 3.24C*). By E14.5, all *Nbeal-2*$^{-/-}$ embryos appeared identical to littermate controls, with the integrity of blood vessels and their surrounding cell network appearing identical to littermate controls (*Figure 3.24B and C*). These results suggest only a minor role for platelet α-granule secretion in maintaining the integrity of the cerebral vasculature.

3.3 Discussion

The primary aim of the work in this chapter was to investigate the basis of the cerebral haemorrhagic defect in CLEC-2 deficient mice. This has involved the generation and characterisation of podoplanin-deficient mice to assist in dissecting the mechanism by which CLEC-2 and podoplanin influence the development of the cerebral vasculature.

Initial characterisation of *Clec-2*$^{-/-}$ mice described the presence of haemorrhages in the CNS at E12.5 (Finney *et al*., 2012). The timing and presentation of haemorrhages were reminiscent of those seen by Tang *et al* (2010) who previously generated *Clec-2*$^{-/-}$ mice, localising haemorrhages to the parenchyma at E12.0 (Tang *et al*., 2010). From this stage in development, podoplanin becomes increasingly restricted to the ependymal lining of the ventricle walls and the choroid plexus (M. C. Williams *et al*., 1996). It therefore became important to investigate the role of CLEC-2 and podoplanin at earlier developmental time points, when podoplanin is expressed throughout the neural tube on neuro-epithelial cells.

To delete podoplanin at this early stage in development, a *PGK-Cre* transgene was used, generating a podoplanin-deficient mouse strain on a C57BL/6 background. The lethality of *Pdpn*$^{fl/fl}$*PGK-Cre* offspring was reminiscent to that observed in podoplanin-deficient mice generated on a 129sv background, whereby the majority of pups died at birth, and is in contrast to mice previously generated on a C57BL/6 background, where 20% of offspring were viable (Uhrin *et al*., 2010; Schacht *et al*., 2003; Ramirez *et al*., 2003). The reason for these differences in viability are unknown, but appear not to be entirely dependent on the strain background, but may instead reflect the efficiency of the genetic

deletion.

This is the first report to describe cerebral haemorrhaging in CLEC-2- and podoplanin-deficient mice to develop between E10.5 and E11.5, a critical time point for neural vascularisation. A comparable pattern of haemorrhaging was seen in a mouse model inducing deletion of podoplanin on neural progenitors, indicating a specific role for podoplanin on neuro-epithelial cells. Interestingly, subcutaneous haemorrhages were also observed in the skin of *Pdpn*$^{fl/fl}$*Nes-Cre* embryos at E14.5, reminiscent of the characteristic blood-lymphatic phenotype observed in CLEC-2- and podoplanin-deficient embryos. Nestin is widely recognised for its expression on neuro-epithelial stem/progenitor cells in the developing CNS, becoming more highly expressed in the proliferative ventricular zones by E14.5, and further restricted to a population of ependymal cells by E16.5, mimicking the expression pattern of podoplanin (Sugawara *et al*., 2002). Interestingly, a number of reports have described nestin to additionally function as a marker for proliferating endothelial cells in both adult CNS and non CNS tumours, as well in normal adult tissues, including the human pancreas (Sugawara *et al*., 2002; Teranishi *et al*., 2007; Klein *et al*., 2003). Furthermore, developmental expression of nestin in proliferating endothelial cells was reported specifically in angiogenic tissues in rats (Mokrý & Nemecek, 1998). Together, these reports provide confounding evidence to support nestin expression on proliferating endothelial cells. The importance of these studies in the context of the cerebral phenotype observed in podoplanin- and CLEC-2-deficient mice is minimal, given that podoplanin is only expressed on lymphatic endothelium, which is absent in the brain. Nevertheless, it remains important to investigate the pattern of recombination of podoplanin by the *Nes-Cre* transgene used in this study. This will be achieved by introducing the *Nes-Cre* transgene into the *Rosa26*^{Yfp}

reporter mouse (obtained from Jackson Laboratories), which produces yellow fluorescent protein (YFP) in all cells expressing cre recombinase (Srinivas *et al*., 2001). A similar strategy was recently used by two independent groups to investigate the expression of PF4-Cre outside of the megakaryocyte/platelet lineage (Pertuy *et al*., 2014; Calaminus *et al*., 2012). Embryos will be collected at different time-points during development and the expression of nestin will be investigated by co-staining with a range of cell markers, e.g. endothelial cell markers. Future studies may also compare the other available Nestin-Cre transgenic mouse models (Tronche *et al*., 1999; Zimmerman *et al*., 1994).

Results so far imply a role for podoplanin specifically on neuro-epithelial cells in preventing cerebral haemorrhage during development. The CLEC-2 expressing cell type proposed to interact with podoplanin in this setting is platelets, given that there is no evidence for significant CLEC-2 expression on any other circulating cell during development. The varying severity of the cerebral phenotype resulting from a megakaryocyte/platelet specific deletion of CLEC-2 or SYK is also apparent in the context of the blood-lymphatic mixing phenotype, for which a wealth of research has been conducted. This variability is thought to result either from incomplete deletion of the genes resulting in a small fraction of platelets expressing CLEC-2 early in development, or the expression of CLEC-2 in megakaryocyte progenitors prior to deletion of the gene, due to the delay in Cre expression downstream of the PF4-promoter (Finney *et al*., 2012). The latter theory is supported by the observation that deleting CLEC-2 or SYK in all haematopoietic lineages using a *Vav-Cre* transgene results in a phenotype comparable to *PF4-Cre* mediated deletion (Bertozzi, Schmaier, *et al*., 2010b; Finney *et al*., 2012). Furthermore, as discussed in detail in *Section 1.41,* blood-lymphatic mixing is also observed in mice lacking functional megakaryocytes (*Meis-1*$^{-/-}$), or following the

inducible ablation of the megakaryocyte/platelet lineage using diphtheria toxin or aspirin treatment, although it should be noted that the latter studies are dependent on the selectivity of *PF4-Cre* and that aspirin is not specific to the megakaryocyte-lineage (Uhrin *et al*., 2010; Carramolino *et al*., 2010). Together these studies support a role for CLEC-2 on platelets, in vascular development.

With this in mind, the mechanism by which activated platelets guide and maintain vascular integrity during development was investigated. Strikingly, a haemorrhagic phenotype was observed in mice deficient in one of the subunits of the major platelet integrin αIIbβ3 at E12.5. Thus, haemorrhaging is presumably influenced by a loss of integrin αIIbβ3-mediated platelet adhesion and/or aggregation. Although this role of the integrin is a component of classical haemostatic function of platelets, this is the first description of haemorrhaging associated specifically with the loss of this pathway during development. Remarkably, however, haemorrhages in αIIb-deficient mice appeared to resolve by E14.5, whereas in *Clec-2*$^{-/-}$ and *Pdpn*$^{fl/fl}$*PGK-Cre* embryos haemorrhages were still prominent at this stage. This suggests an additional mechanism is influenced by the loss of CLEC-2 activation, possibly the angiogenic development of cerebral vessels, leading to a persistent haemorrhagic phenotype. In addition, CLEC-2 drives integrin-dependent platelet aggregation that functions to plug the vessel wall during development.

3-dimensional imaging of the vasculature at E10.5 and E12.5 showed that vessels successfully invade the neural tube from the PNVP by angiogenesis to form a primitive vascular network. However, these nascent vessels appeared tortuous and prone to haemorrhage, indicating the defect lies in the transformation of these ‘leaky’ vessels into a structurally supported vascular system. Several independent studies have shown that

disrupting key signalling mechanisms that are involved in the recruitment of mural cells and ECM proteins to nascent developing vessels, also culminates in cerebral haemorrhaging around the same stage in development (McCarty *et al*., 2002; Hellström *et al*., 2001; Proctor *et al*., 2005; Bader *et al*., 1998; Zhu *et al*., 2002). For example, integrins are key ECM proteins that coat the albuminal vessel wall and mediate the recruitment of perivascular cells, such as pericytes, to aid the maturation of nascent vessels. Mice with a specific loss of the integrin subunit β8 in the neuro-epithelium develop tortuous vessels, owed to defective associations between the endothelium and the surrounding neuro-epithelial and glial cells, reminiscent of the results observed by electron microscopy in *Clec-2*$^{-/-}$ and *Pdpn*$^{fl/fl}$*PGK-Cre* embryos (Proctor *et al*., 2005). Similarly, the PDGFβ-PDGFRβ axis stimulates the recruitment and spreading of perivascular cells across the endothelium. PDGFRβ$^{-/-}$ mice also developed cerebral haemorrhages during development, resulting from endothelial hyperplasia in nascent blood vessels, leaving them fragile and tortuous. Similar to what was observed in the present study, no significant differences were observed in the density, length and branching of vessels, eluding to a role for PDGFRβ in the maturation of an already established primitive vascular network. The fragility of nascent vessels in PDGFRβ$^{-/-}$ mice was instead shown to be attributed to the defective recruitment of pericytes (Hellström *et al*., 2001). A reduction in pericyte recruitment was also observed on tissue sections from *Clec-2*$^{-/-}$ and *Pdpn*$^{fl/fl}$*PGK-Cre* embryos, albeit this phenotype was not replicated in the preliminary analysis of whole-mount, immuno-stained, hindbrains. The question therefore remains as to which of these pathways are related to the role of CLEC-2 and platelets in the development of the cerebral vasculature.

In addition to their adhesive properties, platelets are powerful secretory cells, releasing a

range of bioactive molecules upon activation. In this study, a specific role for α-granules was considered, given their enrichment in growth factors such as VEGF and various other haemostatic proteins, including VWF. However, the mild haemorrhagic phenotype observed in NBEAL-2-deficient mice, with less than 20% exhibiting haemorrhaging, argued against a major role for platelet α-granule secretion in cerebral vascular development and was consistent with the mild bleeding diathesis observed in adult Nbeal-$2^{-/-}$ mice (Deppermann *et al*., 2013).

Independent of α-granules, platelets release a number of lipid mediators, including a range of prostanoids, leukotrienes and the bioactive lipid S1-P, while also critically supporting the formation of lysophosphatidic acid (LPA). Platelets support the generation of LPA through a process that is primarily mediated by binding of extracellular autotaxin to integrin αIIbβ3 (Fulkerson *et al*., 2011). Interestingly, mice deficient in the G-protein coupled LPA receptor, LPA_4, were prone to haemorrhage during gestation as a consequence of the defective recruitment of mural cells to developing blood vessels (Sumida *et al*., 2010). A strikingly similar phenotype was observed in mice deficient in the S1-P receptor, $S1P_1$, both globally and specifically on endothelial cells. A defect in the recruitment of mural cells to developing vessels led to extensive haemorrhaging throughout the developing brain and other organs, culminating in embryonic lethality by E12.5 (Liu *et al*., 2000; Allende *et al*., 2003). Studies in which circulating S1-P levels were eliminated, resulted in an even more severe phenotype, with severe haemorrhaging in the brain by E11.5 and delayed neural tube closure, indicating the involvement of multiple S1-P receptors (Mizugishi *et al*., 2005).

In a recent study, podoplanin and CLEC-2 were reported to play a critical role in the

maintenance of integrity of high endothelial venules through release of S1-P. Whereby the release of S1-P from platelets was found to be CLEC-2-mediated, stimulating up-regulation of V-cadherin in high endothelial venules and preventing blood flow into lymph nodes (Hess *et al*., 2014). It is possible that a similar mechanism takes place during the development of the cerebral vasculature, with S1-P regulating the integrity of endothelial tight junctions. Future studies will involve characterising mice that are deficient in platelet-derived S1-P to determine whether it plays any role in maintaining cerebral vascular integrity during development.

Taken together, a model is proposed whereby during the initial vascularisation of the neural tube, podoplanin on neuro-epithelial cells interacts with CLEC-2, stimulating platelet activation. While platelet aggregates plug the vessel wall to prevent haemorrhage, secreted molecules such as S1-P may function to recruit cells and matrix components to developing vessels to drive their maturation and integrity. In the absence of these interactions, vessels become tortuous and prone to haemorrhage (Summarised in *Figure 3.25*).

CHAPTER 4

EXPRESSION OF MURINE CLEC-2 IN THE HAEMATOPOIETIC SYSTEM

4.1 Introduction

Until now, the focus of research on CLEC-2 and podoplanin has been on their roles in development, but equally important is their role post-development, in particular in maintenance and repair pathways, as these share overlapping features with development. Given the discrepancies in the literature between transcript and protein expression of CLEC-2, it is essential to characterise the expression profile of CLEC-2 in the steady state and during inflammation in order to investigate these questions. Models of CLEC-2 depletion independent of changes in development must also be established.

Over a decade ago, CLEC-2 (gene name *Clec1b*) was identified in a transcriptomics study of human myeloid cells, with *Clec1b* mRNA detected in monocytes, DCs and granulocytes (Colonna *et al*., 2000). A later study identified human *Clec1b* mRNA in fetal liver, bone marrow and in whole blood, although interestingly, *Clec1b* mRNA was absent from leukocytes (*Figure 4.1*). More recent studies that used specific antibodies to CLEC-2, described robust surface expression of CLEC-2 on human platelets, while showing its absence from the surface of leukocytes isolated from whole blood, including monocytes, DCs, neutrophils, T- and B-lymphocytes (Suzuki-Inoue *et al*., 2006; Tang *et al*., 2010; Gitz *et al*., 2014). Together these data show that high-level expression of CLEC-2 is restricted to the platelet lineage in peripheral blood in humans.

A much wider mRNA expression profile was detected in the murine system, with *Clec1b* transcripts detected in placenta, lung, liver, lymph nodes, spleen and bone marrow (*Figure 4.2*) (Xie *et al*., 2008; Wu *et al*., 2009). In the haematopoietic system, serial gene expression analysis (SAGE) identified murine CLEC-2 to be a predominantly

megakaryocyte/platelet specific protein (Senis *et al*., 2006). Surface expression of CLEC-2 was later confirmed on platelets, but was additionally reported for liver Kupffer cells and peripheral blood neutrophils, the latter identified by an independent monoclonal antibody (mAb), 17D9 (Tang *et al*., 2010; Kerrigan *et al*., 2009). Interestingly, CLEC-2 expression was lower on neutrophils resident in the bone marrow and in those isolated from inflammatory sites than circulating neutrophils, suggesting that CLEC-2 is up regulated on these cells during trafficking. In the same study, CLEC-2 expression was induced on peripheral blood monocytes in response to toll-like receptor (TLR) 1or 2 stimulation, while absent under resting conditions (Kerrigan *et al*., 2009). The group of Reis e Sousa used the same antibody, 17D9 (which they had generated), to confirm expression of CLEC-2 on platelets and neutrophils, while also reporting CLEC-2 expression on splenic DCs, peritoneal macrophages, a subset of natural killer cells and B-lymphocytes, in the steady state. Furthermore, CLEC-2 expression was increased on splenic neutrophils, monocytes subsets, DCs, B-lymphocytes and natural killer cells following LPS stimulation (Mourao-Sa *et al*., 2011). This wide CLEC-2 surface expression profile does not correlate with the distribution of *Clec1b* transcript levels identified in the BioGPS database (*Figure 4.2*) and in leukocyte populations, as described in 'The immunological genome project' (*Figure 4.3*). Significant *Clec1b* levels were found only in a population of splenic macrophages, a thioglycolate-elicited population of peritoneal DCs and a population of bone marrow-derived neutrophils (*Figure 4.3*) (Wu *et al*., 2009; Heng *et al*., 2008). An independent study has since verified CLEC-2 to be present at both the mRNA and protein level (using recombinant podoplanin as a 'CLEC-2-specific' ligand) in DCs, albeit at low level, isolated from lymph nodes and skin. Furthermore, CLEC-2 expression was shown to be increased on the surface of DCs in response to LPS challenge (Acton *et al*., 2012).

A limitation of the study by Mourão-Sá *et al* (2011), in which a wide expression pattern of CLEC-2 was observed, is that data for representative staining of leukocytes in CLEC-2-deficient mouse models was described, but not shown (Mourao-Sa *et al*., 2011). Thus, the details of the full spectrum of experiments on the CLEC-2-deficient cells are not known.

The aim of this Chapter was to investigate the expression of CLEC-2 on circulating haematopoietic cells in adult mice, using the commercially available anti-CLEC-2 antibody, 17D9, developed by Mourão-Sá *et al* (2011) and a second murine anti-CLEC-2 antibody, INU1, that was developed by the group of Bernhard Nieswandt (Mourao-Sa *et al*., 2011; May *et al*., 2009). The specificity of these antibodies was validated by flow cytometry on cells isolated from adult CLEC-2-deficient mice. Two methods of CLEC-2 depletion in adult mice were characterised for this study, including the generation of *Clec-2*$^{-/-}$ fetal liver chimeras and tamoxifen-inducible deletion of CLEC-2 using the *ER*^{T2}*Cre* transgene.

4.2 Results

4.2.1 Generation of tamoxifen-inducible CLEC-2-deficient mice

It has previously been shown that constitutive deletion of CLEC-2 (*Clec-2*$^{-/-}$) results in embryonic lethality. For this reason, a mouse model was generated in which CLEC-2 is ubiquitously deleted in adult mice. *Clec-2*$^{fl/fl}$ mice were crossed to mice expressing Cre recombinase upstream of an estrogen receptor T2 cassette (ER^{T2}) driven by the *ROSA*^{26} locus (*Gt(ROSA)26Sortm1Sor)* (*Figure 4.4*) (Soriano, 1999; Hayashi & McMahon, 2002). *Clec-2*$^{fl/fl}$*ER*^{T2}*Cre* mice continuously produce Cre recombinase, which is sequestered in the cytoplasm by the ER^{T2} moiety until tamoxifen is administered, stimulating the release of Cre recombinase, which translocates to the nucleus to excise the floxed allele (*Figure 4.4*).

4.2.2 Initial characterisation of platelets in *Clec-2$^{fl/fl}$ER^{T2}Cre* mice

To characterise the efficiency of recombination of the *Clec-2$^{fl/fl}$* allele by the *ER^{T2}Cre* transgene, *Clec-2$^{fl/fl}$* and *Clec-2$^{fl/fl}$ER^{T2}Cre* mice were administered tamoxifen by i.p. injection and surface CLEC-2 levels on platelets from whole blood were monitored using 17D9 anti-CLEC-2 antibody. 5 consecutive days of tamoxifen dosing led to robust depletion of 17D9 staining from the platelet surface after 1 week, which was maintained at 7 weeks, demonstrating loss of CLEC-2. By 12 weeks, an average of 18% recovery of CLEC-2 protein was detected on the platelet surface (*Figure 4.5*). It was found that reducing injections to 1 or 3 consecutive days was insufficient to provide complete CLEC-2 depletion from the platelet surface in 6 week old mice (*Figure 4.6*). However, in 3 week-old mice, a single injection was sufficient to induce full depletion of CLEC-2 on the platelet surface, although after 4 weeks, a small amount of CLEC-2 was recovered (*Figure 4.7*). These results demonstrate that i.p. injection of tamoxifen successfully induces depletion of CLEC-2 from platelets, but the age of mice and the timeline of their use should be considered in experimental design.

4.2.3 Characterising CLEC-2 depletion on platelets and leukocytes in tamoxifen treated *Clec-2$^{fl/fl}$ER^{T2}Cre* mice

To monitor CLEC-2 depletion on leukocyte populations, many of which have much greater half-lives to that of platelets, alternative tamoxifen administration routes were compared to i.p. injection, due to concerns over the prolonged build up of corn oil in the abdomen, which can be detrimental in certain experimental models (e.g. intravital microscopy) and cause prolonged discomfort to the animal. Tamoxifen was administered in the diet (TAM400, Harlan Laboratories) with an estimated daily dose of 40 mg per kg body weight. It is common for mice to experience significant weight loss on tamoxifen diet (see *Chapter 5*) and so initially 2 weeks of tamoxifen diet was followed by conventional diet for 10 weeks. CLEC-2 expression on leukocytes in peripheral blood was measured using 17D9 at 1 and 12 weeks by flow cytometry. Cells were gated as described in *Figure 4.8*. CLEC-2 depletion on platelets was partial following 1 week on diet, with full deletion seen at 2 weeks (data not shown), which was maintained at 12 weeks (*Figure 4.9*). 17D9 binding was comparable on B-lymphocytes in *Clec-2$^{fl/fl}$* and *Clec-2$^{fl/fl}$ER^{T2}Cre* mice at 1 week, while at 12 weeks a partial reduction was seen in *Clec-2$^{fl/fl}$ER^{T2}Cre* mice (*Figure 4.9*). 17D9 binding to Gr1^{+}Mac-1^{+} myeloid cells (a neutrophil rich population, which will be referred to throughout the text as neutrophils) was comparable between *Clec-2$^{fl/fl}$* and *Clec-2$^{fl/fl}$ER^{T2}Cre* mice at 1 and 12 weeks (*Figure 4.9*). No significant binding of 17D9 was observed on T-lymphocytes.

To investigate depletion of CLEC-2 at the genomic level, DNA was extracted from whole blood of *Clec-2$^{fl/fl}$* and *Clec-2$^{fl/fl}$ER^{T2}Cre* mice treated with tamoxifen diet for 2 weeks followed by 5 weeks conventional diet, or following 7 weeks on continuous tamoxifen diet. Despite the marked presence of *Clec1b* KO DNA after 2 weeks of tamoxifen

treatment, a significant level of floxed *Clec1b* was still present (*Figure 4.10*). This was markedly reduced following 7 weeks of tamoxifen diet.

These results are consistent with binding of 17D9 to CLEC-2 on platelets and on B-lymphocytes, but indicate that 17D9 may also bind to a second site on myeloid cells and on B-lymphocytes (due to the partial rather than complete reduction in binding). Two weeks of tamoxifen diet induced full and sustained excision of the *Clec1b* gene from platelets, but only partial depletion from leukocytes. Genomic *Clec1b* DNA levels indicate that full deletion on leukocytes requires continuous tamoxifen treatment in the diet for a period greater than 7 weeks. Therefore it is important to determine whether 17D9 binding to CLEC-2 'depleted' cells is due to residual levels of CLEC-2, or to 17D9 binding to an alternative ligand.

4.2.4 Investigating the specificity of 17D9 anti-CLEC-2 antibody on leukocytes in whole blood

To further investigate the specificity of 17D9 and the expression profile of CLEC-2 on circulating leukocytes, a number of additional experimental tools were employed. Firstly, tamoxifen-inducible CLEC-2-deficient mice were treated for up to 6-12 months in order to take into account the extended life span of some leukocytes. During this time period *Clec-2*$^{fl/fl}$ and *Clec-2*$^{fl/fl}$*ER*^{T2}*Cre* mice developed a number of phenotypic abnormalities that will be discussed in *Chapter 5*. Secondly, radiation chimeras were generated and reconstituted with CLEC-2-deficient (*Clec-2*$^{-/-}$), or wild-type (+/+) fetal liver cells (C57BL/6). Chimeras were left for 6 weeks to allow donor cells to establish the haematopoietic compartment. Fetal liver chimeras were generated on both a C57BL/6 and on a BoyJ background to allow for donor and recipient cells to be distinguished. Cells from either C57BL/6 or BoyJ origin were distinguished by their expression of distinctive isoforms of the common leukocyte marker CD45, CD45.1 or CD45.2, respectively. The isoforms are functionally identical but can be used for antibody-mediated recognition (*Figure 4.11*). Therefore, leukocytes that may have not turned over during the 6-week irradiation and re-establishment period could be identified.

To investigate the expression of CLEC-2 during immune challenge, systemic inflammation was induced in chimeras by i.p. injection of LPS. LPS is a cell wall component of gram-negative bacteria, such as the common bacterium *Escherichia Coli* (*E.Coli*), and is known to effectively stimulate the innate immune system. An effective immunological response was measured by a simultaneous drop in platelet and white blood cell counts, which were usually concurrent with a small increase in mean platelet volume and circulating monocytes (*Figure 4.12* and *Figure 4.13*). Mice in which the platelet count

did not sufficiently drop were eliminated from the study (*Figure 4.13*, red circles). It is important to note that the data in this chapter was focused only on CLEC-2 expression on platelets and leukocytes in whole blood. Splenic and lymph node leukocyte subsets were analysed independently by Guillaume Desanti alongside this study and will be referred to in the discussion.

4.2.5 Comparing 17D9 and INU1 in un-manipulated C57BL/6 controls

In addition to comparing multiple models of CLEC-2 depletion in adult mice, within some of these models, a direct comparison was made between 17D9 and a second CLEC-2 antibody, INU1. It is important to note that by flow cytometry INU1 gave a much lower shift in fluorescence intensity than 17D9. When compared on platelets isolated from whole blood of unmanipulated control C57BL/6 mice, the geometric mean for INU1 was around 60% lower than 17D9, shown by the left hand shift of the histogram (*Figure 4.14*). INU1 binding was in line with isotype controls on leukocytes, arguing against significant CLEC-2 expression on circulating leukocytes. These results highlighted the importance of studying CLEC-2-deficient cells in order to determine the specificity of 17D9.

4.2.6 Investigating CLEC-2 expression on platelets

Robust expression of CLEC-2 was seen on circulating platelets using either 17D9 or INU1 in both tamoxifen-treated *Clec-2*$^{fl/fl}$ mice and +/+ fetal liver chimeras, while no CLEC-2 expression was seen on platelets isolated from CLEC-2-depleted littermates (*Clec-2*$^{fl/fl}$*ER*^{T2}*Cre* or *Clec-2*$^{-/-}$ chimeras) using either antibody (*Figure 4.15*). Additionally, no difference in CLEC-2 expression on platelets was observed between LPS-treated chimeras or controls, using either 17D9 or INU1 (*Figure 4.15*). Despite efforts to maintain instrument settings between experiments, due to the long period of time over which experiments were conducted, deviations in the baseline fluorescence intensity were introduced, which is reflected in the inter-experimental differences in geometric mean. Importantly, geometric means within single experiments were comparable, maintaining the validity of results. From this data it can be concluded that (i) CLEC-2 is highly expressed on platelets; (ii) both 17D9 and INU1 are suitable for

specifically detecting CLEC-2 on platelets; (iii) CLEC-2 is not up-regulated on platelets after systemic LPS challenge and (iv) both tamoxifen-inducible *ER^{T2}Cre* mediated CLEC-2 depletion (either i.p. or in the diet) and fetal liver chimeras represent effective models for long-term sustained depletion of CLEC-2 in the circulation.

4.2.7 Investigating CLEC-2 expression on B-lymphocytes

In contrast to the partial depletion of CLEC-2 on B-lymphocytes from *Clec-2$^{fl/fl}$ER^{T2}Cre* mice following 2 weeks of tamoxifen diet (*Figure 4.9*), no significant difference in 17D9 binding was observed between *Clec-2$^{fl/fl}$* and *Clec-2$^{fl/fl}$ER^{T2}Cre* mice following 6 months of tamoxifen diet (*Figure 4.16Ai*). A comparable level of binding was also observed with INU1 that was not lost following 6 months of tamoxifen treatment in *Clec-2$^{fl/fl}$ER^{T2}Cre* mice (*Figure 4.16Ci*). This suggests that both 17D9 and INU1 bind to a second site on B-lymphocytes in this model. Furthermore, the CLEC-2-specific site that was labelled by 17D9 following 2 weeks of tamoxifen treatment, was not apparent following prolonged tamoxifen treatment. On the other hand, both 17D9 and INU1 detect a ligand on B-lymphocytes isolated from +/+ fetal liver chimeras that was absent from *Clec-2$^{-/-}$* chimeras (*Figure 4.15A-Dii-iii*). A similar level of 17D9 or INU1 binding was also observed on B-lymphocytes isolated from untreated C57BL/6 controls (*Figure 4.14*), thereby supporting that CLEC-2 is expressed on B-lymphocytes in the steady state. Additionally, no increase in binding of 17D9 or INU1 to B-lymphocytes was observed following LPS challenge (*Figure 4.16A-Dii-iii*). LPS can cause a shift in the fluorescence of isotype controls, but was accounted for by comparing geometric means as apposed to the percentage of positive cells (*Figure 4.15 C-Diii*). Taken together these results suggest that (i) B-lymphocytes isolated from peripheral blood express CLEC-2 that can be

specifically detected by 17D9 and INU1, albeit INU1 exhibits much weaker binding; (ii) CLEC-2 is not upregulated on circulating B-lymphocytes during systemic LPS challenge and (iii) 17D9 and INU1 bind to a second site on B-lymphocytes isolated from peripheral blood of tamoxifen-treated mice.

4.2.8 Investigating CLEC-2 expression on neutrophils ($Gr1^+Mac\text{-}1^+$)

No difference in the binding of 17D9 or INU1 could be observed on peripheral blood neutrophils isolated from *Clec-2*$^{fl/fl}$ or *Clec-2*$^{fl/fl}$*ER*^{T2}*Cre* mice following 2 weeks of tamoxifen diet (*Figure 4.9*), or from *Clec-2*$^{fl/fl}$ or *Clec-2*$^{fl/fl}$*ER*^{T2}*Cre* mice following 6 months on tamoxifen diet (*Figure 4.17A-Di*). This suggests that both 17D9 and INU1 bind to an alternative site on neutrophils. Interestingly, 17D9 binding to circulating neutrophils from +/+ chimeras was substantially higher than in untreated C57BL/6 mice that were measured at the same time, and was much lower in *Clec-2*$^{-/-}$ chimeras (*Figure 4.17A-Bii-iii* and *Figure 4.14*). This suggests that CLEC-2 is upregulated on peripheral blood neutrophils in the chimeric model, which can be specifically detected by 17D9. In addition, 17D9 binding was increased on *Clec-2*$^{-/-}$ chimeras following LPS challenge, thereby demonstrating that 17D9 binds to a second site on peripheral blood neutrophils during systemic inflammation (*Figure 4.17A-Bii-iii*). Although INU1 exhibited substantially weaker binding, there was a trend for increased binding of INU1 to circulating neutrophils isolated from +/+ chimeras (Figure *4.17C-Dii-iii*). On the other hand, INU1 did not detect a second site on neutrophils isolated from *Clec-2*$^{-/-}$ chimeras following systemic LPS challenge (Figure *4.17C-Dii-iii*). Together these results suggest that (i) 17D9 detects a low level of CLEC-2 on peripheral blood neutrophils in the steady state (INU1 binding is too weak to robustly detect this); (ii) CLEC-2 is upregulated on

circulating neutrophils in the chimeric model; (iii) 17D9 binds to a second site on circulating neutrophils during systemic inflammation and (iv) both 17D9 and INU1 detect an alternative ligand on circulating neutrophils isolated from tamoxifen-treated mice.

4.2.9 Investigating CLEC-2 expression on T-lymphocytes

No evidence for CLEC-2 expression was observed using the 17D9 or INU1 antibodies on T-lymphocytes isolated from peripheral blood using either the *ER^{T2}Cre* model or the chimeric model (*Figure 4.18*). Therefore, it can be concluded that CLEC-2 is not expressed at a significant level on T-lymphocytes.

4.3 Discussion

The primary aim of the work in this chapter was to investigate the expression of CLEC-2 on leukocytes in peripheral blood. Alongside this investigation, the same models were used to determine the expression level of CLEC-2 on leukocytes derived from secondary lymphoid tissues. This line of work builds on previous publications that showed surface expression of CLEC-2 on a range of leukocyte subsets in the steady state, including peripheral blood neutrophils (Kerrigan *et al*., 2009; Tang *et al*., 2010), splenic DCs, peritoneal macrophages, subsets of natural killer cells and B-lymphocytes (Mourao-Sa *et al*., 2011) and on splenic neutrophils, DCs, B-lymphocytes, natural killer cells and other monocyte subsets following inflammation (Kerrigan *et al*., 2009; Mourao-Sa *et al*., 2011). Importantly, neither study showed results to confirm antibody specificity by also staining CLEC-2-deficient cells. This comparison has since been made by Acton *et al* (2012), albeit they only analysed DCs derived from the bone marrow, skin or lymph nodes, and used recombinant podoplanin to detect CLEC-2 as apposed to the commercially available 17D9 anti-CLEC-2 antibody used in the previous studies (Acton *et al*., 2012). In this thesis, the expression level of CLEC-2 on platelets and leukocyte subsets was investigated using two antibody clones to CLEC-2, 17D9 and INU1, and using two animal models of CLEC-2 depletion, a tamoxifen-inducible system and *Clec-2*$^{-/-}$ fetal liver chimeras.

In agreement with the literature, CLEC-2 was expressed at a high level on platelets isolated from peripheral blood, and on platelets isolated from the spleen or mesenteric lymph node (Guillaume Desanti, data not shown). This was shown by robust and sustained knockdown of CLEC-2 on platelets following two weeks or long-term tamoxifen-induced CLEC-2 depletion in the *ER*^{T2}*Cre* model, or through the generation of

Clec-2$^{-/-}$ fetal liver chimeras.

While CLEC-2 was expressed on circulating B-lymphocytes in the steady state, this was not upregulated during systemic LPS challenge. Furthermore, no significant level of CLEC-2 was detected on B-lymphocytes isolated from the spleen or lymph nodes in the steady state, or following systemic LPS challenge (Guillaume Desanti, data not shown). In the present study, both 17D9 and INU1 bound to an alternative site on B-lymphocytes, isolated from tamoxifen-treated *Clec-2*$^{fl/fl}$*ER*^{T2}*Cre* mice. The expression profile of CLEC-2 on B-lymphocytes contradicts findings by Sousa *et al* (2011), who showed evidence for 17D9 binding to wild-type splenic B-lymphocytes in the steady-state, which was upregulated during systemic LPS challenge (Mourao-Sa *et al*., 2011). In light of the current findings, this is suggested to represent binding to a second, uncharacterised site, and highlights the importance of comparing 17D9 binding on wild-type cells to that of CLEC-2-depleted cells, derived from a well-characterised animal model. Future studies will also confirm that the levels of CLEC-2 detected on B-lymphocytes were not derived from platelet microparticles. Platelet microparticles are derived from activated platelets and are abundant in the circulation, where they share many functional properties to platelets, including their ability to adhere to leukocytes (Italiano *et al*., 2010). Platelet microparticles are characterised by their small size and expression of CD41 and therefore should have been removed when gating for leukocytes (Figure 4.8). However, the absence of CD41-positive platelet microparticles on B-lymphocytes will be confirmed using flow cytometry studies.

Interestingly, CLEC-2 was shown to be expressed at a low level on peripheral blood neutrophils in the steady state and markedly upregulated in the chimeric model. Conversely, no specific CLEC-2 expression was found on neutrophils isolated from the spleen or lymph nodes in the steady state, or following systemic LPS challenge (Guillaume Desanti, data not shown). Again, this contradicts findings by Sousa *et al* (2011), who showed an increase in 17D9 binding to splenic neutrophils during LPS-induced inflammation (Mourao-Sa *et al*., 2011). In the present study, 17D9 was shown to bind to an off-target site on neutrophils following long-term tamoxifen treatment, or following LPS stimulation. The present study does, however, agree with the work of Kerrigan *et al* (2010), who showed higher expression of CLEC-2 on peripheral blood neutrophils ($Gr1^{+}Mac\text{-}1^{+}$) compared to those isolated from the bone marrow or inflammatory sites. It was proposed that in this scenario, CLEC-2 may be involved in trafficking (Kerrigan *et al*., 2009). This theory is supported by the recent observation that CLEC-2 is required on dendritic cells to support its entry into lymphatic vessels and trafficking to lymph nodes, a process that is dependent on its interaction with podoplanin-expressing LECs and FRCs, respectively (Acton *et al*., 2012).

In this study, CLEC-2 expression was confirmed on platelets, while shown to be absent from leukocyte subsets isolated from the spleen and lymph nodes, which is in contrast to previously published literature. This data was supported by quantitative PCR for *Clec1b* on cell sorted leukocyte populations isolated from the spleen or mesenteric lymph node, showing significant *Clec1b* mRNA levels only in a population of $F4/80^{+}$ splenocytes, which was not upregulated during inflammation (Guillaume Desanti, data not shown). *Clec1b* mRNA was not detected in any other leukocytes isolated from secondary

lymphoid tissue in the steady state, or following systemic inflammatory challenge, including in T-lymphocytes, B-lymphocytes, natural killer cells, neutrophils or DCs, which correlates with *Clec1b* transcript levels identified in the 'The immunological genome project' (*Figure 4.3*) (Guillaume Desanti, data not shown) (Heng *et al*., 2008).

Given the wide expression profile of podoplanin on stromal FRCs, follicular DCs, in tumour environments and throughout the lymphatic network that connects lymphoid tissue, it is likely that podoplanin-CLEC-2 interactions play many key, yet undiscovered roles in immune regulation and responses. This is not hampered by the restricted expression profile of CLEC-2 on leukocytes in secondary lymphoid tissues, given that CLEC-2-podoplanin interactions have been implicated in leukocyte trafficking, a key mechanism in immune regulation. Furthermore, it is well established that platelets interact with leukocytes to regulate their adhesive and migratory properties, in addition to directly regulating the structural integrity and function of lymphoid tissue (van Gils *et al*., 2009; Wagner & Burger, 2003; Herzog *et al*., 2013).

Together these data show that CLEC-2 is expressed on platelets, B-lymphocytes and at low levels on neutrophils in peripheral blood and is restricted to platelets in secondary lymphoid tissues in adult mice. While there was no evidence for CLEC-2 up-regulation following systemic inflammation, only LPS immunisation was studied and it cannot be ruled out that other inflammatory stimuli may elicit different responses. Due to the complexity of DC subsets, more in depth analysis is required to deduce the expression pattern of CLEC-2 on DCs isolated from different tissues, in the steady state, and during inflammation. However, it can be concluded that both 17D9 and INU1 are capable of binding to multiple ligands on leukocytes that can be induced in different models, for

example, following tamoxifen treatment, or in response to injury/repair mechanisms that are induced in the chimeric model. It is therefore essential to consistently compare 17D9 binding to binding on CLEC-2 depleted cells.

CHAPTER 5

INVESTIGATING A POSSIBLE ROLE FOR CLEC-2 AND PODOPLANIN IN SAFE-GUARDING THE BARRIERS OF THE ADULT BRAIN

5.1 Introduction

Chapter 3 described a role for podoplanin and CLEC-2 in the development of the BBB, with a specific role for platelet-derived CLEC-2. In Chapter 4, it was shown that during adulthood, surface expression of CLEC-2 was restricted to circulating platelets and B-lymphocytes, with low levels on circulating neutrophils and DC subsets isolated from the skin and lymph nodes (Acton *et al*., 2012). Given the importance of podoplanin and CLEC-2 interactions in cerebral vascular development, it was hypothesised that they may also play a role in the maintenance of the BBB in the steady state, or in response to challenge.

Initial studies aimed to determine the distribution of podoplanin in the adult mouse brain. In Chapter 3, it was shown that podoplanin becomes restricted to the ependymal lining of the ventricles and to the choroid plexus from E14.5. The same pattern of expression has been reported in adult mice by multiple groups (M. C. Williams *et al*., 1996; Kaji *et al*., 2012). However, one group, who originally reported the same finding, later performed a second immunohistological study and showed podoplanin also to be expressed on a broad range of neural cells, including cranial osteoclasts, dura mater, arachnoid, pia mater, as well as in the meninges and on Schwann cells, glial cells and satellite cells of the spinal cord (Tomooka *et al*., 2013). Furthermore, within the brain parenchyma, unidentified populations of cells were said to co-express podoplanin and the astrocyte marker GFAP within the cerebral cortex, hippocampus and the thalamus (Tomooka *et al*., 2013). To date, the function of podoplanin on these cell types has not been identified, yet the wide tissue distribution of podoplanin suggests it may have multiple roles within the nervous system. Furthermore, no study has reported changes in podoplanin expression in response

to challenge, for example during ageing or inflammation.

From work conducted in Chapter 4 and in published literature, we know that platelets isolated from peripheral blood and secondary lymphoid tissues express high levels of CLEC-2. Beyond a role for platelets in maintaining vascular integrity, it is well known that platelets critically support multiple pathways in immune homeostasis, whether this be in the amplification or resolution of inflammation (Summarised in *Section 1.1.4*). Within the cerebral vasculature, which is uniquely adapted to tightly regulate immune homeostasis (*Figure 1.6*), inappropriate platelet activation has been shown to associate with changes in BBB permeability. For example, in HIV-infected individuals, platelet activation was coupled to an increase leukocyte migration across the BBB (Davidson *et al*., 2012). Additionally, in a mouse model of malaria, increased platelet adhesion to the endothelium caused infected erythrocytes to adhere and obstruct cerebral blood flow (Sun *et al*., 2003). Furthermore, as discussed in Chapter 3, platelets are a key source of LPA and following systemic LPS insult, increased LPA was directly linked to increased BBB permeability (On *et al*., 2013).

A role for CLEC-2 in maintaining BBB integrity has not been studied, however, CLEC-2 is known to play a critical role in maintaining vascular integrity at other sites of inflammation. The source of podoplanin in this setting is unknown, but is said to be on infiltrating F4/80 positive macrophages (Boulaftali *et al*., 2013). As discussed previously, CLEC-2-expressing platelets have been shown to 'piggy back' into inflammatory sites on the back of leukocytes (Herzog *et al*., 2013). Furthermore the group of Shannon Turley showed that CLEC-2 expression on DCs was critical for DC trafficking to inflammatory sites (Acton *et al*., 2012). Together these studies imply multiple mechanisms by which

CLEC-2 and podoplanin may interact to regulate immune homeostasis in the brain during inflammation.

The aim of this chapter was to investigate a role for CLEC-2 in the maintenance and repair of the cerebral vasculature in response to inflammatory challenge. This was achieved by stimulating the immune system of CLEC-2-deficient mice and further assessing the integrity of the BBB. The expression pattern of podoplanin in the brains of adult mice in the steady state or following immune challenge was also studied, with an aim to dissect out a potential mechanism for their interaction.

5.2 Results

5.2.1 Identifying a suitable adult CLEC-2-deficient mouse model

The initial aim of the work in this Chapter was to identify a suitable CLEC-2-deficient, adult mouse model, to study the role of CLEC-2 in cerebral vascular integrity, since constitutive deficiency of CLEC-2 during development caused neonatal lethality. Deletion of CLEC-2 specifically in the megakaryocyte/platelet lineage (*Clec-2*$^{fl/fl}$*PF4-Cre*) overcame this lethality, however, the platelet count in these mice was reduced by 30% compared to *Clec-2*$^{fl/fl}$ littermates (*Figure 5.1*). The reduced platelet count was confirmed not to be due to a defect in platelet production (*Figure 5.2*) or lifetime (*Figure 5.3*). Instead, Finney *et al* (2012) showed that adult *Clec-2*$^{fl/fl}$*PF4-Cre* mice harbored defective lymphatics, with blood visible in mesenteric lymphatic vessels, and a build-up of chylous fluid was noted in the abdomen (Finney *et al*., 2012). With this in mind, it is likely that the reduced platelet count was due to blood-lymphatic mixing and therefore, a greater net vascular volume. It is possible that due to the longer lifetime of white blood cells and red blood cells, they are able to compensate for the linked vasculatures, resulting in largely unaffected cell counts (*Figure 5.1*). In the present study, it was also found that *Clec-2*$^{fl/fl}$*PF4-Cre* mothers were unable to adequately wean entire litters (*Figure 5.4*). The cause for this remains to be established, but given that lymphatics play a crucial role in milk production for newborns, it is likely that *Clec-2*$^{fl/fl}$*PF4-Cre* mothers were unable to sufficiently nourish their offspring, resulting in a large number of deaths within first postnatal days (*Figure 5.4*). Given that litter sizes are rarely recorded immediately after birth, the reduction in total litter size most likely reflects the loss of pups before P1 (*Figure 5.4*). In conclusion, given the significantly lower platelet count in *Clec-2*$^{fl/fl}$*PF4-Cre* mice, this was considered an unsuitable model to investigate the role of CLEC-2 in

the maintenance and repair of the blood-brain barrier.

To remove the developmental influence of CLEC-2, *Clec-2*$^{fl/fl}$ mice were crossed to mice expressing Cre recombinase driven by the ER^{T2} transgene, which mediates induced recombination of the floxed allele following tamoxifen administration (*Section 4.2.1; Figure 4.4*). Platelet counts and other peripheral blood cell counts in *Clec-2*$^{fl/fl}$*ER*^{T2}*Cre* mice treated with tamoxifen diet for 12 weeks were identical to *Clec-2*$^{fl/fl}$ controls, making this a more suitable model (*Figure 5.5*).

5.2.2 Investigating the effect of ageing on *Clec-2$^{fl/fl}$* and *Clec-2$^{fl/fl}$ER^{T2}Cre* tamoxifen treated mice

One of the greatest challenges to the immune system is ageing, which has been shown to play a fundamental role in the regulation of immune homeostasis in the CNS, with direct links to the development and/or progression of a number of neurodegenerative disorders (Perry & Teeling, 2013). To investigate any influence of CLEC-2 depletion on the integrity of the BBB during ageing, *Clec-2$^{fl/fl}$ER^{T2}Cre* mice and *Clec-2$^{fl/fl}$* littermates were fed tamoxifen diet from 8 weeks old for 6-12 months. At 6 months, blood could be seen to accumulate in the ascites fluid of the abdomen in *Clec-2$^{fl/fl}$ER^{T2}Cre* mice but not in *Clec-2$^{fl/fl}$* controls, persisting at 10 and 12 months, albeit this did not noticeably increase in severity. Between 10 and 12 months, the health of *Clec-2$^{fl/fl}$ER^{T2}Cre* mice, but not *Clec-2$^{fl/fl}$* controls, began to deteriorate rapidly, with fur coats appearing starry and grey in colour and small patches of alopecia were noticeable around the head and nose (*Figure 5.6B* and *C*). Isinguinal lymph nodes were noticeably blood-filled in *Clec-2$^{fl/fl}$ER^{T2}Cre* mice at 12 months (*Figure 5.6C*). Interestingly, circulating white blood cell counts were seen to decrease from 3 to 12 months in *Clec-2$^{fl/fl}$ER^{T2}Cre* and *Clec-2$^{fl/fl}$* mice, while circulating monocytes increased significantly in *Clec-2$^{fl/fl}$ER^{T2}Cre* mice, only at 6 and 10 months (*Figure 5.5*). These data suggest that tamoxifen elicited immunosuppressive effects regardless of CLEC-2 depletion, but despite this, *Clec-2$^{fl/fl}$ER^{T2}Cre* mice appeared to have a sustained active innate immune response, reflected in the sustained increase circulating monocytes, suggesting they have a sustained low-grade level of inflammation. Platelet counts did not change significantly over the 12 months, but a significant increase in mean platelet volume was seen in *Clec-2$^{fl/fl}$ER^{T2}Cre* mice at 12 months, the cause for this is unknown (*Figure 5.5*). The increase in circulating monocytes in CLEC-2-deficient mice was reflected by a consistent increase in spleen size from 10 months, albeit this was

not significant (*Figure 5.7A*). No significant difference was observed in the weights of other tissues, including the heart, lung, kidneys, brain or liver dissected from *Clec-2$^{fl/fl}$ER^{T2}Cre* or *Clec-2$^{fl/fl}$* littermates (*Figure 5.7A*). Between 10 and 12 months, the ill health of *Clec-2$^{fl/fl}$ER^{T2}Cre* mice was reflected in a small decline in total body weight compared to the steady increase in weight of *Clec-2$^{fl/fl}$* littermates over the 12 month period (*Figure 5.7B*). Within the first week of tamoxifen diet, it was common for *Clec-2$^{fl/fl}$ER^{T2}Cre* and *Clec-2$^{fl/fl}$* littermates to experience weight loss that almost always recovered by two weeks. It was considered that mice initially found it difficult to transition to the new diet. Occasionally mice lost >20% of their body weight during the first week of tamoxifen diet and were culled in line with UK Home Office regulations. Mice that were fed tamoxifen diet continuously did not experience significant weight gain over the 6-month period compared to mice treated with tamoxifen intraperitoneally, for which weights were shown to increase steadily over the 6-month period (*Figure 5.7B*).

These results showed that inducible deletion of CLEC-2 in adult mice gave rise to a distinct phenotype to that of *Clec-2$^{-/-}$* chimeras and *Clec-2$^{fl/fl}$PF4-Cre* mice. No reduction in platelet count was observed and there was no evidence for blood-lymphatic mixing on tissue sections (data not shown). However, blood was seen in the lymph nodes of *Clec-2$^{fl/fl}$ER^{T2}Cre* mice, similar to what was observed in *Clec-2$^{-/-}$* chimeras and *Clec-2$^{fl/fl}$PF4-Cre* mice, previously shown to result from defective vascular integrity (Herzog *et al*., 2013; Bénézech *et al*., 2014). The impaired integrity of the vasculature most likely also accounts for the blood seen in the peritoneum. During ageing, CLEC-2 depletion appeared to cause a consistent pro-inflammatory state that may be responsible for the rapid deterioration of mice between 10-12 months.

5.2.3 Determining the effect of ageing on vascular permeability in CLEC-2-deficient mice

The brain has been shown to become vulnerable to systemic infection with ageing, whereby resident microglia are 'primed' by repeated immune stimuli, making them either unresponsive, or over-activated, in response to further systemic immune challenge (Perry & Teeling, 2013; Püntener *et al*., 2012). While it has been shown that the microvascular endothelium increases expression of immune molecules such as MHCII and TLRs during ageing, few studies have addressed the impact of this 'pro-inflammatory' state on BBB integrity (Henry *et al*., 2009). Given the heightened monocyte counts in *Clec-2*$^{fl/fl}$*ER*^{T2}*Cre* mice and the disrupted integrity of lymph nodes, it was of interest to check whether CLEC-2 depletion had an effect on vascular integrity in the aged brain. However, no evidence of BBB leakage could be observed in any area of the brain following 12 months of tamoxifen diet (representative images are shown from the hippocampus, cortex and cerebellum), as detected by immunohistochemistry for IgG using F(ab)$_2$-HRP (*Figure 5.8*).

5.2.4 Determining the effect of systemic inflammatory challenge on vascular permeability in CLEC-2-deficient mice

Systemic inflammatory challenge is well known to elicit inflammatory responses across CNS barriers and into the brain parenchyma. A role for platelets in the maintenance of barrier properties during infection has already been described. Here, the most extensively characterised endotoxin, LPS, was used to stimulate the peripheral immune system. LPS cannot cross the BBB, but acts directly on brain endothelium through TLRs, notably TLR4, to influence local cytokine production and stimulate the innate immune system (Mallard, 2012). Both 100 μg and 150 μg of LPS induced a characteristic drop in platelet counts after 24 hours, resulting from platelets becoming sequestered in the liver and spleen (*Figure 5.9A*). A corresponding drop in white blood cell counts reflects leukocytes trafficking to lymphoid organs, while the proportion of circulating monocytes increased, presumably to help control levels of the bacterial pathogen (*Figure 5.9A*). The integrity of the BBB in tamoxifen-treated *Clec-2*$^{fl/fl}$*ER*^{T2}*Cre* or *Clec-2*$^{fl/fl}$ mice, stimulated with LPS, was investigated by immunohistochemistry on paraffin sections, using F(ab)$_2$-HRP, or by immunofluorescence of frozen sections, using F(ab)$_2$-FITC. No evidence of IgG-leakage into the parenchymal tissue was observed in any area of the brain, shown here in the hippocampus and the cortex for mice treated with 150 μg of LPS (*Figure 5.9B* and *C*). To confirm that the drop in platelet count did not influence the sustained integrity of the BBB, thioglycolate was used to stimulate the peripheral immune system. Thioglycolate is commonly used in mouse models of peritonitis, in which it acts as a potent stimulator of the innate immune system. A rapid immune response is initiated, followed by a drastic increase in peripheral blood neutrophil counts at 2 hours, which was shown to resolve by 4 hours (*Figure 5.10C*). To quantify BBB permeability, mice were injected with Evans blue dye and absorbance measurements were calculated from perfused brain tissue.

Initially, the basal level of Evans blue dye absorbance was measured in untreated *Clec-2$^{fl/fl}$ER^{T2}Cre* and *Clec-2$^{fl/fl}$* mice, which showed no significant difference. Brain weights were recorded as a marker of even perfusion of brain tissue (*Figure 5.10A*). Evans blue absorbance measurements were then taken from the brain tissue of tamoxifen-treated *Clec-2$^{fl/fl}$ER^{T2}Cre* and *Clec-2$^{fl/fl}$* mice, stimulated with thioglycolate. A marginal increase in Evans blue absorbance was observed in the thioglycolate-treated mice, but this was not significant (*Figure 5.10B*). A drastic increase in Evans blue absorbance was measured from one CLEC-2-deficient mouse, but this did not correlate with a high monocyte count (*Figure 5.10 B* and *C*). Furthermore, no evidence of BBB permeability was observed by immunohistochemistry (data not shown). The data presented in this Chapter so far demonstrates that a single immune stimulus, or ageing in the absence of significant immune challenge, is not sufficient to induce any change in BBB permeability, in the presence or absence of CLEC-2.

Recent studies have supported the absence of BBB permeability following a single immune stimulus and instead suggest that repeated systemic challenge substantially heightens inflammatory responses within the brain (Püntener *et al*., 2012). Tamoxifen-treated *Clec-2$^{fl/fl}$ER^{T2}Cre* and *Clec-2$^{fl/fl}$* mice were given a sub-lethal bolus of attenuated *Salmonella Typhimurium* (SL3261) to simulate bacterial infection. While the majority of bacteria are taken up by the liver and spleen, those that reach the brain can interact with TLR2 and TLR4 on brain endothelium and on circumventricular organs, including the choroid plexus, resulting in a pro-longed up regulation of MHCII and MHCI (S. E. Peters *et al*., 2009). It was proposed that subsequent systemic challenge with LPS might exacerbate this response, resulting in changes in BBB permeability. LPS was administered 7 days after *Salmonella* infection, when the vast majority of bacteria have been cleared.

The deleterious effects of *Salmonella* treatment alone, or in combination with LPS, were reflected in animal weight loss (*Figure 5.11B*). It has been well characterised that mice infected with *Salmonella* develop thrombi in the liver vasculature by day 7, which was reflected by a drop in platelet count in *Clec-2*$^{fl/fl}$ mice (*Figure 5.11*); (Hitchcock, submitted). In the same study, it was shown that the loss of CLEC-2 on platelets, using the *Clec-2*$^{fl/fl}$*PF4-Cre* model, was protective against *Salmonella*-induced thrombus formation, resulting in a sustained platelet count, a phenomenon that was also observed in tamoxifen-treated *Clec-2*$^{fl/fl}$*ER*^{T2}*Cre* mice (*Figure 5.11*). In line with previous results (*Figure 5.9*), LPS treatment caused a further drop in platelet count and a co-ordinate increase in platelet volume, while the number of circulating monocytes increased in both infected groups (*Figure 5.11C*). Preliminary results showed that *Salmonella* infection alone had no significant effect on BBB permeability, and although a marked variation in Evans blue absorbance was seen in both *Clec-2*$^{fl/fl}$*ER*^{T2}*Cre* and *Clec-2*$^{fl/fl}$ mice treated with *Salmonella* in combination with LPS, this was not significant. The analysis of further mice would be required to confirm these outcomes (*Figure 5.11A*). In cases where an increase in Evans blue absorbance from brain tissue was observed, this could not be seen by immunohistochemistry for IgG leakage on brain sections (data not shown).

Special consideration was taken to eliminate any immunosuppressive effects of tamoxifen treatment (apart from in aged mice) by giving mice 6 weeks of normal diet prior to immune challenge. However, it has already been shown that sustained tamoxifen treatment was required to obtain a pro-longed depletion of CLEC-2 at the genomic level, on circulating leukocytes (*Figure 4.10*). Therefore, in the current model, while it is certain that CLEC-2 is depleted on platelets, it cannot be excluded that residual levels of CLEC-2 remain on B-lymphocytes, neutrophils or DCs, which could also play important roles in

maintaining BBB integrity. For this reason, C57BL/6 mice were irradiated and reconstituted with wild-type or *Clec-2*$^{-/-}$ fetal liver cells and left for 6 weeks to reconstitute the haematopoietic niche. No evidence of BBB permeability was seen under basal conditions, or following systemic challenge in wild-type or *Clec-2*$^{-/-}$ chimeras, nor was their evidence for increased permeability at the choroid plexus (*Figure 5.12*). In line with Home Office restrictions, the dose of LPS was lower than the previous experiments (25 μg), but still considered sufficient to stimulate the innate immune system, confirmed by the drop in platelet and white blood cell counts and an increase in circulating monocytes (*Figure 4.12*).

Taken together, the data presented in this Chapter showed that ageing, or systemic immune challenge with LPS, thioglycolate, *Salmonella* or *Salmonella* + LPS, did not induce BBB permeability under the applied conditions, in the presence or absence of CLEC-2. Therefore, it can be concluded that CLEC-2 depletion does not pre-dispose the cerebral vasculature to alterations in BBB permeability. However, in the absence of a robust model to induce BBB permeability in healthy, untreated mice, a role for CLEC-2 in maintenance and repair pathways cannot be excluded.

5.2.5 Characterising podoplanin expression in the CNS of healthy adult mice

In order to investigate a role for CLEC-2 in regulating cerebral vascular integrity, a more in depth analysis into the expression profile of its only endogenous ligand, podoplanin, was required. In support of previous studies, immunohistochemistry for podoplanin on brain sections from untreated C57BL/6 mice, detected its expression on the apical surface of the choroid plexus, the ependymal lining of the ventricle walls and on the interface between the cortex and the meninges (*Figure 5.13*). Interestingly, podoplanin could also be detected on vessels descending from the meninges into the cortex and on other unidentified vessels throughout the brain (*Figure 5.13*). Immunostaining of sequential brain sections for collagen IV and podoplanin, identified isolated podoplanin-positive vessels that were negative for collagen IV (*Figure 5.14*, top panel), while vessels co-expressing collagen IV and podoplanin were also observed (*Figure 5.14*, bottom panel). Interestingly, podoplanin was often found to line areas of the brain in contact with CSF, including the choroid plexus, ependyma and meninges, and so it was no surprise to see podoplanin-positive cells lining the venous sinus and descending between the two cerebral hemispheres (*Figure 5.14B,* yellow arrows). However, the origin and function of these cells was unknown. Interestingly, single podoplanin-positive cells that were reminiscent of lymphatic endothelial cells, were seen to penetrate the adjacent parenchymal tissue (*Figure 5.14B*, white arrow). It is well accepted that the brain lacks a lymphatic system, however, the marked presence of the lymphatic markers, podoplanin and Lyve-1, on cells that border the major structures of the CSF drainage system, begin to challenge this view. Furthermore, in this study, podoplanin and Lyve-1 positive-cells were seen to line isolated vessels throughout the brain parenchyma, suggesting that they were lymphatic in origin (*Figure 5.14C*).

Taken together, these results postulate a new line of research to investigate the existence of a lymphatic-like drainage system in the brain, in which podoplanin may play a role.

5.2.6 Characterising podoplanin expression in the adult brain in response to challenge

Previous studies have described podoplanin up-regulation or down-regulation to cause either pro- or anti- inflammatory effects, depending on the tissue and its local environment (*Section 1.8.3*). For example, *Salmonella* infection was associated with induced expression of podoplanin on blood endothelium, which was linked to venous thrombosis (Hitchcock, submitted). In aged tamoxifen-treated *Clec-2*$^{fl/fl}$*ER*^{T2}*Cre* and *Clec-2*$^{fl/fl}$ mice, podoplanin was detected on vessels within the cortex, in line with observations in control mice. There was no evidence for increased expression of podoplanin in any area of the brain during ageing, or following systemic challenge with LPS, thioglycolate, *Salmonella* or *Salmonella* + LPS, nor were any changes observed between +/+ and *Clec-2*$^{-/-}$ fetal liver chimeras treated with LPS or PBS only (data not shown). Diffuse expression of podoplanin was observed at varying levels around capillaries in the hippocampus in C57BL/6 brain sections and aged *Clec-2*$^{fl/fl}$*ER*^{T2}*Cre* mice. Tomooka *et al* (2013) reported co-expression of podoplanin with the astrocyte marker GFAP, however the pattern of staining seen here did not correlate with that of astrocytes and was instead thought to be non-specific (*Figure 5.13* and *Figure 5.15*) (Tomooka *et al*., 2013).

Earlier in this thesis, constitutive deficiency of podoplanin was shown to be lethal (*Table 3.2*), as was *Nes-Cre* driven deletion of podoplanin (*Table 3.3*). Furthermore, tamoxifen-inducible deletion of podoplanin in adult mice was associated with lethality, and where mice were viable, only a partial deletion of podoplanin was observed (Guillaume Desanti, data not shown). For these reasons, it was not possible in this study to investigate the effects of podoplanin depletion on BBB permeability, in the adult brain. However, podoplanin has also been detected on MS-inducing T_H17 cells and F4/80+ macrophages

isolated from the spleen and the inflamed peritoneum, albeit, the mechanisms that guide their recruitment, and the contribution of individual subsets to the enhancement or resolution of inflammation, remain controversial (*Section 1.8.3*) (A. Peters *et al*., 2011; Hou *et al*., 2010). Through the generation of *Pdpn*$^{fl/fl}$ and *Pdpn*$^{fl/fl}$*PGK-Cre* fetal liver chimeras, it was confirmed that the loss of podoplanin on haematopoietic cells did not pre-dispose mice to impaired BBB integrity following systemic infection with *Salmonella* Typhimurium (*Figure 5.16*). In line with previous results, there were no obvious changes in podoplanin expression throughout the brain following systemic bacterial infection (data not shown). These results demonstrate that podoplanin expression in the brain is unaltered during ageing, or in response to systemic inflammatory challenge, whether this be in the presence or absence of CLEC-2, or the presence or absence of haematopoietic podoplanin.

5.2.7 Investigating a role for podoplanin in leukocyte trafficking

A key finding in this study was the observation of podoplanin lining the areas of the brain in contact with CSF. CSF is produced by the choroid plexus and flows through the four ventricles of the brain into the sub-arachnoid space, where it drains through arachnoid granulations into the venous sinuses. Venous sinuses provide an entry route for venous circulating blood cells and an exit route for CSF into the venous system (Johansson *et al*., 2008). For this reason, the sub-arachnoid space is a key surveillance channel for immune cells, such as F4/80$^+$ and CD11b$^+$ DCs. This was demonstrated using immunofluorescence staining on embryo tissue sections to identify F4/80$^+$ cells and CD11b$^+$ DCs, which were seen to circulate around the brain parenchyma in CSF (*Figure 5.17A*). There was no change in the number of F4/80$^+$ or CD11b$^+$ DCs in CLEC-2-deficient embryos, nor was their any evidence for their infiltration into the parenchymal tissue (*Figure 5.17C*). Interestingly, F4/80$^+$ and CD11b$^+$ DCs could be seen to adhere to podoplanin-positive ependyma and choroidal epithelium in both wild-type and CLEC-2-deficient embryos (*Figure 5.17D*). These preliminary observations imply that podoplanin interacts with immune cells in the CSF through an independent ligand to CLEC-2. Prior to this finding, an *in vitro* model was tested to mimic barrier properties of choroidal epithelium, whereby, the electrical resistance was measured across choroid plexus epithelial cell monolayers (confirmed to express podoplanin, data not shown). Platelets were found to have no effect on the resistance of choroid plexus epithelial cell monolayers (*Figure 5.18*). However, platelets were shown to increase the migration of choroid plexus epithelial cells, which was found to be CLEC-2-dependent (*Figure 5.19*). Further studies are required to investigate the function of podoplanin on the choroid plexus, a structure known to be the key site of leukocyte trafficking. It is possible that multiple mechanisms exist to traffic both CLEC-2 and non-CLEC-2 expressing leukocytes.

5.3 Discussion

The primary aim of the work described in this chapter was to determine whether CLEC-2 and podoplanin play any role in the maintenance or repair of the cerebral vasculature in the steady state, or in response to challenge, such as inflammation. Age is the most common risk factor for a number of inflammatory-associated diseases, including arthritis, cancers, atherosclerosis and neurodegenerative diseases. While a multitude of risk factors contribute to the development of age-related disease over time, a significant factor is the decline in function of the adaptive immune system, resulting in a low-grade chronic-inflammatory state (Perry & Teeling, 2013). Monocyte numbers were consistently increased at 6 and 10 months following tamoxifen-induced CLEC-2 depletion, suggesting that the loss of CLEC-2 may accelerate the development of a chronic inflammatory state. Interestingly, draining isinguinal lymph nodes were noticeably blood-filled in 6-12 month old tamoxifen-treated *Clec-2*$^{fl/fl}$*ER*^{T2}*Cre* mice, reminiscent of *Clec-2*$^{fl/fl}$*PF4-Cre* mice, *Clec-2*$^{-/-}$ chimeras and *Pdpn*$^{-/-}$ chimeras, which supports the hypothesis that CLEC-2 on platelets interacts with podoplanin on lymph node FRCs to support the integrity of HEVs (Herzog *et al*., 2013). Interestingly Bénézech *et al* (2014) showed that loss of lymph node vascular integrity was directly linked to an impaired adaptive immune response (Bénézech *et al*., 2014). It would therefore be interesting to investigate any association between podoplanin and CLEC-2 in the decline of immune function during ageing.

During ageing, peripheral inflammatory signals are continually communicated to the CNS, causing resident cells such as microglia to become 'primed' and sensitised to future inflammatory challenges (Püntener *et al*., 2012). Furthermore, the expression of pro-inflammatory molecules, such as MHCII, were increased on the endothelium of

normal/healthy aged patients (Godbout *et al*., 2005). Despite the pro-inflammatory state of aged *Clec-2*$^{fl/fl}$*ER*^{T2}*Cre* mice and the drastic defects on vascular integrity in other tissues, no change was observed in BBB permeability. Given the unique resistant barrier properties of the cerebral microvasculature, this was not entirely surprising, but suggested that the loss of CLEC-2 did not pre-dispose to a loss of barrier function. A similar scenario was seen following a single systemic inflammatory challenge with LPS or thioglycolate, where no change in BBB function was observed in CLEC-2-sufficient or CLEC-2-deficient mice. Peripheral LPS challenge has been shown to elicit a much higher inflammatory response in aged mice, however, due to the deteriorating health of aged *Clec-2*$^{fl/fl}$*ER*^{T2}*Cre* mice, it was not possible to study this model (Henry *et al*., 2009). Püntener *et al* (2012) reported increasing levels of cytokines in the brain parenchyma following repeated LPS challenges, which eventually declined, indicative of tolerance. Alternatively, following bacterial infection with *Salmonella*, they observed a sustained pro-inflammatory response, with pro-longed up-regulation of MHCII on the microvascular endothelium (Püntener *et al*., 2012). In the present study, it was found that despite the pro-inflammatory state of the microvasculature, no change in BBB permeability was observed in the presence of absence of CLEC-2, following *Salmonella* infection alone, or following a second systemic stimulus of LPS. Together, these studies imply that systemic inflammatory mediators are transmitted into the CNS across an intact BBB. Furthermore, loss of CLEC-2 does not affect BBB integrity in the inflammatory models used. In this study, the induction of BBB permeability in control mice was not achieved and therefore, it was not possible to investigate a role for CLEC-2 in the prevention of BBB permeability, or in its repair. Future work would involve testing new models, such as the hypoxia/reoxygenation model that has been shown to induce BBB permeability in a model of stroke (Suidan *et al*., 2013).

In this study, the effects of CLEC-2 depletion on the infiltration of leukocytes and microglial function were not explored. In neurodegenerative disorders such as MS, systemic infections have been shown to induce relapse of disease by exacerbating inflammatory responses within the CNS. Similarly, systemic infection was associated with rapid cognitive decline in patients with Alzheimer's disease and the exacerbation of disease symptoms in a mouse models of prion disease. Importantly, these effects were reported to take place in the presence of an intact BBB (Perry & Teeling, 2013; Cunningham *et al*., 2005). In these neuro-degenerative disease models, the progression of disease symptoms was commonly associated with increased cytokine levels in the brain parenchyma. These cytokines are unable to cross the BBB, but transmit messages to resident microglia via perivascular macrophages that are situated at circumventricular organs, albeit, the detailed mechanism of transmission is not known (Dantzer *et al*., 2008). In this study, podoplanin was detected in all areas of the brain lining CSF, specifically the meninges and choroid plexus, which are key entry and exit routes for leukocytes trafficking to and from the venous system. It was postulated that podoplanin might act as a regulator of epithelial barrier function and therefore, a regulator of leukocyte trafficking, across the choroid plexus. In preliminary studies, the loss of CLEC-2 had no effect on blood-CSF barrier integrity *in vitro*; however, CLEC-2-expressing platelets significantly increased the migratory properties of choroid plexus epithelial cells in an *in vitro* migration assay that was shown to be CLEC-2 dependent. In cancer cell lines, the acquisition of a migratory phenotype has been shown to be linked to down-regulation of epithelial markers, such as E-cadherin, resulting in increased cell motility (Martin-Villar *et al*., 2006). It can be suggested that the binding of CLEC-2-expressing cells to podoplanin, induces an alteration in epithelial barrier function, to specifically aid leukocyte migration across an otherwise intact choroidal epithelium. Future work will

investigate the expression of key junctional proteins such as ZO-1 and CL-1 on choroidal epithelium, in the presence and absence of podoplanin. However, this research is currently limited to *in vitro* studies, due to the lack of a robust model to deplete podoplanin in adult mice.

While $F4/80^+$ and $CD11b^+$ DCs from both +/+ and *Clec-2*$^{-/-}$ fetal liver chimeras were seen to interact with podoplanin-expressing ependyma and choroidal epithelium, it cannot be confirmed that they were effectively trafficked across these barriers. Given that CLEC-2 expression was shown to be restricted to subsets of leukocytes, it is likely that CLEC-2-independent mechanisms exist to regulate leukocyte trafficking into the brain parenchyma. For example, podoplanin is known to interact with the chemokine CCL21, yet the significance of this interaction has not been explored (Kerjaschki *et al*., 2004). Additionally, a role for platelets cannot be ruled out, given the critical interplay between platelets and leukocytes in mediating leukocyte tethering, rolling and migration across endothelium (Ley *et al*., 2007). This process is highly dependent on platelets or leukocytes binding to endothelial P-selectin, which is stored and released from Weibel-Palade bodies in endothelial cells. Interestingly, Weibel-Palade bodies that are found in endothelial cells in the brain parenchyma do not store P-selectin, however, P-selectin is stored in Weibel-Palade bodies that reside in meningeal endothelial cells (Engelhardt, 2008). While *in vivo* visualisation of leukocyte trafficking across the choroid plexus is limited by the depth of the tissue, leukocyte tethering to meningeal vessels has been visualised by intravital microscopy in a mouse model of MS, whereby disease progression was directly linked to platelet function (Langer *et al*., 2012). Furthermore, platelets were seen within T-lymphocyte-rich MS lesions, which have previously been shown to be abundant in podoplanin-expressing T_H17 cells. These studies demonstrate the capacity of platelets and

leukocytes to infiltrate inflamed nervous tissue and suggest new points of interaction between CLEC-2 and podoplanin that should be further investigated (Langer *et al*., 2012; A. Peters *et al*., 2011).

The trafficking of platelets and leukocytes across meningeal vessels is particularly interesting, given that earlier in this chapter, podoplanin was shown to be expressed on isolated meningeal vessels. Future work should investigate the significance of this finding and identify whether podoplanin can interact with CLEC-2-expressing platelets or leukocytes on the meningeal endothelium, to mediate their adhesion and trafficking into the CNS parenchyma. Platelets, in particular, are powerful secretory cells that release a number of chemokines and soluble factors that can influence the recruitment and adhesion of leukocytes to the endothelium (Danese *et al*., 2007). It would be interesting to investigate whether podoplanin-induced platelet activation through CLEC-2, contributes to this process. This hypothesis represents a novel mechanism of action for CLEC-2 and podoplanin, given that podoplanin expression has not been reported on any other blood endothelial vessel in the steady state.

A final consideration is whether podoplanin-expressing vessels play any role in CSF drainage in the brain. An association between CSF and lymph has been reported for over 100 years, where tracer molecules were injected into the CSF and eventually found in lymphatic vessels, reviewed in (Koh *et al*., 2005). However, few studies have attempted to characterise their connections. It has been shown that CSF moves by bulk flow through the ventricles into the sub-arachnoid space, where it is absorbed into the venous sinuses through arachnoid granulations (Johansson *et al*., 2008). While one group described the venous sinuses to be a direct exit route for CSF into the venous system, another suggested

that this pathway of CSF drainage was used only under circumstances of increased intracranial pressure. Instead, they proposed that in the steady state, CSF flows from the sub-arachnoid compartment, along olfactory nerves, where it drains over the cribiform plate and into the nasal submucosa, where the CSF is absorbed by extracranial lymphatics (Papaiconomou *et al*., 2002; Mollanji *et al*., 2002). The present study reported the expression of two lymphatic specific markers, podoplanin and Lyve-1, that line areas of the brain involved in CSF drainage into the lymphatic compartments. Podoplanin and Lyve-1 were also seen on isolated vessels in brain parenchyma. These results postulate a role for podoplanin in CSF drainage into the lymphatic system and open up a new line of research for future study. In Chapter 3, the generation of a *podoplanin*$^{fl/fl}$ mouse was described that can be used as a useful tool to target the tissue-specific deletion of podoplanin in the adult brain, for example, on the endothelium, or on the choroid plexus. Molecular dyes of varying molecular weight can be used to monitor CSF flow and the passive, or regulated movement of molecules across the barriers of the brain, in podoplanin sufficient or podoplanin-deficient mice.

CHAPTER 6

GENERAL DISCUSSION

6.1 Summary of results

In this thesis, a unique mechanism was described for the receptor CLEC-2 on platelets and its endogenous ligand podoplanin in directing the development and integrity of the cerebral vasculature. It is proposed that podoplanin on neuro-epithelial cells induces platelet activation through its receptor, CLEC-2, mediating αIIbβ3-dependant platelet aggregation to plug the vessel wall, while secreted molecules (possibly S1-P) may direct supporting mural cells to the vessel wall, together preventing lethal haemorrhage.

In order to investigate a role for CLEC-2 in cerebral vascular integrity during adulthood, the surface expression profile of CLEC-2 on leukocytes in adult mice was first investigated. CLEC-2 was found to be expressed at a high level on platelets isolated from the blood and secondary lymphoid organs, while CLEC-2 expression on leukocytes was restricted to peripheral blood B-lymphocytes and, at low level on neutrophils, with CLEC-2 expression induced in the chimeric model. No evidence was found for CLEC-2 up-regulation on platelets or leukocytes following systemic LPS challenge. By using animal models, in which CLEC-2 was depleted during adulthood, the loss of CLEC-2 was shown to be dispensable for maintaining blood-brain barrier integrity during adulthood in the steady state, or in response to systemic LPS challenge. However, a role for CLEC-2 and podoplanin in vascular repair, a process that shares many mechanistic similarities with vascular development, is still to be investigated.

6.2 Evolution of platelets and CLEC-2

We have come along way since the first identification of platelets, described as 'novel morphological elements' with important roles in haemorrhage and thrombosis, reviewed in (Ribatti & Crivellato, 2007). It is now well appreciated that platelets play fundamental roles that extend beyond these pathways and that their origin may lie in their nucleated evolutionary ancestors. Anucleate platelets are specialised cell fragments, unique to mammals. Non-mammalian vertebrates have nucleated thrombocytes and invertebrates harbor an even more primitive cell, the amebocyte (or haemocyte), which is their only blood cell and as such elicits a multitude of functions (McNicol & Israels, 2008). In fact, amebocytes are reminiscent of macrophages, expressing immune molecules such as TLRs. It is thought that platelets and leukocytes diverged from this single cell type, evolving to perform their specialised roles (Semple *et al*., 2011). It is highly likely that platelets may have retained some immune-like molecules to augment their roles in inflammatory processes. In support of platelets functioning as inflammatory cells, proteomics studies provided evidence for platelets to secrete a vast range of proteins upon activation, which included some inflammatory mediators, such as interleukin-1 (Coppinger *et al*., 2007). In addition, platelets have been shown to secrete a range of molecules that are involved in pro- and anti-angiogenic pathways, including VEGF, S1-P, TGF-β, PDGF, Ang-1, PF4 and matrix metalloproteases (Italiano *et al*., 2007). These additional roles for platelets are thought to reflect the high platelet counts in mammals, given that adverse effects of haemostasis only occur when the platelet count falls below 5 $x10^{10}$, a third lower than the physiological range (15-40 $x10^{10}$) (Levin, 2012; Navarro-Nunez *et al*., 2013). The secretion of bioactive molecules relies on platelet activation, which can be induced through multiple receptors. The work in this thesis focused on the platelet ITAM receptor,

CLEC-2. While other ITAM receptors can be traced back as far as zebrafish; due to the divergence of the C-type lectin family, only one ortholog was identified in zebrafish (CLEC14), while other C-type lectins, including CLEC-2, were found to be restricted to mammals (Hughes, 2010). Similarly, the sequence domain within the podoplanin gene that permits its interaction with platelet CLEC-2, was found to emerge after the divergence of avians and mammals (Kaneko *et al*., 2006). It can therefore be considered, that mammalian anucleate platelets have adapted to their specialised roles outside of haemostasis by exploiting novel receptor-ligand interactions, such as CLEC-2 and podoplanin, which have evolved to become physiologically fundamental for survival.

6.3 Platelets in cerebral vascular development; clinical implications

Thrombocytopenia is the most common risk factor for intraventricular haemorrhage (IVH) in pre-term infants, affecting over 12 000 infants every year (Ballabh, 2010). At the time of onset, cerebral haemorrhage is generally asymptomatic, but often results in substantial morbidity and mortality in neonates. Outcomes can be within a range of neurological disorders, including cerebral palsy, hydrocephalus, mental retardation and cognitive deficits that can cause a number of developmental disabilities (Ballabh, 2010). While diagnostic methods for IVH have significantly improved, there has been little clinical development of preventative medicines, which is reflected by the consistent level of mortality rates over the past three decades (Hanley, 2009). A significant proportion of IVH cases are derived from germinal matrix haemorrhaging, an area of the developing neural tube that is located beneath the ventricular ependymal. IVH is associated with blood leakage into the developing brain ventricles, attributable to increased fragility and

disturbed blood flow in developing cerebral vessels (Winkler *et al*., 2011). The fragility of vessels has been postulated to result from a paucity of pericytes, specifically in the germinal matrix region (Braun *et al*., 2007). The molecular mechanisms that govern pericyte recruitment were discussed in *Section 1.6.4*, notably involving the PDGF-β, Ang-1, TGF-β and S1-P signalling axes, with the present findings further implicating the CLEC-2-podoplanin axis. However, these pathways have not been targeted for therapeutic intervention of IVH. In the United States of America, glucocorticoids remain one of the only clinical drugs administered for the prevention of germinal matrix-derived IVH and are given to up to 75% of women in preterm labor, which encompasses over 12.5% of all births (Vinukonda *et al*., 2010). The molecular mechanisms that govern their effects are unknown, but they were recently shown to elicit anti-angiogenic properties through inhibition of VEGF, while increasing levels of TGF-β to guide the maturation and stabilisation of germinal matrix vessels and prevent haemorrhage (Vinukonda *et al*., 2010). In addition, it was recently reported that platelet infusions in high-risk preterm infants enhance haemostasis and reduce the risk of IVH (Coen, 2013). These findings provide exciting new prospects to target the CLEC-2-podoplanin axis, or other associated pathways for non-invasive therapeutic prevention of IVH. Additionally, these findings argue against the use of anti-platelet drugs such as clopidogrel during pregnancy to reduce the risk of cerebral haemorrhage mid-gestation.

6.4 Targeting platelet interactions in inflammation

In this thesis, evidence was provided to argue against a role for CLEC-2 and podoplanin in safeguarding the integrity of the BBB in the steady state, or in response to systemic inflammatory challenge. Simultaneously, no evidence for podpolanin expression on cells that constitute the BBB could be observed during inflammation to complement this finding. Instead, podpolanin was found to be highly expressed on the choroid plexus, venous sinus and on meningeal vessels, key sites of immune cell trafficking. A role for the CLEC-2-podoplanin axis in immune cell trafficking has already been shown, whereby CLEC-2-expressing DCs interact with podoplanin on lymphatic vessels and lymph node FRCs to guide their recruitment (Acton *et al*., 2012). At the lymph node, it has been shown that podoplanin-expressing FRCs induce platelet activation through CLEC-2, initiating the release of S1-P (Herzog *et al*., 2013). Interestingly, S1-P gradients have been shown to be critical in directing immune cell trafficking between secondary lymphoid organs and inflammatory sites (Chun & Hartung, 2010). In a recent study, using targeted depletion of podoplanin-expressing FRCs in mice, it was demonstrated that while trafficking of naïve T-lymphocytes is chemokine-dependent, once activated, retention of T-lymphocytes in the lymph node is instead dependent on their relative expression of the S1PR (Denton *et al*., 2014). A role for the S1PR in T-lymphocyte trafficking is supported by a recent study, whereby inhibition of the S1-P pathway was associated with reduced pathogenesis of MS. The recently licensed drug for treatment of MS, FTY720 (fingolimod), directly mimics S1-P when phosphorylated *in vivo*, interacting with S1PRs to antagonise their function. It has been shown that FTY720 down-regulates S1PRs on lymphocytes, preventing their egress from lymphoid tissue to the CNS. This is coupled to a reduced clinical score in the MS animal model, EAE (Mohammad *et al*., 2014). In other

models, FTY720 was also shown to inhibit DC trafficking, thereby suppressing the activation of T-lymphocytes and reducing disease pathogenesis (Idzko *et al*., 2006). There are however concerns over disrupting the intricate balance of the immune system, with some studies showing long-term exacerbation of auto-inflammatory disease and others claiming an increased risk of infections resulting from impaired leukocyte trafficking (Mohammad *et al*., 2014). In *Section 5.3* it was discussed that MS lesions are rich in podoplanin-expressing T_H17 cells and that platelets are directly implicated in the progression of MS (Langer *et al*., 2012; A. Peters *et al*., 2011). In addition, work in this thesis identified podoplanin on meningeal vessels and in the sub-arachnoid compartment, which are key points of surveillance for leukocytes in the CNS. This thesis also demonstrated for the first time that in addition to CLEC-2 expression on circulating platelets, CLEC-2 is also expressed on circulating B-lymphocytes and at low levels on circulating neutrophils. Together, these findings raise the possibility that CLEC-2 on platelets and leukocyte subsets interact with podoplanin in the CNS to regulate the recruitment of immune cells. Future studies should investigate this hypothesis both in the steady state, and in animal models of disease that are associated with increased leukocyte infiltration into the brain parenchymal tissue, such as the EAE model.

6.5 Final considerations

Since the mergence of the CLEC-2-podoplanin pathways nearly a decade ago, a number of high impact studies have demonstrated that they occupy fundamental roles in development, including the correct separation of the blood and lymphatic vasculatures, the formation of lymph nodes and in cerebral vascular development. More specifically,

CLEC-2 on platelets and platelet signalling through SYK has been specifically implicated during development. Beyond development, the role of the CLEC-2 signalling pathway outside of its classical haemostatic function remains largely elusive, but is considered to play diverse roles throughout the body, likely reflecting the wide tissue expression pattern of podoplanin during adulthood. Importantly, there are many aspects of podoplanin biology that remain unanswered. Firstly, podoplanin signalling pathways, for which the majority of research has been conducted in tumour environments or *in vitro* (*Section 1.3.3*), thereby presenting prosperous new lines of research that may lead to therapeutic targets. Secondly, the significance of the emerging ligands for podoplanin, such as chemokine CCL21 and galectin-8, which have been implicated in a multitude of pathways, including in immune cell trafficking and the dissemination of *Salmonella* infection, respectively (Denton *et al*., 2014; Thurston *et al*., 2013). Finally, the binding partners of podoplanin, which include the tetraspanin CD9 and the hyaluronan receptor CD44 (Lyve-1), which are specifically implicated in regulating podoplanin function (*Section 1.3.4*), yet their significance in *in vivo* molecular processes remains to be established. A third potential binding partner for podoplanin that was identified in this thesis is the intermediate filament protein, nestin. Like podoplanin, nestin is highly expressed on neural progenitors during development and becomes simultaneously down-regulated following cell differentiation (Sugawara *et al*., 2002). Nestin-driven deletion of podoplanin results in a characteristic blood-lymphatic mixing phenotype (*Section 3.2.8*), which is thought to result from the loss of podoplanin on lymphatic endothelium, given the evidence for nestin expression on proliferating endothelial cells (Sugawara *et al*., 2002). Future studies should establish the extent of podoplanin-nestin co-expression and the significance of this relationship.

To summarise, this thesis has discussed many of the emerging roles of podoplanin and CLEC-2 in both physiological and pathophysiological molecular pathways. Future studies will investigate the mechanisms that govern these processes, specifically investigating the pathological elements of their interactions, thereby paving the way for new therapeutic targets with wide potential clinical implications.

REFERENCES

Abtahian, F., Guerriero, A., Sebzda, E., Lu, M.-M., Zhou, R., Mocsai, A., Myers, E.E., Huang, B., Jackson, D.G., Ferrari, V.A., Tybulewicz, V., Lowell, C.A., Lepore, J.J., Koretzky, G.A. & Kahn, M.L. (2003) Regulation of blood and lymphatic vascular separation by signaling proteins SLP-76 and Syk. *Science*, 299 (5604), pp.247–251.

Acton, S.E., Astarita, J.L., Malhotra, D., Lukacs-Kornek, V., Franz, B., Hess, P.R., Jakus, Z., Kuligowski, M., Fletcher, A.L., Elpek, K.G., Bellemare-Pelletier, A., Sceats, L., Reynoso, E.D., Gonzalez, S.F., Graham, D.B., Chang, J., Peters, A., Woodruff, M., Kim, Y.-A., Swat, W., Morita, T., Kuchroo, V., Carroll, M.C., Kahn, M.L., Wucherpfennig, K.W. & Turley, S.J. (2012) Podoplanin-rich stromal networks induce dendritic cell motility via activation of the C-type lectin receptor CLEC-2. *Immunity*, 37 (2), pp.276–289.

Albers, C.A., Cvejic, A., Favier, R., Bouwmans, E.E., Alessi, M.-C., Bertone, P., Jordan, G., Kettleborough, R.N.W., Kiddle, G., Kostadima, M., Read, R.J., Sipos, B., Sivapalaratnam, S., Smethurst, P.A., Stephens, J., Voss, K., Nurden, A., Rendon, A., Nurden, P. & Ouwehand, W.H. (2011) Exome sequencing identifies NBEAL2 as the causative gene for gray platelet syndrome. *Nature Publishing Group*, 43 (8), pp.735–737.

Alberts, B. (2008) *Molecular Biology of the Cell*. Garland Science.

Allende, M.L., Yamashita, T. & Proia, R.L. (2003) G-protein-coupled receptor S1P1 acts within endothelial cells to regulate vascular maturation. *Blood*, 102 (10), pp.3665–3667.

Anon (1998) Kaufmann: The atlas of mouse development (second printing) - Google Scholar. *Proceedings of the National Academy of Sciences*.

Armulik, A., Genové, G., Mäe, M., Nisancioglu, M.H., Wallgard, E., Niaudet, C., He, L., Norlin, J., Lindblom, P., Strittmatter, K., Johansson, B.R. & Betsholtz, C. (2010) Pericytes regulate the blood–brain barrier. *Nature*, 468 (7323), pp.557–561.

Bader, B.L., Rayburn, H., Crowley, D. & Hynes, R.O. (1998) Extensive vasculogenesis, angiogenesis, and organogenesis precede lethality in mice lacking all alpha v integrins. *Cell*, 95 (4), pp.507–519.

Ballabh, P. (2010) Intraventricular hemorrhage in premature infants: mechanism of disease. *Pediatric research*, 67 (1), pp.1–8.

Ballabh, P., Braun, A. & Nedergaard, M. (2004) The blood–brain barrier: an overview. *Neurobiology of Disease*, 16 (1), pp.1–13.

Bekiaris, V., Withers, D., Glanville, S.H., McConnell, F.M., Parnell, S.M., Kim, M.Y., Gaspal, F.M.C., Jenkinson, E., Sweet, C., Anderson, G. & Lane, P.J.L. (2007) Role of CD30 in B/T Segregation in the Spleen. *The Journal of Immunology*, 179 (11), pp.7535–7543.

Bertozzi, C.C., Hess, P.R. & Kahn, M.L. (2010a) Platelets: covert regulators of lymphatic development. *Arteriosclerosis, Thrombosis, and Vascular Biology*, 30 (12), pp.2368–

2371.

Bertozzi, C.C., Schmaier, A.A., Mericko, P., Hess, P.R., Zou, Z., Chen, M., Chen, C.-Y., Xu, B., Lu, M.-M., Zhou, D., Sebzda, E., Santore, M.T., Merianos, D.J., Stadtfeld, M., Flake, A.W., Graf, T., Skoda, R., Maltzman, J.S., Koretzky, G.A. & Kahn, M.L. (2010b) Platelets regulate lymphatic vascular development through CLEC-2-SLP-76 signaling. *Blood*, 116 (4), pp.661–670.

Bénézech, C., Nayar, S., Finney, B.A., Withers, D.R., Lowe, K., Desanti, G.E., Marriott, C.L., Watson, S.P., Caamaño, J.H., Buckley, C.D. & Barone, F. (2014) CLEC-2 is required for development and maintenance of lymph nodes. *Blood*, 123 (20), pp.3200–3207.

Bohmer, R., Neuhaus, B., BUhren, S., Zhang, D., Stehling, M., Bock, B. & Kiefer, F. (2010) Regulation of developmental lymphangiogenesis by Syk(+) leukocytes. *Developmental cell*, 18 (3), pp.437–449.

Boulaftali, Y., Hess, P.R., Getz, T.M., Cholka, A., Stolla, M., Mackman, N., Owens, A.P., Ware, J., Kahn, M.L. & Bergmeier, W. (2013) Platelet ITAM signaling is critical for vascular integrity in inflammation. *Journal of Clinical Investigation*, 123 (2), pp.908–916.

Braun, A., Xu, H., Hu, F., Kocherlakota, P., Siegel, D., Chander, P., Ungvari, Z., Csiszar, A., Nedergaard, M. & Ballabh, P. (2007) Paucity of Pericytes in Germinal Matrix Vasculature of Premature Infants. *Journal of Neuroscience*, 27 (44), pp.12012–12024.

Breier, G. & Risau, W. (1996) The role of vascular endothelial growth factor in blood vessel formation. *Trends in cell biology*, 6 (12), pp.454–456.

Breier, G., Albrecht, U., Sterrer, S. & Risau, W. (1992) Expression of vascular endothelial growth factor during embryonic angiogenesis and endothelial cell differentiation. *Development*, 114 (2), pp.521–532.

Breiteneder-Geleff, S., Matsui, K., Soleiman, A., Meraner, P., Poczewski, H., Kalt, R., Schaffner, G. & Kerjaschki, D. (1997) Podoplanin, novel 43-kd membrane protein of glomerular epithelial cells, is down-regulated in puromycin nephrosis. *The American journal of pathology*, 151 (4), pp.1141–1152.

Bretscher, A., Edwards, K. & Fehon, R.G. (2002) ERM proteins and merlin: integrators at the cell cortex. *Nature Reviews Molecular Cell Biology*, 3 (8), pp.586–599.

Bryan, L., Kordula, T., Spiegel, S. & Milstien, S. (2008) Regulation and functions of sphingosine kinases in the brain. *Biochimica et biophysica acta*, 1781 (9), pp.459–466.

Calaminus, S.D.J., Guitart, A., Sinclair, A., Schachtner, H., Watson, S.P., Holyoake, T.L., Kranc, K.R. & Machesky, L.M. (2012) Lineage Tracing of Pf4-Cre Marks Hematopoietic Stem Cells and Their Progeny K. Freson ed. *PLoS ONE*, 7 (12), p.e51361.

Cambier, S., Gline, S., Mu, D., Collins, R., Araya, J., Dolganov, G., Einheber, S., Boudreau, N. & Nishimura, S.L. (2005) Integrin alpha(v)beta8-mediated activation of transforming growth factor-beta by perivascular astrocytes: an angiogenic control switch. *The American journal of pathology*, 166 (6), pp.1883–1894.

Carramolino, L., Fuentes, J., Garcia-Andres, C., Azcoitia, V., Riethmacher, D. & Torres, M. (2010) Platelets Play an Essential Role in Separating the Blood and Lymphatic Vasculatures During Embryonic Angiogenesis. *Circulation Research*, 106 (7), pp.1197–1201.

Chaipan, C., Soilleux, E.J., Simpson, P., Hofmann, H., Gramberg, T., Marzi, A., Geier, M., Stewart, E.A., Eisemann, J., Steinkasserer, A., Suzuki-Inoue, K., Fuller, G.L., Pearce, A.C., Watson, S.P., Hoxie, J.A., Baribaud, F. & Pohlmann, S. (2006) DC-SIGN and CLEC-2 Mediate Human Immunodeficiency Virus Type 1 Capture by Platelets. *Journal of virology*, 80 (18), pp.8951–8960.

Chauvet, S., Burk, K. & Mann, F. (2013) Navigation rules for vessels and neurons: cooperative signaling between VEGF and neural guidance cues. *Cellular and Molecular Life Sciences*, 70 (10), pp.1685–1703.

Cheng, A.M., Rowley, B., Pao, W., Hayday, A., Bolen, J.B. & Pawson, T. (1995) Syk tyrosine kinase required for mouse viability and B-cell development. *Nature*, 378 (6554), pp.303–306.

Christou, C.M., Pearce, A.C., Watson, A.A., Mistry, A.R., Pollitt, A.Y., Fenton-May, A.E., Johnson, L.A., Jackson, D.G., Watson, S.P. & O'callaghan, C.A. (2008) Renal cells activate the platelet receptor CLEC-2 through podoplanin. *Biochemical Journal*, 411 (1), p.133.

Chun, J. & Hartung, H.-P. (2010) Mechanism of Action of Oral Fingolimod (FTY720) in Multiple Sclerosis. *Clinical Neuropharmacology*, 33 (2), pp.91–101.

Clements, J.L. (1998) Requirement for the Leukocyte-Specific Adapter Protein SLP-76 for Normal T Cell Development. *Science*, 281 (5375), pp.416–419.

Clements, J.L., Lee, J.R., Gross, B., Yang, B., Olson, J.D., Sandra, A., Watson, S.P., Lentz, S.R. & Koretzky, G.A. (1999) Fetal hemorrhage and platelet dysfunction in SLP-76-deficient mice. *Journal of Clinical Investigation*, 103 (1), pp.19–25.

Coen, R.W. (2013) Preventing germinal matrix layer rupture and intraventricular hemorrhage. *Frontiers in pediatrics*, 1, p.22.

Colonna, M., Samaridis, J. & Angman, L. (2000) Molecular characterization of two novel C-type lectin-like receptors, one of which is selectively expressed in human dendritic cells. *European Journal of Immunology*, 30 (2), pp.697–704.

Copp, A.J., Greene, N.D.E. & Murdoch, J.N. (2003) The genetic basis of mammalian neurulation. *Nature Reviews Genetics*, 4 (10), pp.784–793.

Coppinger, J.A., O'Connor, R., Wynne, K., Flanagan, M., Sullivan, M., Maguire, P.B., Fitzgerald, D.J. & Cagney, G. (2007) Moderation of the platelet releasate response by aspirin. *Blood*, 109 (11), pp.4786–4792.

Cueni, L.N. & Detmar, M. (2009) Galectin-8 interacts with podoplanin and modulates lymphatic endothelial cell functions. *Experimental cell research*, 315 (10), pp.1715–1723.

Cueni, L.N., Chen, L., Zhang, H., Marino, D., Huggenberger, R., Alitalo, A., Bianchi, R.

& Detmar, M. (2010) Podoplanin-Fc reduces lymphatic vessel formation in vitro and in vivo and causes disseminated intravascular coagulation when transgenically expressed in the skin. *Blood*, 116 (20), pp.4376–4384.

Cunningham, C., Wilcockson, D.C., Campion, S., Lunnon, K. & Perry, V.H. (2005) Central and systemic endotoxin challenges exacerbate the local inflammatory response and increase neuronal death during chronic neurodegeneration. *Journal of Neuroscience*, 25 (40), pp.9275–9284.

Daneman, R., Agalliu, D., Zhou, L., Kuhnert, F., Kuo, C.J. & Barres, B.A. (2009) Wnt/beta-catenin signaling is required for CNS, but not non-CNS, angiogenesis. *Proceedings of the National Academy of Sciences of the United States of America*, 106 (2), pp.641–646.

Danese, S., Dejana, E. & Fiocchi, C. (2007) Immune Regulation by Microvascular Endothelial Cells: Directing Innate and Adaptive Immunity, Coagulation, and Inflammation. *The Journal of Immunology*, 178 (10), pp.6017–6022.

Dantzer, R., O'Connor, J.C., Freund, G.G., Johnson, R.W. & Kelley, K.W. (2008) From inflammation to sickness and depression: when the immune system subjugates the brain. *Nature Reviews Neuroscience*, 9 (1), pp.46–56.

Davidson, D.C., Hirschman, M.P., Sun, A., Singh, M.V., Kasischke, K. & Maggirwar, S.B. (2012) Excess soluble CD40L contributes to blood brain barrier permeability in vivo: implications for HIV-associated neurocognitive disorders. *PLoS ONE*, 7 (12), p.e51793.

de Castro, F., López-Mascaraque, L. & De Carlos, J.A. (2007) Cajal: Lessons on brain development. *Brain Research Reviews*, 55 (2), pp.481–489.

Del Rey, M.J., Faré, R., Izquierdo, E., Usategui, A., Rodríguez-Fernández, J.L., Suárez-Fueyo, A., Cañete, J.D. & Pablos, J.L. (2014) Clinicopathological Correlations of Podoplanin (gp38) Expression in Rheumatoid Synovium and Its Potential Contribution to Fibroblast Platelet Crosstalk K. Freson ed. *PLoS ONE*, 9 (6), p.e99607.

Denton, A.E., Roberts, E.W., Linterman, M.A. & Fearon, D.T. (2014) Fibroblastic reticular cells of the lymph node are required for retention of resting but not activated CD8+ T cells. *Proceedings of the National Academy of Sciences*, 111 (33), pp.12139–12144.

Deppermann, C., Cherpokova, D., Nurden, P., Schulz, J.-N., Thielmann, I., Kraft, P., Vögtle, T., Kleinschnitz, C., Dütting, S., Krohne, G., Eming, S.A., Nurden, A.T., Eckes, B., Stoll, G., Stegner, D. & Nieswandt, B. (2013) Gray platelet syndrome and defective thrombo-inflammation in Nbeal2-deficient mice. *Journal of Clinical Investigation*, 123 (8), pp.3331–3342.

Dumont, D.J., Gradwohl, G., Fong, G.H., Puri, M.C., Gertsenstein, M., Auerbach, A. & Breitman, M.L. (1994) Dominant-negative and targeted null mutations in the endothelial receptor tyrosine kinase, tek, reveal a critical role in vasculogenesis of the embryo. *Genes & Development*, 8 (16), pp.1897–1909.

Dumont, D.J., Jussila, L., Taipale, J., Lymboussaki, A., Mustonen, T., Pajusola, K., Breitman, M. & Alitalo, K. (1998) Cardiovascular failure in mouse embryos deficient in

VEGF receptor-3. *Science*, 282 (5390), pp.946–949.

D'Agostino, P.M., Gottfried-Blackmore, A., Anandasabapathy, N. & Bulloch, K. (2012) Brain dendritic cells: biology and pathology. *Acta Neuropathologica*, 124 (5), pp.599–614.

Emambokus, N.R. & Frampton, J. (2003) The glycoprotein IIb molecule is expressed on early murine hematopoietic progenitors and regulates their numbers in sites of hematopoiesis. *Immunity*, 19 (1), pp.33–45.

Emerich, D.F., Skinner, S.J.M., Borlongan, C.V., Vasconcellos, A.V. & Thanos, C.G. (2005) The choroid plexus in the rise, fall and repair of the brain. *BioEssays*, 27 (3), pp.262–274.

Engelhardt, B. (2008) Immune cell entry into the central nervous system: involvement of adhesion molecules and chemokines. *Journal of the neurological sciences*, 274 (1-2), pp.23–26.

Engelhardt, B. & Sorokin, L. (2009) The blood–brain and the blood–cerebrospinal fluid barriers: function and dysfunction. *Seminars in Immunopathology*, 31 (4), pp.497–511.

Engelmann, B. & Massberg, S. (2013) Thrombosis as an intravascular effector of innate immunity. *Nature Reviews Immunology*, 13 (1), pp.34–45.

Fantin, A., Vieira, J.M., Plein, A., Maden, C.H. & Ruhrberg, C. (2013) The embryonic mouse hindbrain as a qualitative andquantitative model for studying the molecular andcellular mechanisms of angiogenesis. *Nature Protocols*, 8 (2), pp.418–429.

Farkas, L.M. & Huttner, W.B. (2008) The cell biology of neural stem and progenitor cells and its significance for their proliferation versus differentiation during mammalian brain development. *Current Opinion in Cell Biology*, 20 (6), pp.707–715.

Farr, A.G., Berry, M.L., Kim, A., Nelson, A.J., Welch, M.P. & Aruffo, A. (1992) Characterization and cloning of a novel glycoprotein expressed by stromal cells in T-dependent areas of peripheral lymphoid tissues. *The Journal of experimental medicine*, 176 (5), pp.1477–1482.

Fehon, R.G., McClatchey, A.I. & Bretscher, A. (2010) Organizing the cell cortex: the role of ERM proteins. *Nature Reviews Molecular Cell Biology*, 11 (4), pp.276–287.

Ferrara, N., Carver-Moore, K., Chen, H., Dowd, M., Lu, L., O'Shea, K.S., Powell-Braxton, L., Hillan, K.J. & Moore, M.W. (1996) Heterozygous embryonic lethality induced by targeted inactivation of the VEGF gene. *Nature*, 380 (6573), pp.439–442.

Finney, B.A., Schweighoffer, E., Navarro-Nunez, L., Bénézech, C., Barone, F., Hughes, C.E., Langan, S.A., Lowe, K.L., Pollitt, A.Y., Mourao-Sa, D., Sheardown, S., Nash, G.B., Smithers, N., Reis e Sousa, C., Tybulewicz, V.L.J. & Watson, S.P. (2012) CLEC-2 and Syk in the megakaryocytic/platelet lineage are essential for development. *Blood*, 119 (7), pp.1747–1756.

Fitzgerald, J.R., Foster, T.J. & Cox, D. (2006) The interaction of bacterial pathogens with platelets. *Nature Reviews Microbiology*, 4 (6), pp.445–457.

François, M., Caprini, A., Hosking, B., Orsenigo, F., Wilhelm, D., Browne, C., Paavonen, K., Karnezis, T., Shayan, R., Downes, M., Davidson, T., Tutt, D., Cheah, K.S.E., Stacker, S.A., Muscat, G.E.O., Achen, M.G., Dejana, E. & Koopman, P. (2008) Sox18 induces development of the lymphatic vasculature in mice. *Nature*, 456 (7222), pp.643–647.

Fu, J., Gerhardt, H., McDaniel, J.M., Xia, B., Liu, X., Ivanciu, L., Ny, A., Hermans, K., Silasi-Mansat, R., McGee, S., Nye, E., Ju, T., Ramirez, M.I., Carmeliet, P., Cummings, R.D., Lupu, F. & Xia, L. (2008) Endothelial cell O-glycan deficiency causes blood/lymphatic misconnections and consequent fatty liver disease in mice. *Journal of Clinical Investigation*, 118 (11), pp.3725–3737.

Fulkerson, Z., Wu, T., Sunkara, M., Kooi, C.V., Morris, A.J. & Smyth, S.S. (2011) Binding of autotaxin to integrins localizes lysophosphatidic acid production to platelets and mammalian cells. *Journal of Biological Chemistry*, 286 (40), pp.34654–34663.

Gaengel, K., Genove, G., Armulik, A. & Betsholtz, C. (2009) Endothelial-Mural Cell Signaling in Vascular Development and Angiogenesis. *Arteriosclerosis, Thrombosis, and Vascular Biology*, 29 (5), pp.630–638.

Gawaz, M., Langer, H. & May, A.E. (2005) Platelets in inflammation and atherogenesis. *Journal of Clinical Investigation*, 115 (12), pp.3378–3384.

Gay, L.J. & Felding-Habermann, B. (2011) Contribution of platelets to tumour metastasis. *Nature Reviews Cancer*, 11 (2), pp.123–134.

Gerhardt, H., Golding, M., Fruttiger, M., Ruhrberg, C., Lundkvist, A., Abramsson, A., Jeltsch, M., Mitchell, C., Alitalo, K., Shima, D. & Betsholtz, C. (2003) VEGF guides angiogenic sprouting utilizing endothelial tip cell filopodia. *The Journal of Cell Biology*, 161 (6), pp.1163–1177.

Gerhardt, H., Ruhrberg, C., Abramsson, A., Fujisawa, H., Shima, D. & Betsholtz, C. (2004) Neuropilin-1 is required for endothelial tip cell guidance in the developing central nervous system. *Developmental Dynamics*, 231 (3), pp.503–509.

Gibbins, J.M. (2004) Platelet adhesion signalling and the regulation of thrombus formation. *Journal of Cell Science*, 117 (16), pp.3415–3425.

Gittenberger-De Groot, A.C., Mahtab, E.A.F., Hahurij, N.D., Wisse, L.J., DeRuiter, M.C., Wijffels, M.C.E.F. & Poelmann, R.E. (2007) Nkx2.5-negative myocardium of the posterior heart field and its correlation with podoplanin expression in cells from the developing cardiac pacemaking and conduction system. *Anatomical record (Hoboken, N.J. : 2007)*, 290 (1), pp.115–122.

Gitz, E., Pollitt, A.Y., Gitz-Francois, J.J., Alshehri, O., Mori, J., Montague, S., Nash, G.B., Douglas, M.R., Gardiner, E.E., Andrews, R.K., Buckley, C.D., Harrison, P. & Watson, S.P. (2014) CLEC-2 expression is maintained on activated platelets and on platelet microparticles. *Blood*.

Godbout, J.P., Chen, J., Abraham, J., Richwine, A.F., Berg, B.M., Kelley, K.W. & Johnson, R.W. (2005) Exaggerated neuroinflammation and sickness behavior in aged mice following activation of the peripheral innate immune system. *FASEB journal : official publication of the Federation of American Societies for Experimental Biology*, 19

(10), pp.1329–1331.

Götz, M. & Huttner, W.B. (2005) The cell biology of neurogenesis. *Nature Reviews Molecular Cell Biology*, 6 (10), pp.777–788.

Green, A.R. (2011) *Postgraduate Haematology*. John Wiley & Sons.

Greene, N.D.E. & Copp, A.J. (2009) Development of the vertebrate central nervous system: formation of the neural tube L. Chitty & G. Pilu eds. *Prenatal Diagnosis*, 29 (4), pp.303–311.

Gunay-Aygun, M., Falik-Zaccai, T.C., Vilboux, T., Zivony-Elboum, Y., Gumruk, F., Cetin, M., Khayat, M., Boerkoel, C.F., Kfir, N., Huang, Y., Maynard, D., Dorward, H., Berger, K., Kleta, R., Anikster, Y., Arat, M., Freiberg, A.S., Kehrel, B.E., Jurk, K., Cruz, P., Mullikin, J.C., White, J.G., Huizing, M. & Gahl, W.A. (2011) NBEAL2 is mutated in gray platelet syndrome and is required for biogenesis of platelet α-granules. *Nature Publishing Group*, 43 (8), pp.732–734.

Hanley, D.F. (2009) Intraventricular hemorrhage: severity factor and treatment target in spontaneous intracerebral hemorrhage. *Stroke*, 40 (4), pp.1533–1538.

Hata, M., Amano, I., Tsuruga, E., Kojima, H. & Sawa, Y. (2010) Immunoelectron microscopic study of podoplanin localization in mouse salivary gland myoepithelium. *ACTA HISTOCHEMICA ET CYTOCHEMICA*, 43 (2), pp.77–82.

Hawkins, B.T. & Davis, T.P. (2005) The blood-brain barrier/neurovascular unit in health and disease. *Pharmacological reviews*, 57 (2), pp.173–185.

Hayashi, S. & McMahon, A.P. (2002) Efficient Recombination in Diverse Tissues by a Tamoxifen-Inducible Form of Cre: A Tool for Temporally Regulated Gene Activation/Inactivation in the Mouse. *Developmental Biology*, 244 (2), pp.305–318.

Hägerling, R., Pollmann, C., Andreas, M., Schmidt, C., Nurmi, H., Adams, R.H., Alitalo, K., Andresen, V., Schulte-Merker, S. & Kiefer, F. (2013) A novel multistep mechanism for initial lymphangiogenesis in mouse embryos based on ultramicroscopy. *The EMBO journal*, 32 (5), pp.629–644.

Hellström, M., Gerhardt, H., Kalén, M., Li, X., Eriksson, U., Wolburg, H. & Betsholtz, C. (2001) Lack of pericytes leads to endothelial hyperplasia and abnormal vascular morphogenesis. *The Journal of Cell Biology*, 153 (3), pp.543–553.

Heng, T.S.P., Painter, M.W.Immunological Genome Project Consortium (2008) The Immunological Genome Project: networks of gene expression in immune cells. *Nature Immunology*, 9 (10), pp.1091–1094.

Henry, C.J., Huang, Y., Wynne, A.M. & Godbout, J.P. (2009) Brain, Behavior, and Immunity. *Brain Behavior and Immunity*, 23 (3), pp.309–317.

Herzog, B.H., Fu, J., Wilson, S.J., Hess, P.R., Sen, A., McDaniel, J.M., Pan, Y., Sheng, M., Yago, T., Silasi-Mansat, R., McGee, S., May, F., Nieswandt, B., Morris, A.J., Lupu, F., Coughlin, S.R., McEver, R.P., Chen, H., Kahn, M.L. & Xia, L. (2013) Podoplanin maintains high endothelial venule integrity by interacting with platelet CLEC-2. *Nature*,

pp.1–7.

Hess, P.R., Rawnsley, D.R., Jakus, Z., Yang, Y., Sweet, D.T., Fu, J., Herzog, B., Lu, M., Nieswandt, B., Oliver, G., Makinen, T., Xia, L. & Kahn, M.L. (2014) Platelets mediate lymphovenous hemostasis to maintain blood-lymphatic separation throughout life. *Journal of Clinical Investigation*, 124 (1), pp.273–284.

Ho-Tin-Noe, B., Demers, M. & Wagner, D.D. (2011) How platelets safeguard vascular integrity. *Journal of thrombosis and haemostasis : JTH*, 9 Suppl 1, pp.56–65.

Hodivala-Dilke, K.M., McHugh, K.P., Tsakiris, D.A., Rayburn, H., Crowley, D., Ullman-Culleré, M., Ross, F.P., Coller, B.S., Teitelbaum, S. & Hynes, R.O. (1999) β3-integrin–deficient mice are a model for Glanzmann thrombasthenia showing placental defects and reduced survival. *Journal of Clinical Investigation*, 103 (2), pp.229–238.

Hou, T.Z., Bystrom, J., Sherlock, J.P., Qureshi, O., Parnell, S.M., Anderson, G., Gilroy, D.W. & Buckley, C.D. (2010) A distinct subset of podoplanin (gp38) expressing F4/80+ macrophages mediate phagocytosis and are induced following zymosan peritonitis. *FEBS Letters*, 584 (18), pp.3955–3961.

Hughes, C.E. (2010) Comparison of CLEC-2 and GPVI signaling in platelets: the role of adaptor proteins.

Hughes, C.E., Navarro-Nunez, L., Finney, B.A., Mourao-Sa, D., Pollitt, A.Y. & Watson, S.P. (2010) CLEC-2 is not required for platelet aggregation at arteriolar shear. *Journal of thrombosis and haemostasis : JTH*, 8 (10), pp.2328–2332.

Ichise, H., Ichise, T., Ohtani, O. & Yoshida, N. (2008) Phospholipase C 2 is necessary for separation of blood and lymphatic vasculature in mice. *Development*, 136 (2), pp.191–195.

Idzko, M., Hammad, H., Nimwegen, M.V., Kool, M., Müller, T., Soullié, T., Willart, M.A.M., Hijdra, D., Hoogsteden, H.C. & Lambrecht, B.N. (2006) Local application of FTY720 to the lung abrogates experimental asthma by altering dendritic cell function. *Journal of Clinical Investigation*, 116 (11), pp.2935–2944.

Italiano, J.E. & Shivdasani, R.A. (2003) Megakaryocytes and beyond: the birth of platelets. *Journal of thrombosis and haemostasis : JTH*, 1 (6), pp.1174–1182.

Italiano, J.E., Jr, Mairuhu, A.T. & Flaumenhaft, R. (2010) Clinical relevance of microparticles from platelets and megakaryocytes. *Current Opinion in Hematology*, 17 (6), pp.578–584.

Italiano, J.E., Richardson, J.L., Patel-Hett, S., Battinelli, E., Zaslavsky, A., Short, S., Ryeom, S., Folkman, J. & Klement, G.L. (2007) Angiogenesis is regulated by a novel mechanism: pro- and antiangiogenic proteins are organized into separate platelet granules and differentially released. *Blood*, 111 (3), pp.1227–1233.

Jain, R.K. (2003) Molecular regulation of vessel maturation. *Nature Medicine*, 9 (6), pp.685–693.

Janeway, C. (2001) *Immunobiology Five*. Garland Publishing.

Johansson, P.A., Dziegielewska, K.M., Liddelow, S.A. & Saunders, N.R. (2008) The blood–CSF barrier explained: when development is not immaturity. *BioEssays*, 30 (3), pp.237–248.

Kahr, W.H., Hinckley, J., Li, L., Schwertz, H., Christensen, H., Rowley, J.W., Pluthero, F.G., Urban, D., Fabbro, S., Nixon, B., Gadzinski, R., Storck, M., Wang, K., Ryu, G.-Y., Jobe, S.M., Schutte, B.C., Moseley, J., Loughran, N.B., Parkinson, J., Weyrich, A.S. & Di Paola, J. (2011) Mutations in. *Nature Publishing Group*, 43 (8), pp.738–740.

Kaji, C., Tomooka, M., Kato, Y., Kojima, H. & Sawa, Y. (2012) The expression of podoplanin and classic cadherins in the mouse brain. *Journal of Anatomy*, 220 (5), pp.435–446.

Kaneko, M., Kato, Y., Kunita, A., Fujita, N., Tsuruo, T. & Osawa, M. (2004) Functional sialylated O-glycan to platelet aggregation on Aggrus (T1alpha/Podoplanin) molecules expressed in Chinese hamster ovary cells. *The Journal of biological chemistry*, 279 (37), pp.38838–38843.

Kaneko, M.K., Kato, Y., Kitano, T. & Osawa, M. (2006) Conservation of a platelet activating domain of Aggrus/podoplanin as a platelet aggregation-inducing factor. *Gene*, 378, pp.52–57.

Karkkainen, M.J., Haiko, P., Sainio, K., Partanen, J., Taipale, J., Petrova, T.V., Jeltsch, M., Jackson, D.G., Talikka, M., Rauvala, H., Betsholtz, C. & Alitalo, K. (2003) Vascular endothelial growth factor C is required for sprouting of the first lymphatic vessels from embryonic veins. *Nature Immunology*, 5 (1), pp.74–80.

Kato, Y., Fujita, N., Kunita, A., Sato, S., Kaneko, M., Osawa, M. & Tsuruo, T. (2003) Molecular identification of Aggrus/T1alpha as a platelet aggregation-inducing factor expressed in colorectal tumors. *The Journal of biological chemistry*, 278 (51), pp.51599–51605.

Katsura, Y. (2002) Redefinition of lymphoid progenitors. *Nature Reviews Immunology*, 2 (2), pp.127–132.

Kaufman, M.H. (1992) *The Atlas of Mouse Development*.

Kaushansky, K. (2005) The molecular mechanisms that control thrombopoiesis. *Journal of Clinical Investigation*, 115 (12), pp.3339–3347.

Kawasaki, T., Kitsukawa, T., Bekku, Y., Matsuda, Y., Sanbo, M., Yagi, T. & Fujisawa, H. (1999) A requirement for neuropilin-1 in embryonic vessel formation. *Development*, 126 (21), pp.4895–4902.

Kerjaschki, D., Regele, H.M., Moosberger, I., Nagy-Bojarski, K., Watschinger, B., Soleiman, A., Birner, P., Krieger, S., Hovorka, A. & Silberhumer, G. (2004) Lymphatic neoangiogenesis in human kidney transplants is associated with immunologically active lymphocytic infiltrates. *Journal of the American Society of Nephrology*, 15 (3), pp.603–612.

Kerrigan, A.M., Dennehy, K.M., Mourao-Sa, D., Faro-Trindade, I., Willment, J.A., Taylor, P.R., Eble, J.A., Reis e Sousa, C. & Brown, G.D. (2009) CLEC-2 Is a Phagocytic

Activation Receptor Expressed on Murine Peripheral Blood Neutrophils. *The Journal of Immunology*, 182 (7), pp.4150–4157.

Kerrigan, A.M., Navarro-Nunez, L., PYZ, E., Finney, B.A., Willment, J.A., Watson, S.P. & Brown, G.D. (2012) Podoplanin-expressing inflammatory macrophages activate murine platelets via CLEC-2. *Journal of Thrombosis and Haemostasis*, 10 (3), pp.484–486.

Klein, T., Ling, Z., Heimberg, H., Madsen, O.D., Heller, R.S. & Serup, P. (2003) Nestin Is Expressed in Vascular Endothelial Cells in the Adult Human Pancreas. *Journal of Histochemistry & Cytochemistry*, 51 (6), pp.697–706.

Koh, L., Zakharov, A. & Johnston, M. (2005) Integration of the subarachnoid space and lymphatics: is it time to embrace a new concept of cerebrospinal fluid absorption? *Cerebrospinal Fluid Research*, 2, p.6.

Komatsu, M., Carraway, C.A.C., Fregien, N.L. & Carraway, K.L. (1997) Reversible disruption of cell-matrix and cell-cell interactions by overexpression of sialomucin complex. *The Journal of biological chemistry*, 272 (52), pp.33245–33254.

Kono, M., Tucker, A.E., Tran, J., Bergner, J.B., Turner, E.M. & Proia, R.L. (2014) Sphingosine-1-phosphate receptor 1 reporter mice reveal receptor activation sites in vivo. *Journal of Clinical Investigation*, 124 (5), pp.2076–2086.

Lallemand, Y., Luria, V., Haffner-Krausz, R. & Lonai, P. (1998) Maternally expressed PGK-Cre transgene as a tool for early and uniform activation of the Cre site-specific recombinase. *Transgenic Research*, 7 (2), pp.105–112.

Langer, H.F., Choi, E.Y., Zhou, H., Schleicher, R., Chung, K.J., Tang, Z., Gobel, K., Bdeir, K., Chatzigeorgiou, A., Wong, C., Bhatia, S., Kruhlak, M.J., Rose, J.W., Burns, J.B., Hill, K.E., Qu, H., Zhang, Y., Lehrmann, E., Becker, K.G., Wang, Y., Simon, D.I., Nieswandt, B., Lambris, J.D., Li, X., Meuth, S.G., Kubes, P. & Chavakis, T. (2012) Platelets Contribute to the Pathogenesis of Experimental Autoimmune Encephalomyelitis. *Circulation Research*, 110 (9), pp.1202–1210.

Levin, J. (2012) *The Evolution of Mammalian Platelets*. Third Edition. Elsevier Inc.

Ley, K., Laudanna, C., Cybulsky, M.I. & Nourshargh, S. (2007) Getting to the site of inflammation: the leukocyte adhesion cascade updated. *Nature Reviews Immunology*, 7 (9), pp.678–689.

Liebner, S., Corada, M., Bangsow, T., Babbage, J., Taddei, A., Czupalla, C.J., Reis, M., Felici, A., Wolburg, H., Fruttiger, M., Taketo, M.M., Melchner, von, H., Plate, K.H., Gerhardt, H. & Dejana, E. (2008) Wnt/ -catenin signaling controls development of the blood-brain barrier. *The Journal of Cell Biology*, 183 (3), pp.409–417.

Liscovitch, N. & Chechik, G. (2013) Specialization of gene expression during mouse brain development. *PLoS computational biology*, 9 (9), p.e1003185.

Liu, Y., Wada, R., Yamashita, T., Mi, Y., Deng, C.X., Hobson, J.P., Rosenfeldt, H.M., Nava, V.E., Chae, S.S., Lee, M.J., Liu, C.H., Hla, T., Spiegel, S. & Proia, R.L. (2000) Edg-1, the G protein-coupled receptor for sphingosine-1-phosphate, is essential for vascular maturation. *Journal of Clinical Investigation*, 106 (8), pp.951–961.

Lowe, K.L., Navarro-Nunez, L. & Watson, S.P. (2012) Platelet CLEC-2 and podoplanin in cancer metastasis. *Thrombosis research*, 129 Suppl 1, pp.S30–7.

Mahtab, E.A.F., Wijffels, M.C.E.F., Van Den Akker, N.M.S., Hahurij, N.D., Lie-Venema, H., Wisse, L.J., DeRuiter, M.C., Uhrin, P., Zaujec, J., Binder, B.R., Schalij, M.J., Poelmann, R.E. & Gittenberger-De Groot, A.C. (2008) Cardiac malformations and myocardial abnormalities inpodoplanin knockout mouse embryos: Correlation with abnormal epicardial development. *Developmental Dynamics*, 237 (3), pp.847–857.

Mallard, C. (2012) Innate immune regulation by toll-like receptors in the brain. *ISRN neurology*, 2012, p.701950.

Marcelo, K.L., Goldie, L.C. & Hirschi, K.K. (2013) Regulation of endothelial cell differentiation and specification. *Circulation Research*, 112 (9), pp.1272–1287.

Martin-Villar, E., Megias, D., Castel, S., Yurrita, M.M., Vilaro, S. & Quintanilla, M. (2006) Podoplanin binds ERM proteins to activate RhoA and promote epithelial-mesenchymal transition. *Journal of Cell Science*, 119 (21), pp.4541–4553.

Martín-Villar, E., Fernández-Muñoz, B., Parsons, M., Yurrita, M.M., Megías, D., Pérez-Gómez, E., Jones, G.E. & Quintanilla, M. (2010) Podoplanin associates with CD44 to promote directional cell migration. *Molecular biology of the cell*, 21 (24), pp.4387–4399.

May, F., Hagedorn, I., Pleines, I., Bender, M., Vogtle, T., Eble, J., Elvers, M. & Nieswandt, B. (2009) CLEC-2 is an essential platelet-activating receptor in hemostasis and thrombosis. *Blood*, 114 (16), pp.3464–3472.

McCarty, J.H., Monahan-Earley, R.A., Brown, L.F., Keller, M., Gerhardt, H., Rubin, K., Shani, M., Dvorak, H.F., Wolburg, H., Bader, B.L., Dvorak, A.M. & Hynes, R.O. (2002) Defective Associations between Blood Vessels and Brain Parenchyma Lead to Cerebral Hemorrhage in Mice Lacking v Integrins. *Molecular and Cellular Biology*, 22 (21), pp.7667–7677.

McNicol, A. & Israels, S.J. (2008) Beyond hemostasis: the role of platelets in inflammation, malignancy and infection. *Cardiovascular & hematological disorders drug targets*, 8 (2), pp.99–117.

Mebius, R.E. & Kraal, G. (2005) Structure and function of the spleen. *Nature Reviews Immunology*, 5 (8), pp.606–616.

Mizugishi, K., Yamashita, T., Olivera, A., Miller, G.F., Spiegel, S. & Proia, R.L. (2005) Essential Role for Sphingosine Kinases in Neural and Vascular Development. *Molecular and Cellular Biology*, 25 (24), pp.11113–11121.

Mohammad, M.G., Tsai, V.W.W., Ruitenberg, M.J., Hassanpour, M., Li, H., Hart, P.H., Breit, S.N., Sawchenko, P.E. & Brown, D.A. (2014) Immune cell trafficking from the brain maintains CNS immune tolerance. *Journal of Clinical Investigation*, 124 (3), pp.1228–1241.

Mokrý, J. & Nemecek, S. (1998) Angiogenesis of extra- and intraembryonic blood vessels is associated with expression of nestin in endothelial cells. *Folia biologica*, 44 (5), pp.155–161.

Mollanji, R., Bozanovic-Sosic, R., Zakharov, A., Makarian, L. & Johnston, M.G. (2002) Blocking cerebrospinal fluid absorption through the cribriform plate increases resting intracranial pressure. *American journal of physiology. Regulatory, integrative and comparative physiology*, 282 (6), pp.R1593–9.

Mourao-Sa, D., Robinson, M.J., Zelenay, S., Sancho, D., Chakravarty, P., Larsen, R., Plantinga, M., Van Rooijen, N., Soares, M.P., Lambrecht, B. & Reis e Sousa, C. (2011) CLEC-2 signaling via Syk in myeloid cells can regulate inflammatory responses. *European Journal of Immunology*, 41 (10), pp.3040–3053.

Nakazawa, Y., Sato, S., Naito, M., Kato, Y., Mishima, K., Arai, H., Tsuruo, T. & Fujita, N. (2008) Tetraspanin family member CD9 inhibits Aggrus/podoplanin-induced platelet aggregation and suppresses pulmonary metastasis. *Blood*, 112 (5), pp.1730–1739.

Navarro, A., Perez, R.E., Rezaiekhaligh, M., Mabry, S.M. & Ekekezie, I.I. (2008) T1alpha/podoplanin is essential for capillary morphogenesis in lymphatic endothelial cells. *American journal of physiology. Lung cellular and molecular physiology*, 295 (4), pp.L543–51.

Navarro-Nunez, L., Langan, S.A., Nash, G.B. & Watson, S.P. (2013) The physiological and pathophysiological roles of platelet CLEC-2. *Thrombosis and Haemostasis*, 109 (6), pp.991–998.

Nieswandt, B., Pleines, I. & Bender, M. (2011) Platelet adhesion and activation mechanisms in arterial thrombosis and ischaemic stroke. *Journal of thrombosis and haemostasis : JTH*, 9 Suppl 1, pp.92–104.

Nose, K., Saito, H. & Kuroki, T. (1990) Isolation of a gene sequence induced later by tumor-promoting 12-O-tetradecanoylphorbol-13-acetate in mouse osteoblastic cells (MC3T3-E1) and expressed constitutively in ras-transformed cells. *Cell growth & differentiation : the molecular biology journal of the American Association for Cancer Research*, 1 (11), pp.511–518.

Obermeier, B., Daneman, R. & Ransohoff, R.M. (2013) Development, maintenance and disruptionof the blood-brain barrier. *Nature Medicine*, 19 (12), pp.1584–1596.

On, N.H., Savant, S., Toews, M. & Miller, D.W. (2013) Rapid and reversible enhancement of blood–brain barrier permeability using lysophosphatidic acid. 33 (12), pp.1944–1954.

Papaiconomou, C., Bozanovic-Sosic, R., Zakharov, A. & Johnston, M. (2002) Does neonatal cerebrospinal fluid absorption occur via arachnoid projections or extracranial lymphatics? *American journal of physiology. Regulatory, integrative and comparative physiology*, 283 (4), pp.R869–76.

Partanen, J., Puri, M.C., Schwartz, L., Fischer, K.D., Bernstein, A. & Rossant, J. (1996) Cell autonomous functions of the receptor tyrosine kinase TIE in a late phase of angiogenic capillary growth and endothelial cell survival during murine development. *Development*, 122 (10), pp.3013–3021.

Perry, V.H. & Teeling, J. (2013) Microglia and macrophages of the central nervous system: the contribution of microglia priming and systemic inflammation to chronic

neurodegeneration. *Seminars in Immunopathology*, 35 (5), pp.601–612.

Perry, V.H., Cunningham, C. & Holmes, C. (2007) Systemic infections and inflammation affect chronic neurodegeneration. *Nature Reviews Immunology*, 7 (2), pp.161–167.

Pertuy, F., Aguilar, A., Strassel, C., Eckly, A., Freund, J.N., Duluc, I., Gachet, C., Lanza, F. & Léon, C. (2014) Broader expression of the mouse platelet factor 4-cre transgene beyond the megakaryocyte lineage. *Journal of Thrombosis and Haemostasis*, 13 (1), pp.115–125.

Peters, A., Pitcher, L.A., Sullivan, J.M., Mitsdoerffer, M., Acton, S.E., Franz, B., Wucherpfennig, K., Turley, S., Carroll, M.C., Sobel, R.A., Bettelli, E. & Kuchroo, V.K. (2011) Th17 cells induce ectopic lymphoid follicles in central nervous system tissue inflammation. *Immunity*, 35 (6), pp.986–996.

Peters, S.E., Paterson, G.K., Bandularatne, E.S.D., Northen, H.C., Pleasance, S., Willers, C., Wang, J., Foote, A.K., Constantino-Casas, F., Scase, T.J., Blacklaws, B.A., Bryant, C.E., Mastroeni, P., Charles, I.G. & Maskell, D.J. (2009) Salmonella enterica Serovar Typhimurium trxA Mutants Are Protective against Virulent Challenge and Induce Less Inflammation than the Live-Attenuated Vaccine Strain SL3261. *Infection and Immunity*, 78 (1), pp.326–336.

Petersen, P.H., Zou, K., Hwang, J.K., Jan, Y.N. & Zhong, W. (2002) Progenitor cell maintenance requires numb and numblike during mouse neurogenesis. *Nature*, 419 (6910), pp.929–934.

Pivniouk, V., Tsitsikov, E., Swinton, P., Rathbun, G., Alt, F.W. & Geha, R.S. (1998) Impaired viability and profound block in thymocyte development in mice lacking the adaptor protein SLP-76. *Cell*, 94 (2), pp.229–238.

Prinz, M., Priller, J., Sisodia, S.S. & Ransohoff, R.M. (2011) Heterogeneity of CNS myeloid cells and their roles in neurodegeneration. *Nature Neuroscience*, 13 (10), pp.1227–1235.

Proctor, J.M., Zang, K., Wang, D., Wang, R. & Reichardt, L.F. (2005) Vascular development of the brain requires beta8 integrin expression in the neuroepithelium. *Journal of Neuroscience*, 25 (43), pp.9940–9948.

Puri, M.C., Rossant, J., Alitalo, K., Bernstein, A. & Partanen, J. (1995) The receptor tyrosine kinase TIE is required for integrity and survival of vascular endothelial cells. *The EMBO journal*, 14 (23), pp.5884–5891.

Püntener, U., Booth, S.G., Perry, V.H. & Teeling, J.L. (2012) Long-term impact of systemic bacterial infection on the cerebral vasculature and microglia. *Journal of neuroinflammation*, 9, p.146.

Ramirez, M.I., Millien, G., Hinds, A., Cao, Y., Seldin, D.C. & Williams, M.C. (2003) T1α, a lung type I cell differentiation gene, is required for normal lung cell proliferation and alveolus formation at birth. *Developmental Biology*, 256 (1), pp.62–73.

Randolph, G.J., Angeli, V. & Swartz, M.A. (2005) Dendritic-cell trafficking to lymph nodes through lymphatic vessels. *Nature Reviews Immunology*, 5 (8), pp.617–628.

Ransohoff, R.M. & Brown, M.A. (2012) Innate immunity in the central nervous system. *Journal of Clinical Investigation*, 122 (4), pp.1164–1171.

Ransohoff, R.M. & Cardona, A.E. (2010) The myeloid cells of the central nervous system parenchyma. *Nature*, 468 (7321), pp.253–262.

Ribatti, D. & Crivellato, E. (2007) *Giulio Bizzozero and the discovery of platelets.*

Risau, W. (1997) Mechanisms of angiogenesis. *Nature*, 386 (6626), pp.671–674.

Ruhrberg, C., Gerhardt, H., Golding, M., Watson, R., Ioannidou, S., Fujisawa, H., Betsholtz, C. & Shima, D.T. (2002) Spatially restricted patterning cues provided by heparin-binding VEGF-A control blood vessel branching morphogenesis. *Genes & Development*, 16 (20), pp.2684–2698.

Sato, T.N., Tozawa, Y., Deutsch, U., Wolburg-Buchholz, K., Fujiwara, Y., Gendron-Maguire, M., Gridley, T., Wolburg, H., Risau, W. & Qin, Y. (1995) Distinct roles of the receptor tyrosine kinases Tie-1 and Tie-2 in blood vessel formation. *Nature*, 376 (6535), pp.70–74.

Schacht, V., Ramirez, M.I., Hong, Y.-K., Hirakawa, S., Feng, D., Harvey, N., Williams, M., Dvorak, A.M., Dvorak, H.F., Oliver, G. & Detmar, M. (2003) T1alpha/podoplanin deficiency disrupts normal lymphatic vasculature formation and causes lymphedema. *The EMBO journal*, 22 (14), pp.3546–3556.

Scholl, F.G., Gamallo, C., Vilaro, S. & Quintanilla, M. (1999) Identification of PA2.26 antigen as a novel cell-surface mucin-type glycoprotein that induces plasma membrane extensions and increased motility in keratinocytes. *Journal of Cell Science*, 112 (Pt 24), pp.4601–4613.

Schulte-Merker, S., Sabine, A. & Petrova, T.V. (2011) Lymphatic vascular morphogenesis in development, physiology, and disease. *The Journal of Cell Biology*, 193 (4), pp.607–618.

Schwartz, M., Kipnis, J., Rivest, S. & Prat, A. (2013) How Do Immune Cells Support and Shape the Brain in Health, Disease, and Aging? *Journal of Neuroscience*, 33 (45), pp.17587–17596.

Sebzda, E., Hibbard, C., Sweeney, S., Abtahian, F., Bezman, N., Clemens, G., Maltzman, J.S., Cheng, L., Liu, F. & Turner, M. (2006) Syk and Slp-76 Mutant Mice Reveal a Cell-Autonomous Hematopoietic Cell Contribution to Vascular Development. *Developmental cell*, 11 (3), pp.349–361.

Semple, J.W., Italiano, J.E. & Freedman, J. (2011) Platelets and the immune continuum. *Nature Reviews Immunology*, 11 (4), pp.264–274.

Senis, Y.A., Tomlinson, M.G., Garcia, A., Dumon, S., Heath, V.L., Herbert, J., Cobbold, S.P., Spalton, J.C., Ayman, S., Antrobus, R., Zitzmann, N., Bicknell, R., Frampton, J., Authi, K.S., Martin, A., Wakelam, M.J.O. & Watson, S.P. (2006) A Comprehensive Proteomics and Genomics Analysis Reveals Novel Transmembrane Proteins in Human Platelets and Mouse Megakaryocytes Including G6b-B, a Novel Immunoreceptor Tyrosine-based Inhibitory Motif Protein. *Molecular & Cellular Proteomics*, 6 (3),

pp.548–564.

Soriano, P. (1999) Generalized lacZ expression with the ROSA26 Cre reporter strain. *Nature genetics*, 21 (1), pp.70–71.

Srinivas, S., Watanabe, T., Lin, C.S., William, C.M., Tanabe, Y., Jessell, T.M. & Costantini, F. (2001) Cre reporter strains produced by targeted insertion of EYFP and ECFP into the ROSA26 locus. *BMC developmental biology*, 1, p.4.

Srinivasan, R.S., Dillard, M.E., Lagutin, O.V., Lin, F.J., Tsai, S., Tsai, M.J., Samokhvalov, I.M. & Oliver, G. (2007) Lineage tracing demonstrates the venous origin of the mammalian lymphatic vasculature. *Genes & Development*, 21 (19), pp.2422–2432.

Stenman, J.M., Rajagopal, J., Carroll, T.J., Ishibashi, M., McMahon, J. & McMahon, A.P. (2008) Canonical Wnt signaling regulates organ-specific assembly and differentiation of CNS vasculature. *Science*, 322 (5905), pp.1247–1250.

Sugawara, K.-I., Kurihara, H., Negishi, M., Saito, N., Nakazato, Y., Sasaki, T. & Takeuchi, T. (2002) Nestin as a marker for proliferative endothelium in gliomas. *Laboratory investigation; a journal of technical methods and pathology*, 82 (3), pp.345–351.

Suidan, G.L., Brill, A., De Meyer, S.F., Voorhees, J.R., Cifuni, S.M., Cabral, J.E. & Wagner, D.D. (2013) Endothelial Von Willebrand Factor Promotes Blood-Brain Barrier Flexibility and Provides Protection From Hypoxia and Seizures in Mice. *Arteriosclerosis, Thrombosis, and Vascular Biology*, 33 (9), pp.2112–2120.

Sumida, H., Noguchi, K., Kihara, Y., Abe, M., Yanagida, K., Hamano, F., Sato, S., Tamaki, K., Morishita, Y., Kano, M.R., Iwata, C., Miyazono, K., Sakimura, K., Shimizu, T. & Ishii, S. (2010) LPA4 regulates blood and lymphatic vessel formation during mouse embryogenesis. *Blood*, 116 (23), pp.5060–5070.

Sun, G., Chang, W.L., Li, J., Berney, S.M., Kimpel, D. & van der Heyde, H.C. (2003) Inhibition of Platelet Adherence to Brain Microvasculature Protects against Severe Plasmodium berghei Malaria. *Infection and Immunity*, 71 (11), pp.6553–6561.

Suzuki-Inoue, K. (2011) Essential in vivo roles of the platelet activation receptor CLEC-2 in tumour metastasis, lymphangiogenesis and thrombus formation. *Journal of biochemistry*, 150 (2), pp.127–132.

Suzuki-Inoue, K., Fuller, G.L.J., García, A., Eble, J.A., Pöhlmann, S., Inoue, O., Gartner, T.K., Hughan, S.C., Pearce, A.C., Laing, G.D., Theakston, R.D.G., Schweighoffer, E., Zitzmann, N., Morita, T., Tybulewicz, V.L.J., Ozaki, Y. & Watson, S.P. (2006) A novel Syk-dependent mechanism of platelet activation by the C-type lectin receptor CLEC-2. *Blood*, 107 (2), pp.542–549.

Suzuki-Inoue, K., Inoue, O., Ding, G., Nishimura, S., Hokamura, K., Eto, K., Kashiwagi, H., Tomiyama, Y., Yatomi, Y., Umemura, K., Shin, Y., Hirashima, M. & Ozaki, Y. (2010) Essential in vivo roles of the C-type lectin receptor CLEC-2: embryonic/neonatal lethality of CLEC-2-deficient mice by blood/lymphatic misconnections and impaired thrombus formation of CLEC-2-deficient platelets. *Journal of Biological Chemistry*, 285 (32), pp.24494–24507.

Suzuki-Inoue, K., Kato, Y., Inoue, O., Kaneko, M.K., Mishima, K., Yatomi, Y., Yamazaki, Y., Narimatsu, H. & Ozaki, Y. (2007) Involvement of the snake toxin receptor CLEC-2, in podoplanin-mediated platelet activation, by cancer cells. *The Journal of biological chemistry*, 282 (36), pp.25993–26001.

Tam, S.J. & Watts, R.J. (2010) Connecting vascular and nervous system development: angiogenesis and the blood-brain barrier. *Annual Review of Neuroscience*, 33 (1), pp.379–408.

Tammela, T. & Alitalo, K. (2010) Lymphangiogenesis: Molecular Mechanisms and Future Promise. *Cell*, 140 (4), pp.460–476.

Tang, T., Li, L., Tang, J., Li, Y., Lin, W.Y., Martin, F., Grant, D., Solloway, M., Parker, L., Ye, W., Forrest, W., Ghilardi, N., Oravecz, T., Platt, K.A., Rice, D.S., Hansen, G.M., Abuin, A., Eberhart, D.E., Godowski, P., Holt, K.H., Peterson, A., Zambrowicz, B.P. & de Sauvage, F.J. (2010) A mouse knockout library for secreted and transmembrane proteins. *Nature Biotechnology*, 28 (7), pp.749–755.

Teranishi, N., Naito, Z., Ishiwata, T., Tanaka, N., Furukawa, K., Seya, T., Shinji, S. & Tajiri, T. (2007) Identification of neovasculature using nestin in colorectal cancer. *International journal of oncology*, 30 (3), pp.593–603.

Thurston, T.L.M., Wandel, M.P., Muhlinen, von, N., Foeglein, Á. & Randow, F. (2013) Galectin 8 targets damaged vesicles for autophagy to defend cells against bacterial invasion. *Nature*, 482 (7385), pp.414–418.

Tiedt, R., Schomber, T., Hao-Shen, H. & Skoda, R.C. (2007) Pf4-Cre transgenic mice allow the generation of lineage-restricted gene knockouts for studying megakaryocyte and platelet function in vivo. *Blood*, 109 (4), pp.1503–1506.

Tomooka, M., Kaji, C., Kojima, H. & Sawa, Y. (2013) Distribution of podoplanin-expressing cells in the mouse nervous systems. *ACTA HISTOCHEMICA ET CYTOCHEMICA*, 46 (6), pp.171–177.

Tronche, F., Kellendonk, C., Kretz, O., Gass, P., Anlag, K., Orban, P.C., Bock, R., Klein, R. & Schutz, G. (1999) Disruption of the glucocorticoid receptor gene in the nervous system results in reduced anxiety. *Nature genetics*, 23 (1), pp.99–103.

Turley, S.J., Fletcher, A.L. & Elpek, K.G. (2010) The stromal and haematopoietic antigen-presenting cells that reside in secondary lymphoid organs. *Nature Reviews Immunology*, 10 (12), pp.813–825.

Turner, M., Mee, P.J., Costello, P.S., Williams, O., Price, A.A., Duddy, L.P., Furlong, M.T., Geahlen, R.L. & Tybulewicz, V.L. (1995) Perinatal lethality and blocked B-cell development in mice lacking the tyrosine kinase Syk. *Nature*, 378 (6554), pp.298–302.

Uhrin, P., Zaujec, J., Breuss, J.M., Olcaydu, D., Chrenek, P., Stockinger, H., Fuertbauer, E., Moser, M., Haiko, P., Fassler, R., Alitalo, K., Binder, B.R. & Kerjaschki, D. (2010) Novel function for blood platelets and podoplanin in developmental separation of blood and lymphatic circulation. *Blood*, 115 (19), pp.3997–4005.

Underhill, D.M. & Goodridge, H.S. (2007) The many faces of ITAMs. *Trends in*

Immunology, 28 (2), pp.66–73.

van Gils, J.M., Zwaginga, J.J. & Hordijk, P.L. (2009) Molecular and functional interactions among monocytes, platelets, and endothelial cells and their relevance for cardiovascular diseases. *Journal of leukocyte biology*, 85 (2), pp.195–204.

Vinukonda, G., Dummula, K., Malik, S., Hu, F., Thompson, C.I., Csiszar, A., Ungvari, Z. & Ballabh, P. (2010) Effect of Prenatal Glucocorticoids on Cerebral Vasculature of the Developing Brain * Supplemental Methods. *Stroke*, 41 (8), pp.1766–1773.

Wagner, D.D. & Burger, P.C. (2003) Platelets in inflammation and thrombosis. *Arteriosclerosis, Thrombosis, and Vascular Biology*, 23 (12), pp.2131–2137.

Walls, J.R., Coultas, L., Rossant, J. & Henkelman, R.M. (2008) Three-Dimensional Analysis of Vascular Development in the Mouse Embryo T. Chan-Ling ed. *PLoS ONE*, 3 (8), p.e2853.

Wang, D., Feng, J., Wen, R., Marine, J.C., Sangster, M.Y., Parganas, E., Hoffmeyer, A., Jackson, C.W., Cleveland, J.L., Murray, P.J. & Ihle, J.N. (2000) Phospholipase Cgamma2 is essential in the functions of B cell and several Fc receptors. *Immunity*, 13 (1), pp.25–35.

Watson, A.A., Brown, J., Harlos, K., Eble, J.A., Walter, T.S. & O'Callaghan, C.A. (2006) The Crystal Structure and Mutational Binding Analysis of the Extracellular Domain of the Platelet-activating Receptor CLEC-2. *Journal of Biological Chemistry*, 282 (5), pp.3165–3172.

Watson, C., Paxinos, G. & Puelles, L. (2012) *The Mouse Nervous System*. Academic Press.

Watson, S.P., Herbert, J.M.J. & Pollitt, A.Y. (2010) GPVI and CLEC-2 in hemostasis and vascular integrity. *Journal of thrombosis and haemostasis : JTH*, 8 (7), pp.1456–1467.

Wetterwald, A., Hoffstetter, W., Cecchini, M.G., Lanske, B., Wagner, C., Fleisch, H. & Atkinson, M. (1996) Characterization and cloning of the E11 antigen, a marker expressed by rat osteoblasts and osteocytes. *Bone*, 18 (2), pp.125–132.

Wicki, A., Lehembre, F., Wick, N., Hantusch, B., Kerjaschki, D. & Christofori, G. (2006) Tumor invasion in the absence of epithelial-mesenchymal transition: Podoplanin-mediated remodeling of the actin cytoskeleton. *Cancer Cell*, 9 (4), pp.261–272.

Wigle, J.T., Harvey, N., Detmar, M., Lagutina, I., Grosveld, G., Gunn, M.D., Jackson, D.G. & Oliver, G. (2002) An essential role for Prox1 in the induction of the lymphatic endothelial cell phenotype. *The EMBO journal*, 21 (7), pp.1505–1513.

Willard-Mack, C.L. (2006) Normal structure, function, and histology of lymph nodes. *Toxicologic pathology*, 34 (5), pp.409–424.

Williams, K., Alvarez, X. & Lackner, A.A. (2001) Central nervous system perivascular cells are immunoregulatory cells that connect the CNS with the peripheral immune system. *Glia*, 36 (2), pp.156–164.

Williams, M.C., Cao, Y., Hinds, A., Rishi, A.K. & Wetterwald, A. (1996) T1 alpha

protein is developmentally regulated and expressed by alveolar type I cells, choroid plexus, and ciliary epithelia of adult rats. *American journal of respiratory cell and molecular biology*, 14 (6), pp.577–585.

Winkler, E.A., Bell, R.D. & Zlokovic, B.V. (2011) Central nervous system pericytes in health and disease. *Nature Neuroscience*, 14 (11), pp.1398–1405.

Wolburg, H. & Paulus, W. (2010) Choroid plexus: biology and pathology. *Acta Neuropathologica*, 119 (1), pp.75–88.

Wu, C., Orozco, C., Boyer, J., Leglise, M., Goodale, J., Batalov, S., Hodge, C.L., Haase, J., Janes, J., Huss, J.W. & Su, A.I. (2009) BioGPS: an extensible and customizable portal for querying and organizing gene annotation resources. *Genome Biology*, 10 (11), p.R130.

Xia, L., Ju, T., Westmuckett, A., An, G., Ivanciu, L., McDaniel, J.M., Lupu, F., Cummings, R.D. & McEver, R.P. (2004) Defective angiogenesis and fatal embryonic hemorrhage in mice lacking core 1-derived O-glycans. *The Journal of Cell Biology*, 164 (3), pp.451–459.

Xie, J., Wu, T., Guo, L., Ruan, Y., Zhou, L., Zhu, H., Yun, X., Hong, Y., Jiang, J., Wen, Y. & Gu, J. (2008) Molecular characterization of two novel isoforms and a soluble form of mouse CLEC-2. *Biochemical and Biophysical Research Communications*, 371 (2), pp.180–184.

Xu, Y., Yuan, L., Mak, J., Pardanaud, L., Caunt, M., Kasman, I., Larrivee, B., del Toro, R., Suchting, S., Medvinsky, A., Silva, J., Yang, J., Thomas, J.L., Koch, A.W., Alitalo, K., Eichmann, A. & Bagri, A. (2010) Neuropilin-2 mediates VEGF-C-induced lymphatic sprouting together with VEGFR3. *The Journal of Cell Biology*, 188 (1), pp.115–130.

Yang, Y., Garcia-Verdugo, J.M., Soriano-Navarro, M., Srinivasan, R.S., Scallan, J.P., Singh, M.K., Epstein, J.A. & Oliver, G. (2012) Lymphatic endothelial progenitors bud from the cardinal vein and intersomitic vessels in mammalian embryos. *Blood*, 120 (11), pp.2340–2348.

Yu, H., Gibson, J.A., Pinkus, G.S. & Hornick, J.L. (2007) Podoplanin (D2-40) Is a Novel Marker for Follicular Dendritic Cell Tumors. *American Journal of Clinical Pathology*, 128 (5), pp.776–782.

Zhu, J., Motejlek, K., Wang, D., Zang, K., Schmidt, A. & Reichardt, L.F. (2002) beta8 integrins are required for vascular morphogenesis in mouse embryos. *Development*, 129 (12), pp.2891–2903.

Zimmerman, L., Parr, B., Lendahl, U., Cunningham, M., McKay, R., Gavin, B., Mann, J., Vassileva, G. & McMahon, A. (1994) Independent regulatory elements in the nestin gene direct transgene expression to neural stem cells or muscle precursors. *Neuron*, 12 (1), pp.11–24.